Magnetic fields in the ISM of the Milky Way and Nearby Galaxies

Kate Pattle

University College London

GISM3 - Banyuls-sur-Mer – 25/07/25

But what about the magnetic fields?

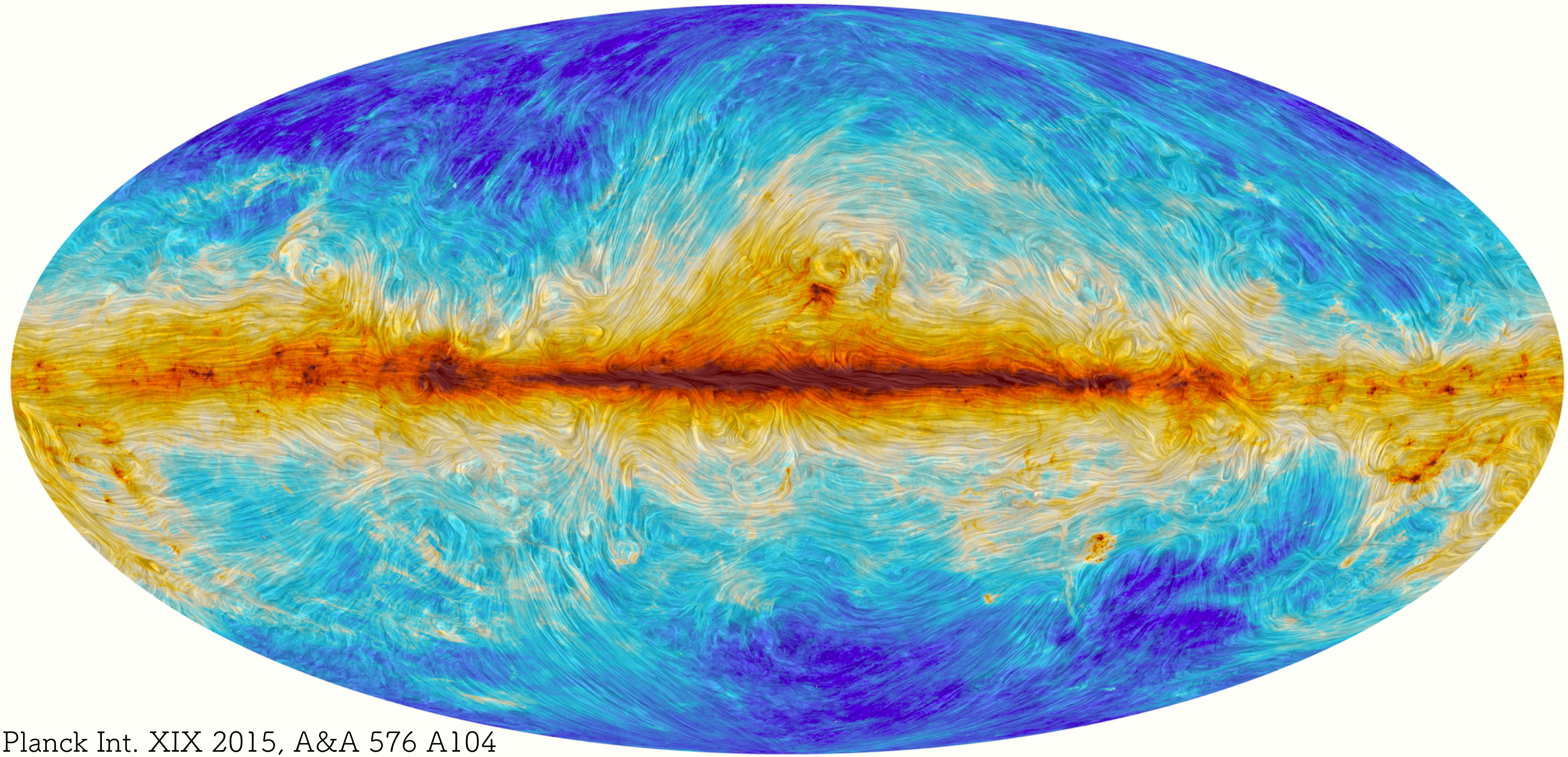

Planck Int. XIX 2015, A&A 576 A104

But what about the magnetic fields?

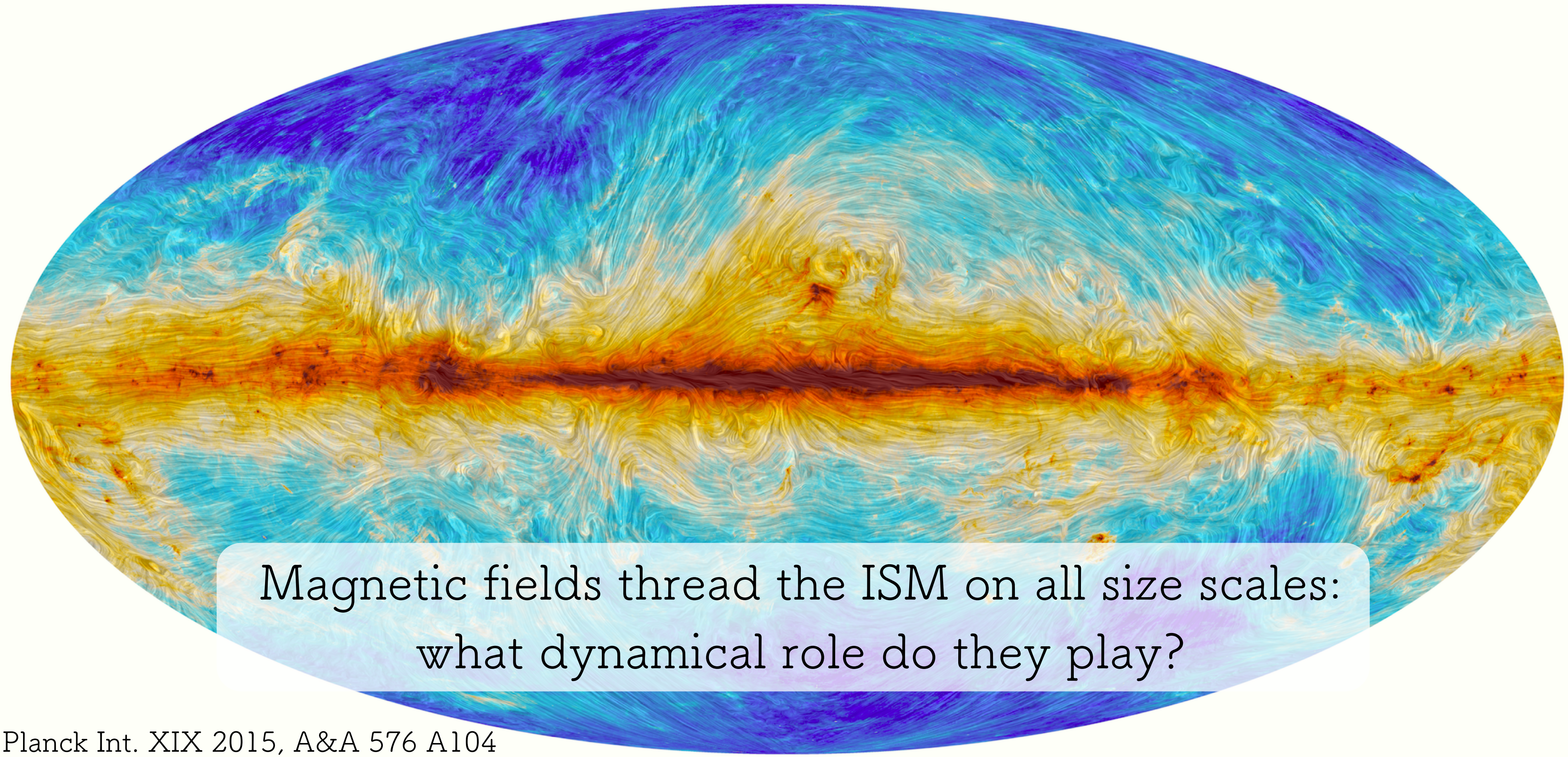

Planck Int. XIX 2015, A&A 576 A104

“The argument in the past has frequently been a process of elimination: one observed certain phenomena, and one investigated what part of the phenomena could be explained; then the unexplained part was taken to show the effects of the magnetic field.

It is clear in this case that, the larger one's ignorance, the stronger the magnetic field.”

- Lodewijk Woltjer (1930 – 2019)
Proceedings of IAU Symposium 31, 1967

Outline

1) Magnetohydrodynamic equations
2) Measuring interstellar magnetic fields
3) Magnetic fields in clouds, filaments and cores
4) Magnetic fields and feedback
5) Magnetic fields in other galaxies
6) Current and future facilities

(1) MHD equations

Maxwell's Equations

$$(1) \quad \nabla \cdot \vec{E} = 4\pi\rho_c$$

$$(2) \quad \nabla \cdot \vec{B} = 0$$

$$(3) \quad \nabla \times \vec{E} = -\frac{1}{c}\frac{\partial \vec{B}}{\partial t}$$

$$(4) \quad \nabla \times \vec{B} = \frac{1}{c}\left(4\pi\vec{J} + \frac{\partial \vec{E}}{\partial t}\right)$$

$$(1) \quad \nabla \cdot \vec{E} = 4\pi\rho_c$$

Gauss's Law

$$(2) \quad \nabla \cdot \vec{B} = 0$$

$$(3) \quad \nabla \times \vec{E} = -\frac{1}{c}\frac{\partial \vec{B}}{\partial t}$$

$$(4) \quad \nabla \times \vec{B} = \frac{1}{c}\left(4\pi\vec{J} + \frac{\partial \vec{E}}{\partial t}\right)$$

$$(1) \quad \nabla \cdot \vec{E} = 4\pi\rho_c$$

$$(2) \quad \nabla \cdot \vec{B} = 0$$

Gauss's Law for Magnetism

$$(3) \quad \nabla \times \vec{E} = -\frac{1}{c}\frac{\partial \vec{B}}{\partial t}$$

$$(4) \quad \nabla \times \vec{B} = \frac{1}{c}\left(4\pi\vec{J} + \frac{\partial \vec{E}}{\partial t}\right)$$

$$(1) \quad \nabla \cdot \vec{E} = 4\pi\rho_c$$

$$(2) \quad \nabla \cdot \vec{B} = 0$$

$$(3) \quad \nabla \times \vec{E} = -\frac{1}{c}\frac{\partial \vec{B}}{\partial t}$$

Faraday's Law of Induction

$$(4) \quad \nabla \times \vec{B} = \frac{1}{c}\left(4\pi\vec{J} + \frac{\partial \vec{E}}{\partial t}\right)$$

$$(1) \quad \nabla \cdot \vec{E} = 4\pi\rho_c$$

$$(2) \quad \nabla \cdot \vec{B} = 0$$

$$(3) \quad \nabla \times \vec{E} = -\frac{1}{c}\frac{\partial \vec{B}}{\partial t}$$

$$(4) \quad \nabla \times \vec{B} = \frac{1}{c}\left(4\pi\vec{J} + \frac{\partial \vec{E}}{\partial t}\right)$$

Ampère's Circuital Law

Lorentz Force

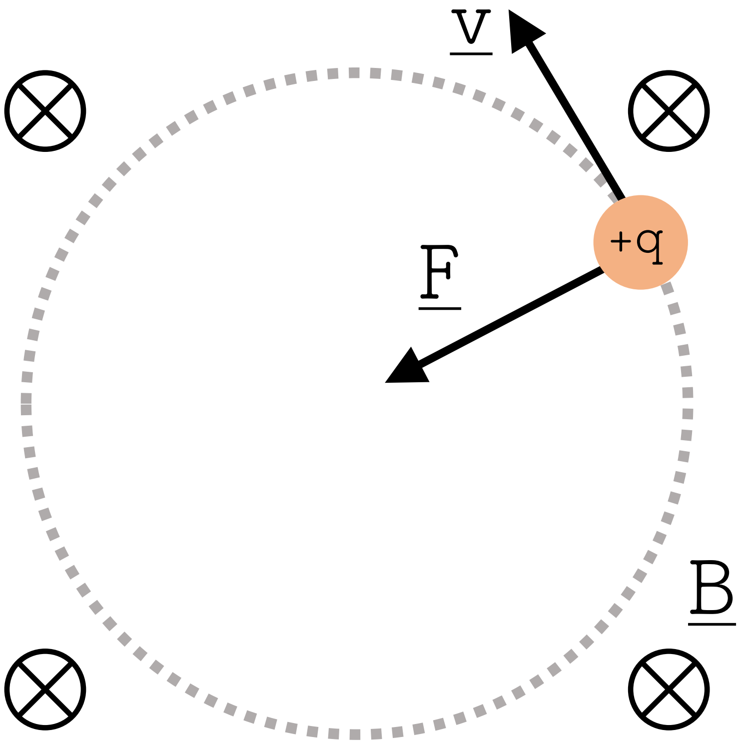

$$\vec{F} = q\left(\vec{E} + \frac{1}{c}\vec{v} \times \vec{B}\right)$$

Ohm's Law

$$\vec{J} = \sigma \left[\vec{E} + \frac{1}{c}(\vec{v} \times \vec{B}) \right]$$

Electric current density
(current per unit area)

Electrical conductivity

We can thus eliminate E from Maxwell's 3rd Law

If v<<c, Maxwell's 4th Law becomes: $\nabla \times \vec{B} = \frac{4\pi}{c}\vec{J}$

Using Ohm's Law, $\vec{E} = \frac{c}{4\pi\sigma}(\nabla \times \vec{B}) - \frac{1}{c}(\vec{v} \times \vec{B})$

Taking curl of both sides...

$$\nabla \times \vec{E} = -\frac{1}{c}\frac{\partial \vec{B}}{\partial t} = \frac{c}{4\pi\sigma}\nabla \times (\nabla \times \vec{B}) - \frac{1}{c}\nabla \times (\vec{v} \times \vec{B})$$

This leads us (using $\nabla \times (\nabla \times \vec{B}) = \nabla(\nabla \cdot \vec{B}) - \nabla^2 \vec{B}$ and Maxwell's 2nd Law ($\nabla \cdot \vec{B} = 0$)) to the **Induction Equation**:

$$\frac{\partial \vec{B}}{\partial t} = \eta \nabla^2 \vec{B} + \nabla \times (\vec{v} \times \vec{B})$$

Where $\eta = c^2/4\pi\sigma$ is magnetic diffusivity

This relates the velocity of a plasma to its magnetic field strength

What other conditions apply to the ISM?

1) Conservation of mass

The mass continuity equation: $$\frac{\partial \rho}{\partial t} + \nabla \cdot (\rho \vec{v}) = 0$$

What other conditions apply to the ISM?

2) Conservation of momentum

The Euler equation (inviscid form of the Navier-Stokes equation):

$$\frac{\partial \vec{v}}{\partial t} + (\vec{v} \cdot \nabla)\vec{v} = \vec{f} - \frac{1}{\rho}\nabla P$$

Body force per unit mass ($\vec{f}$)

Surface force per unit mass ($\frac{1}{\rho}\nabla P$)

Assume that body force term has gravitational and magnetic contributions: $\vec{f} = \vec{f}_G + \vec{f}_B$

Magnetic force per unit mass is given by:

$$\vec{f}_B = \frac{\vec{F}_B}{m} = \frac{\vec{F}_B}{\rho V}$$

$$= \frac{1}{\rho V}\frac{q}{c}\vec{v} \times \vec{B} = \frac{\rho_c}{\rho c}\vec{v} \times \vec{B}$$

$$\vec{f}_B = \frac{1}{\rho c}\vec{J} \times \vec{B}$$

(Noting $\vec{J} = \rho_c \vec{v}$)

Assume that body force term has gravitational and magnetic contributions: $\vec{f} = \vec{f}_G + \vec{f}_B$

Magnetic force per unit mass is given by:

$$\vec{f}_B = \frac{1}{\rho c}\vec{J} \times \vec{B} = \frac{1}{4\pi\rho}(\nabla \times \vec{B}) \times \vec{B}$$

(Using $\nabla \times \vec{B} = \frac{4\pi}{c}\vec{J}$)

The Euler equation then becomes:

$$\frac{\partial \vec{v}}{\partial t} + (\vec{v} \cdot \nabla)\vec{v} = \vec{f}_G - \frac{1}{\rho}\nabla P + \frac{1}{4\pi\rho}(\nabla \times \vec{B}) \times \vec{B}$$

This can be manipulated into:

$$\frac{\partial \vec{v}}{\partial t} + (\vec{v} \cdot \nabla)\vec{v} = \vec{f}_G - \frac{1}{\rho}\nabla \left(P + \frac{B^2}{8\pi} \right) + \frac{1}{4\pi\rho}(\vec{B} \cdot \nabla)\vec{B}$$

Makes use of: $(\nabla \times \vec{B}) \times \vec{B} = (\vec{B} \cdot \nabla)\vec{B} - \nabla(B^2/2)$

$$\frac{\partial \vec{v}}{\partial t} + (\vec{v} \cdot \nabla)\vec{v} = \vec{f}_G - \frac{1}{\rho}\nabla\left(P + \frac{B^2}{8\pi}\right) + \frac{1}{4\pi\rho}(\vec{B} \cdot \nabla)\vec{B}$$

Magnetic pressure term

A gradient in magnetic pressure results in a net force on the plasma

Regions of the ISM with higher B than their surroundings will be overpressured and expand

$$\frac{\partial \vec{v}}{\partial t} + (\vec{v} \cdot \nabla)\vec{v} = \vec{f}_G - \frac{1}{\rho}\nabla\left(P + \frac{B^2}{8\pi}\right) + \frac{1}{4\pi\rho}(\vec{B} \cdot \nabla)\vec{B}$$

Magnetic pressure term

By analogy with thermodynamics, the magnetic energy within a volume V with magnetic field B is:

$$E_B = \frac{B^2 V}{8\pi}$$

$$\frac{\partial \vec{v}}{\partial t} + (\vec{v} \cdot \nabla)\vec{v} = \vec{f}_G - \frac{1}{\rho}\nabla\left(P + \frac{B^2}{8\pi}\right) + \frac{1}{4\pi\rho}(\vec{B} \cdot \nabla)\vec{B}$$

Magnetic pressure term

The ratio of thermal and magnetic pressure is known as **plasma *β***

$$\beta = \frac{n k_{\mathrm{B}} T}{B^2/8\pi}$$

$\beta \gg 1$ Gas pressure-dominated

$\beta \ll 1$ Magnetic pressure-dominated

$$\frac{\partial \vec{v}}{\partial t} + (\vec{v} \cdot \nabla)\vec{v} = \vec{f}_G - \frac{1}{\rho}\nabla\left(P + \frac{B^2}{8\pi}\right) + \frac{1}{4\pi\rho}(\vec{B} \cdot \nabla)\vec{B}$$

Magnetic tension term

Provides a restoring force on a bent magnetic field line

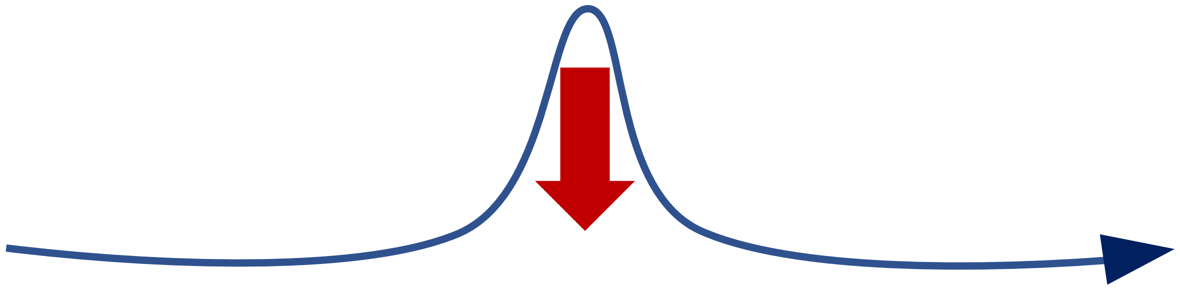

So what happens if we perturb a magnetic field?

Perturb a uniform, static, non-self-gravitating $(\vec{f}_G = 0)$ plasma with a uniform magnetic field $\vec{B}_0$

$$\rho = \rho_0 + \rho_1(\vec{x}, t)$$

$$P = P_0 + P_1(\vec{x}, t)$$

$$\vec{v} = \vec{v}_1(\vec{x}, t)$$

$$\vec{B} = \vec{B}_0 + \vec{B}_1(\vec{x}, t)$$

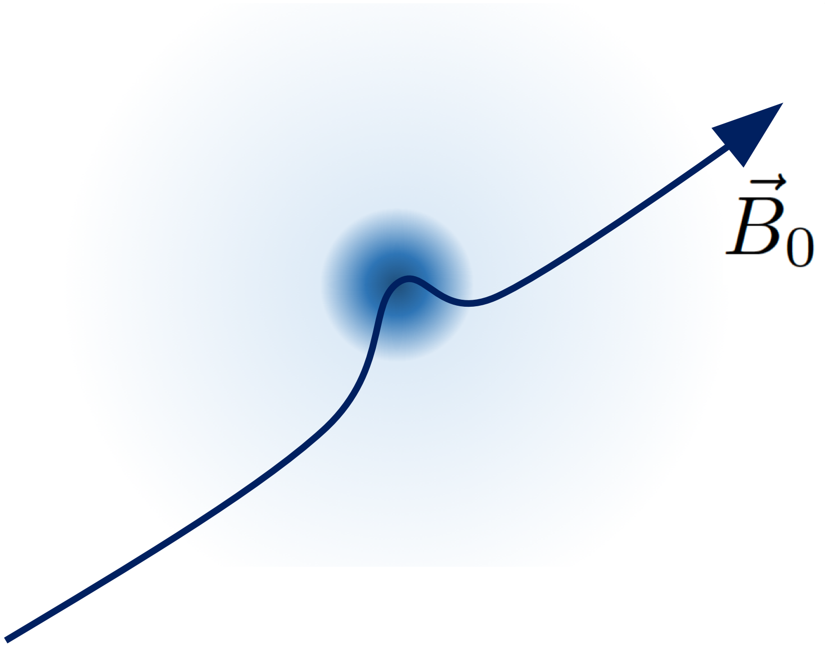

Perturb and linearise...

The continuity equation: $$\frac{\partial \rho}{\partial t} + \nabla \cdot (\rho \vec{v}) = 0$$

The induction equation: $$\frac{\partial \vec{B}}{\partial t} = \eta \nabla^2 \vec{B} + \nabla \times (\vec{v} \times \vec{B})$$

The Euler equation: $$\frac{\partial \vec{v}}{\partial t} + (\vec{v} \cdot \nabla)\vec{v} = -\frac{1}{\rho}\nabla P + \frac{1}{4\pi\rho}(\nabla \times \vec{B}) \times \vec{B}$$

Perturb and linearise...

The continuity equation: $$\frac{\partial \rho_1}{\partial t} + \rho_0 \nabla \cdot \vec{v}_1 = 0$$

The induction equation: $$\frac{\partial \vec{B}_1}{\partial t} = \nabla \times (\vec{v}_1 \times \vec{B}_0)$$

The Euler equation: $$\rho_0 \frac{\partial \vec{v}_1}{\partial t} = -c_s^2 \nabla \rho_1 + \frac{1}{4\pi} (\nabla \times \vec{B}_1) \times \vec{B}_0$$

In the final case, we have used the ideal gas law, $P_1 = c_s^2 \rho_1$

Differentiating the perturbed Euler equation w.r.t. time, and substituting in the perturbed continuity and induction equations gives:

$$\frac{\partial^2 \vec{v}_1}{\partial t^2} = c_s^2 \nabla(\nabla \cdot \vec{v}_1) + \frac{1}{4\pi\rho_0}\left(\nabla \times \left[\nabla \times (\vec{v}_1 \times \vec{B}_0)\right]\right) \times \vec{B}_0$$

We define the **Alfvén velocity**: $$\vec{v}_A = \frac{\vec{B}_0}{\sqrt{4\pi\rho_0}}$$

Note: $\underline{v}_A$ is along magnetic field direction

And so,

$$\frac{\partial^2 \vec{v}_1}{\partial t^2} = c_s^2 \nabla(\nabla \cdot \vec{v}_1) + \nabla \times [\nabla \times (\vec{v}_1 \times \vec{v}_A)] \times \vec{v}_A$$

$$\frac{\partial^2 \vec{v}_1}{\partial t^2} = c_s^2 \nabla(\nabla \cdot \vec{v}_1) + \nabla \times [\nabla \times (\vec{v}_1 \times \vec{v}_A)] \times \vec{v}_A$$

This is starting to look like a wave equation, so we consider the case in which the perturbations vary as $\exp(i[\vec{k} \cdot \vec{x} - \omega t])$

Thus, $\partial/\partial t \rightarrow -i\omega$ and $\nabla \rightarrow i\vec{k}$

Our differentiated Euler equation then becomes

$$\omega^2 \vec{v}_1 = (c_s^2 + v_A^2)(\vec{k} \cdot \vec{v}_1)\vec{k} + (\vec{v}_A \cdot \vec{k}) \left[(\vec{v}_A \cdot \vec{k})\vec{v}_1 - (\vec{v}_A \cdot \vec{v}_1)\vec{k} - (\vec{k} \cdot \vec{v}_1)\vec{v}_A \right]$$

This is a dispersion relation!

Consider the particular case where the perturbation is transverse, i.e. $\underline{v}_A.\underline{v}_1 = 0$ ($\underline{B}_0.\underline{v}_1 = 0$) and $\underline{k}.\underline{v}_1 = 0$.

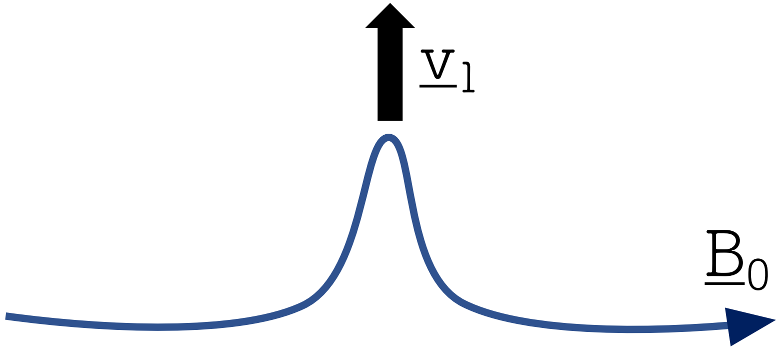

The dispersion equation reduces to: $\omega^2 = (\vec{v}_A \cdot \vec{k})^2$

The group velocity of a transverse wave is thus:

$$\vec{v}_g = \nabla_{\vec{k}}\omega = \vec{v}_A$$

Transverse perturbations propagate along magnetic field lines at the Alfvén velocity, $\vec{v}_A = \vec{B}_0/\sqrt{4\pi\rho_0}$

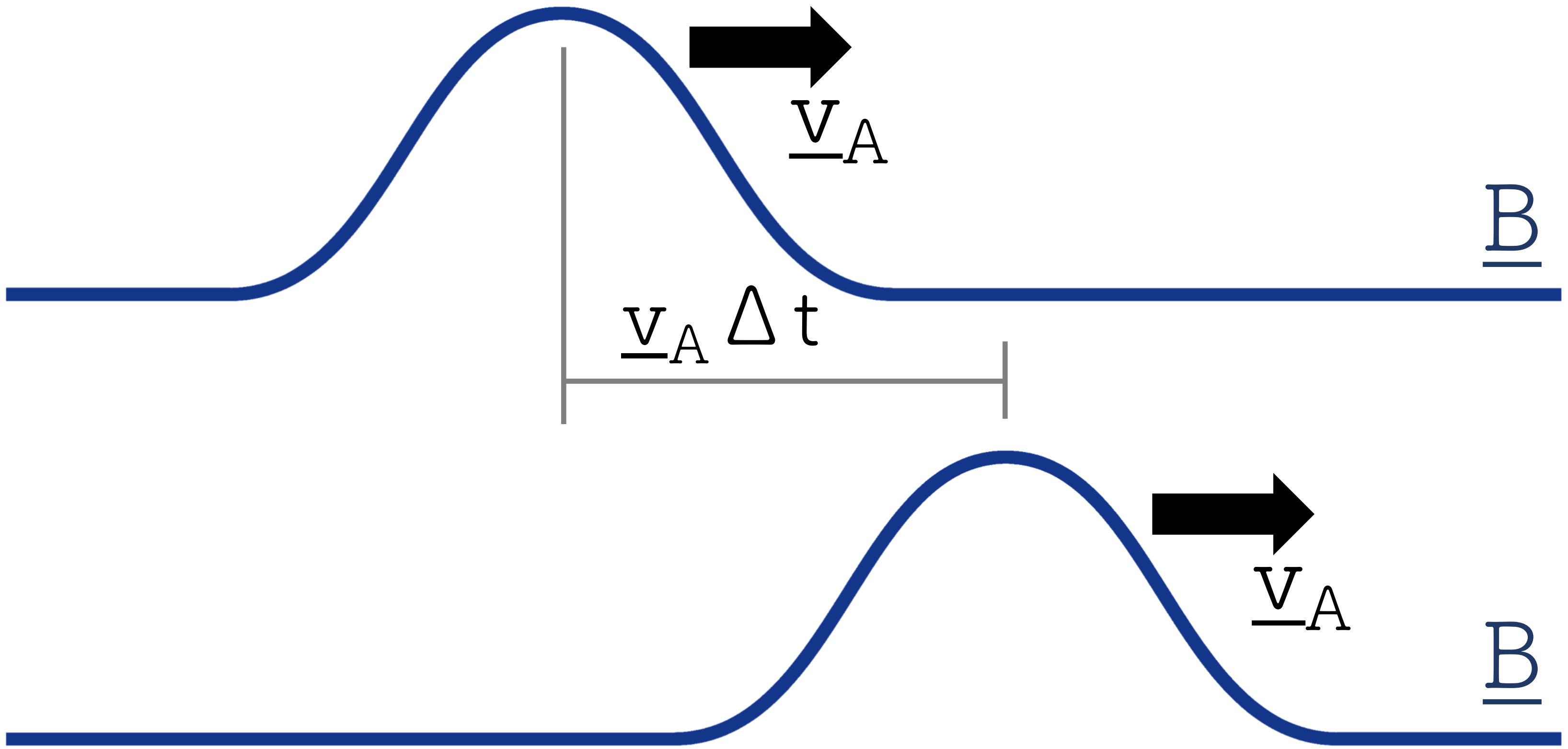

The Alfvén speed determines how quickly a magnetic field can react to a perturbation: analogous to sound speed in a gas

Alfvén Mach Number

The ratio of the speed of a non-thermal plasma flow and the Alfvén speed (analogous to sonic Mach number):

$$\mathcal{M}_A = \frac{v_{plasma}}{v_A}$$

For turbulent gas motions:

$$\mathcal{M}_{A,turb} = \frac{\sigma_{v,\mathrm{NT},1D}\sqrt{2}}{v_A}$$

Sub-Alfvénic: $\mathcal{M}_A < 1$ Magnetic fields direct gas flows

Super-Alfvénic: $\mathcal{M}_A > 1$ Gas flows direct magnetic fields

$M_A = 0.6$

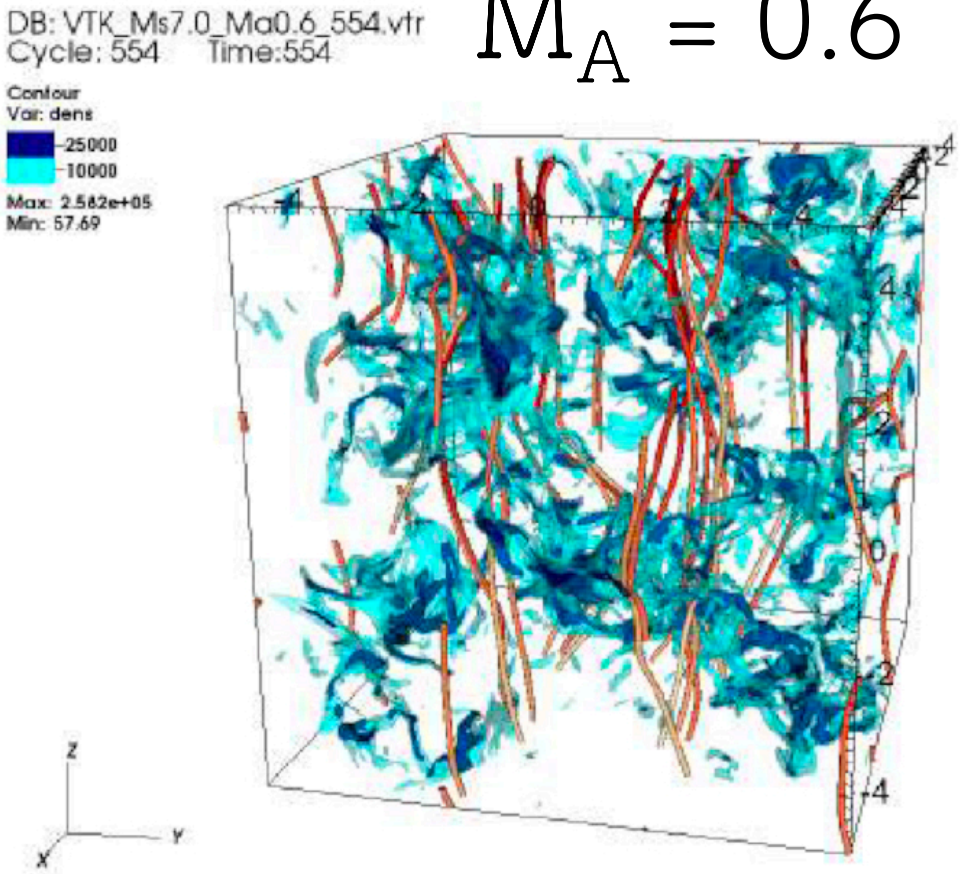

$M_A = 2.0$

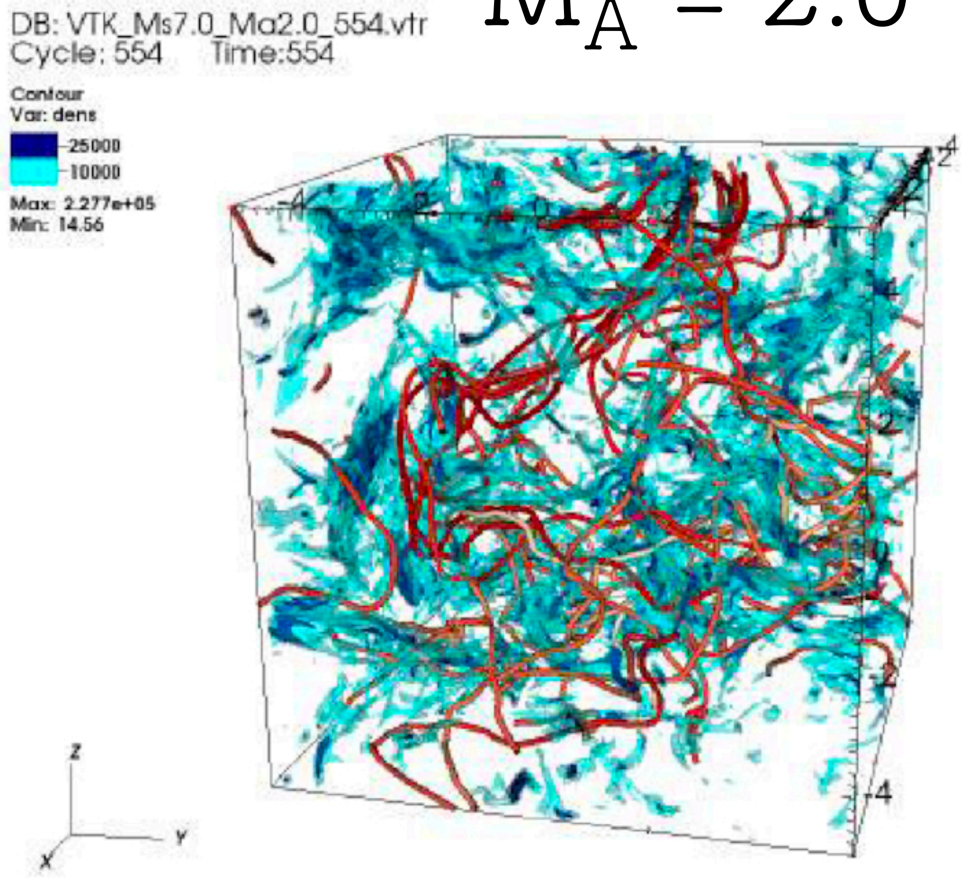

Baretto-Mora et al. 2021

Magnetic Reynolds Number

Induction Equation:

$$\frac{\partial \vec{B}}{\partial t} = \eta \nabla^2 \vec{B} + \nabla \times (\vec{v} \times \vec{B})$$

Diffusion term

Advection term

Magnetic field "diffuses" through plasma

Bulk motions; magnetic field moves with plasma flow

Magnetic Reynolds Number

Induction Equation:

$$\frac{\partial \vec{B}}{\partial t} = \eta \nabla^2 \vec{B} + \nabla \times (\vec{v} \times \vec{B})$$

Diffusion term | Advection term

Magnetic Reynolds Number:

$$\mathcal{R}_M = \frac{vB/L}{\eta B/L^2} = \frac{vL}{\eta}$$

For a plasma with characteristic length scale L

$\mathcal{R}_M \ll 1$ Diffusion-dominated

$\mathcal{R}_M \gg 1$ Advection-dominated

Magnetic Reynolds Number:

$$\mathcal{R}_M = \frac{vB/L}{\eta B/L^2} = \frac{vL}{\eta}$$

In most environments in the ISM, L is very large, so $\mathcal{R}_M \gg 1$ and the magnetic field evolution is advection-dominated, i.e.:

$$\frac{\partial \vec{B}}{\partial t} \approx \nabla \times (\vec{v} \times \vec{B})$$

Flux Freezing

For any quantity Q for which $\frac{d\vec{Q}}{dt} = \nabla \times (\vec{v} \times \vec{Q})$, it can be shown that the flux through surface S is constant with time.

Alfvén's principle of flux freezing:

$$\frac{d}{dt}\int_S \vec{B} \cdot d\vec{S} = 0$$

The magnetic field and the plasma move together

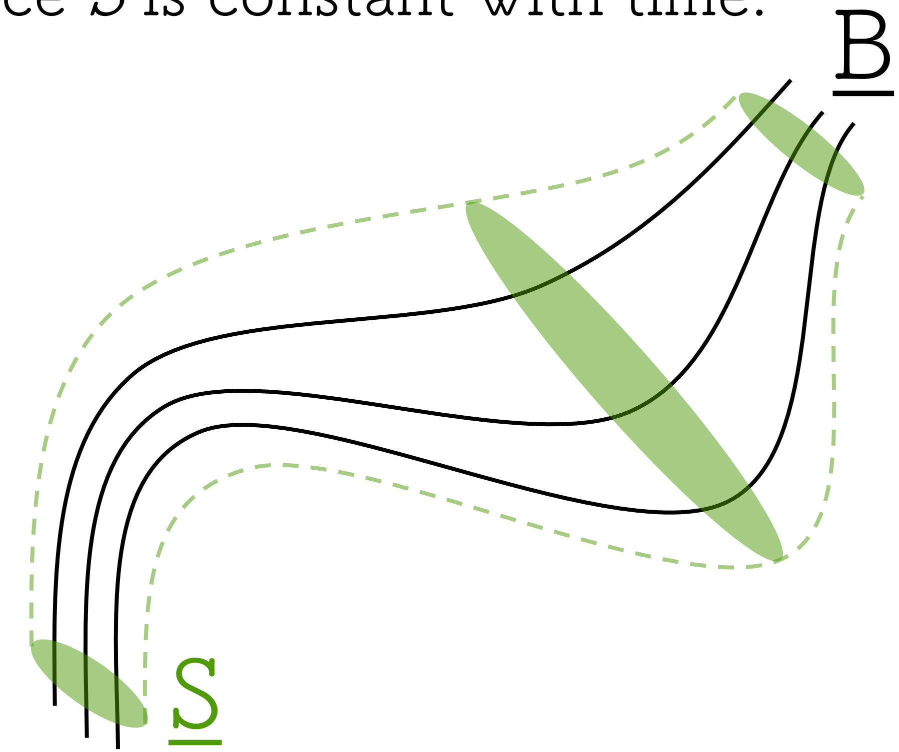

Flux Freezing

For any quantity Q for which $\frac{d\vec{Q}}{dt} = \nabla \times (\vec{v} \times \vec{Q})$, it can be shown that the flux through surface S is constant with time.

Alfvén's principle of flux freezing:

$$\frac{d}{dt}\int_S \vec{B} \cdot d\vec{S} = 0$$

The magnetic field and the plasma move together

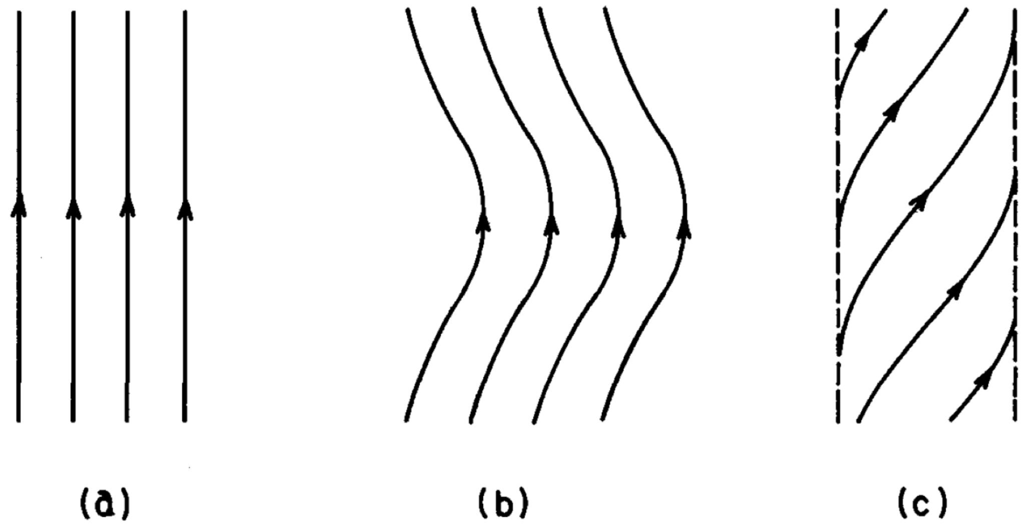

Choudhuri 2014, Chapter 6

Flux Freezing

Why should magnetic fields be frozen into neutral gas?

Alfvén's principle of flux freezing:

$$\frac{d}{dt}\int_S \vec{B}\cdot d\vec{S} = 0$$

The magnetic field and the plasma move together

Ion-neutral Coupling

While the mean free path for ion-neutral collisions is sufficiently short, ions and neutrals are coupled, and so the neutral gas and the magnetic field move together.

Key metrics

Mass-to-flux ratio: magnetic fields vs. gravity ("subcritical" = magnetically dominated)

$$\left(\frac{M}{\Phi}\right)_{crit} = \frac{1}{2\pi\sqrt{G}} \quad \mu_\Phi = \frac{(M/\Phi)}{(M/\Phi)_{crit}} = 2\pi\sqrt{G}\mu m_{\mathrm{H}}\left(\frac{N}{B}\right)$$

Alfvén Mach number: magnetic fields vs. non-thermal motions

("sub-Alfvénic" = magnetically dominated)

$$\mathcal{M}_A = \frac{v_{plasma}}{v_A}$$

Plasma beta: magnetic pressure vs. thermal pressure

$$\beta = \frac{n k_{\mathrm{B}} T}{B^2/8\pi}$$

$$E_B = \frac{B^2 V}{8\pi}$$

(2) Measuring magnetic fields

Polarization

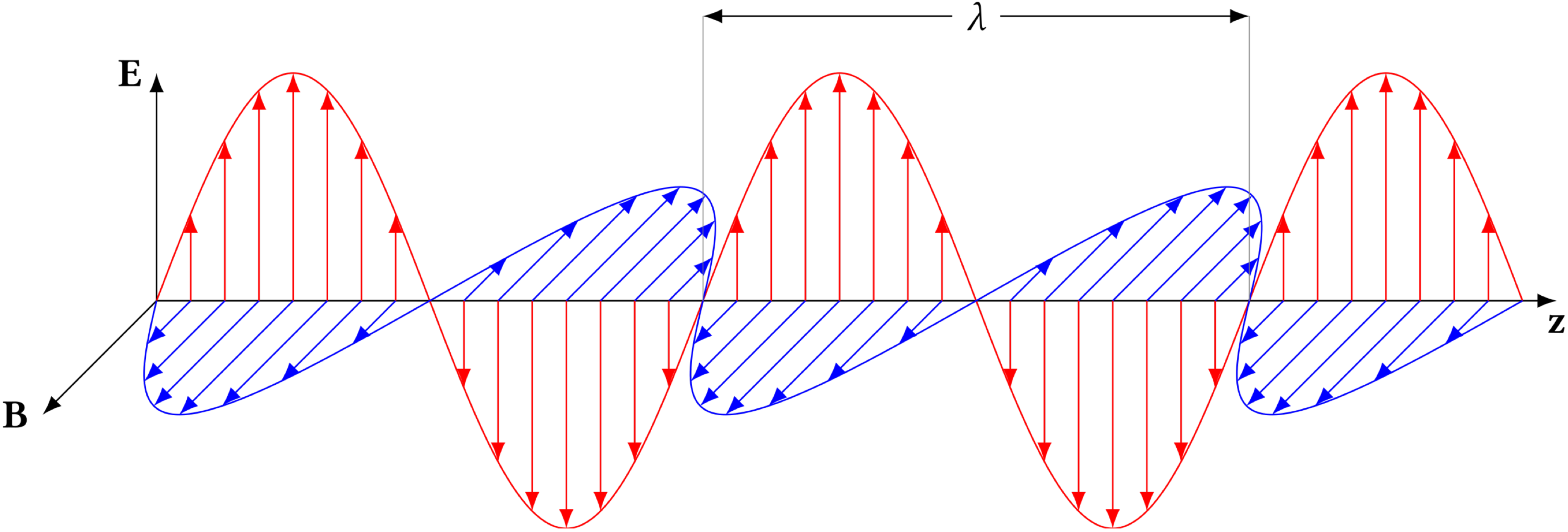

Linear polarization

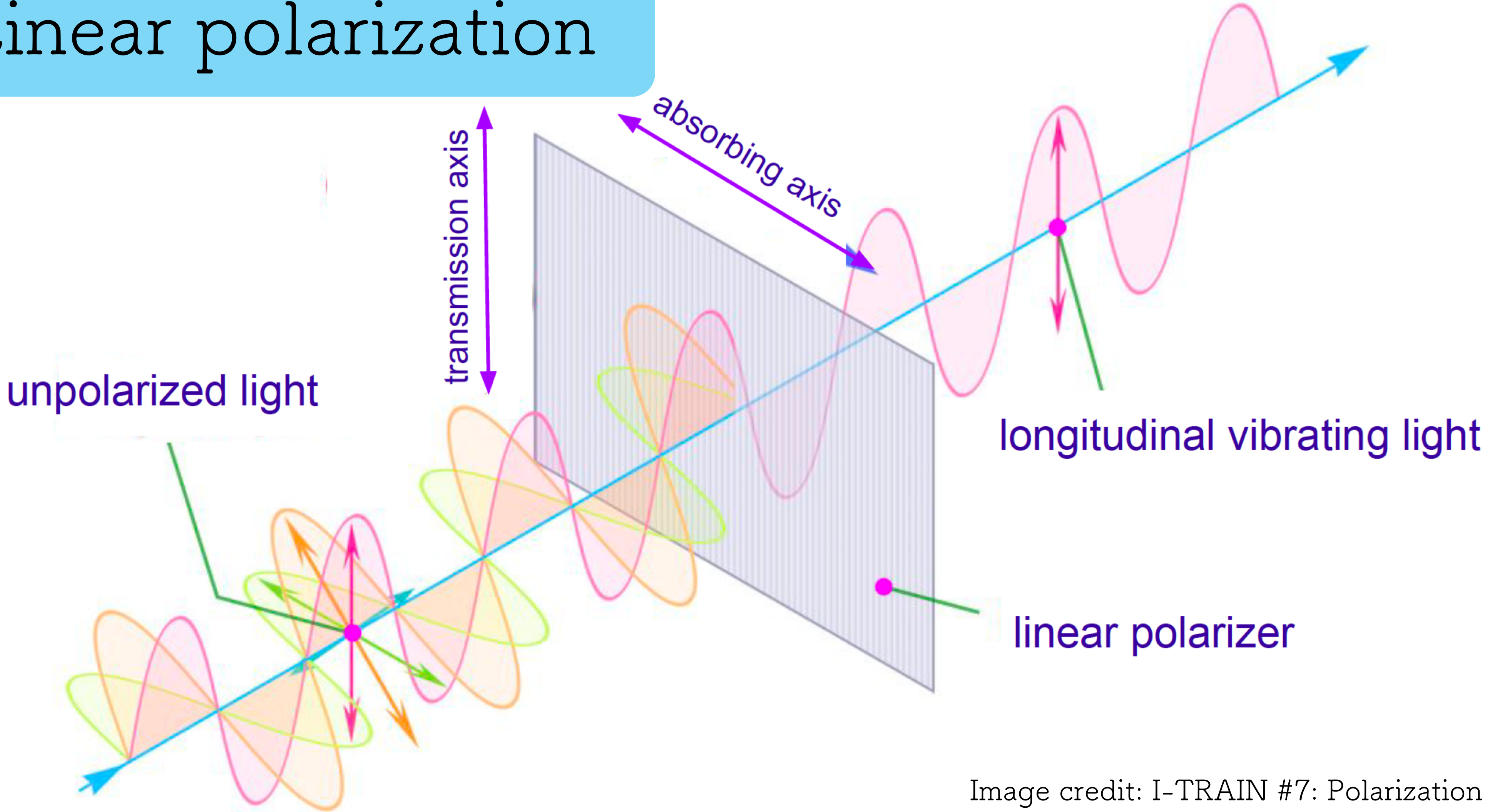

Image credit: I-TRAIN #7: Polarization observations with ALMA, Paladino et al.

Circular polarization

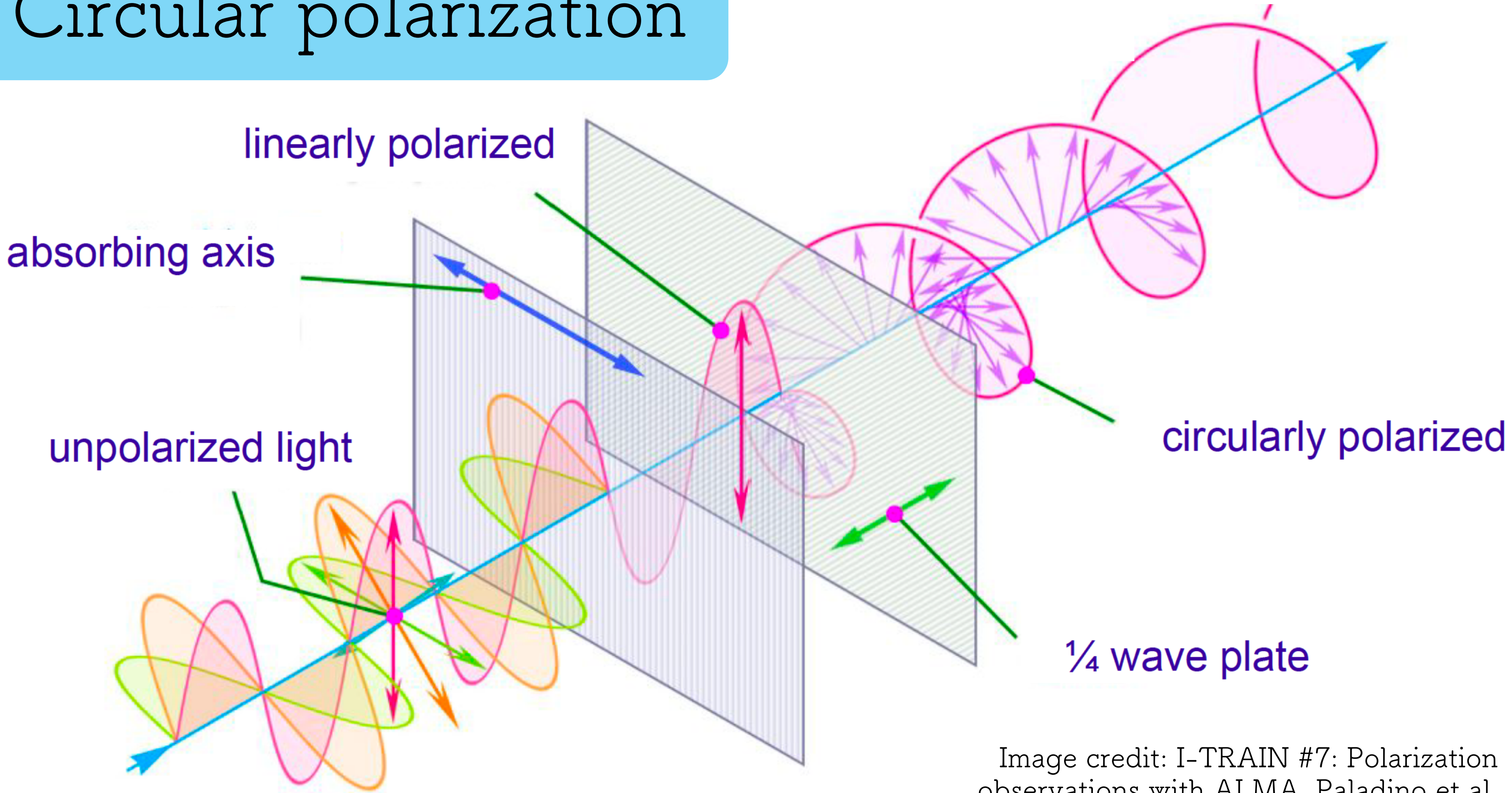

Image credit: I-TRAIN #7: Polarization observations with ALMA, Paladino et al.

Stokes Parameters

$$\begin{pmatrix} I \\ Q \\ U \\ V \end{pmatrix}$$

Total intensity

} Linearly polarized intensity

Circularly polarized intensity

This is **IAU Convention**

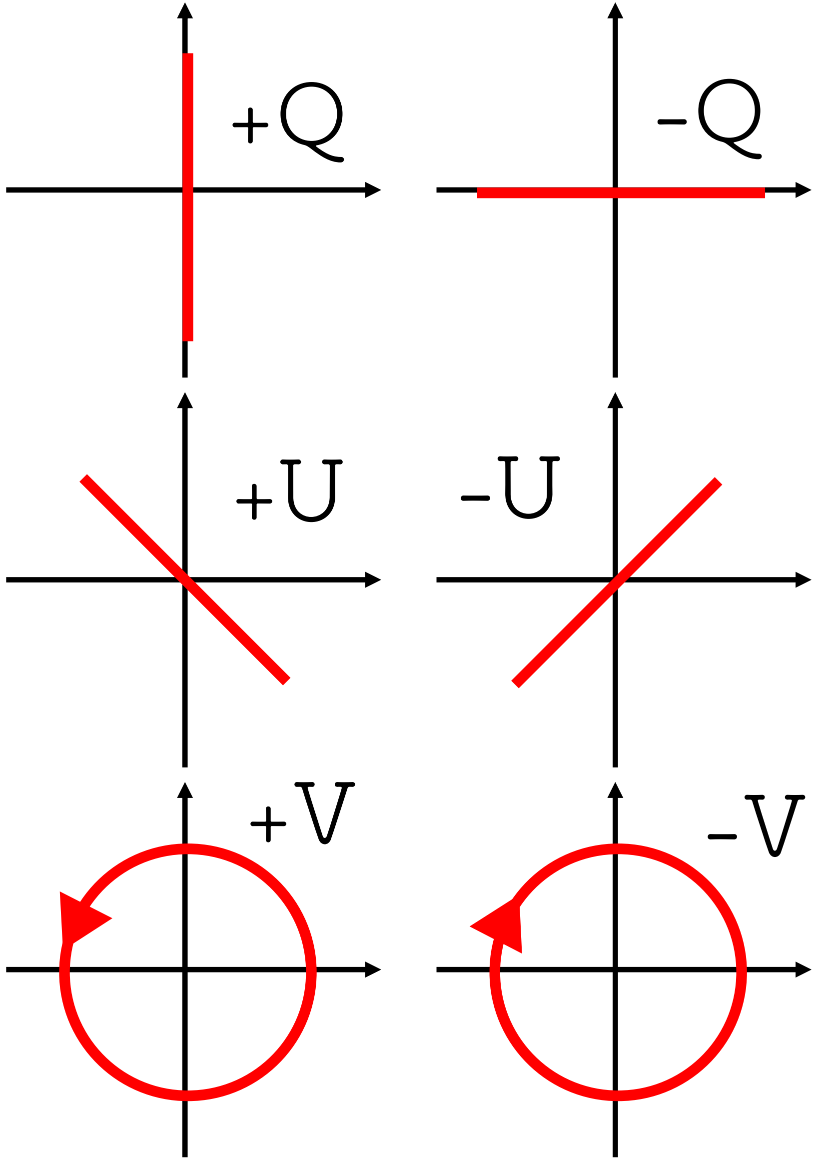

Stokes Parameters

$$\begin{pmatrix} I \\ Q \\ U \\ V \end{pmatrix}$$

Total intensity

} Linearly polarized intensity

Circularly polarized intensity

This is **Cosmology Convention**

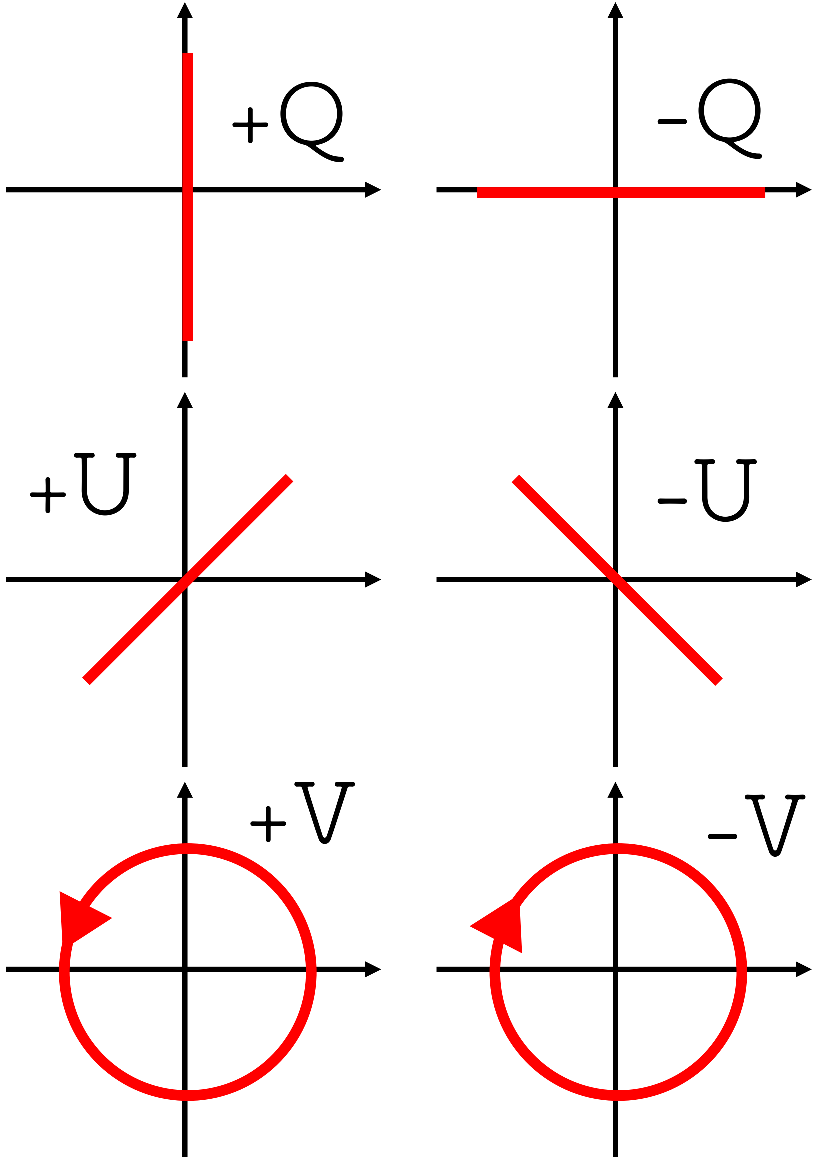

Methods for measuring magnetic fields

The Zeeman Effect

- Directly measures the line-of-sight (LOS) field component through splitting of spectral lines in the presence of a magnetic field
- Requires a species with a magnetic dipole moment, i.e. a paramagnetic species: HI, OH, CN…
- Pencil-beam and very observationally intensive

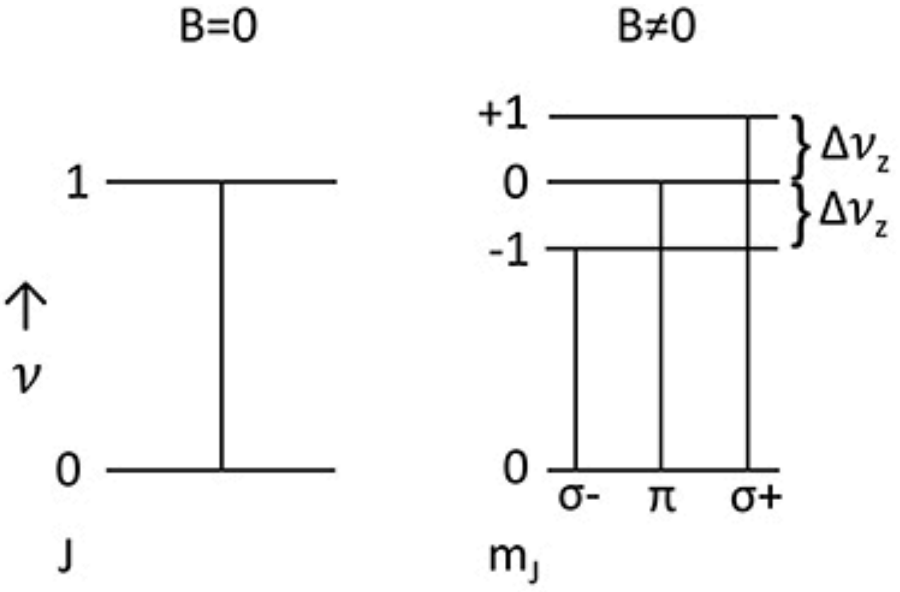

Crutcher & Kemball 2019, FrASS 6 66

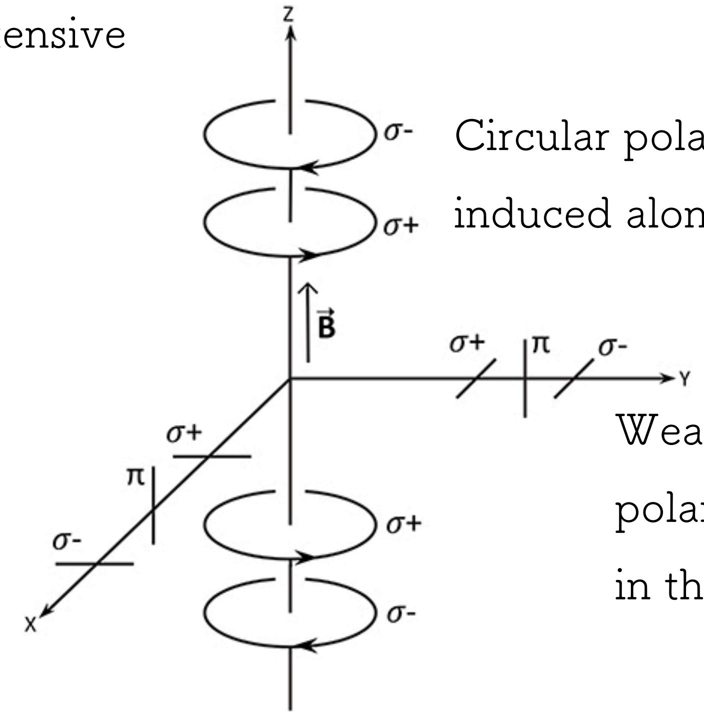

Circular polarization induced along the LOS

Weaker linear polarization induced in the POS

Methods for measuring magnetic fields

Faraday rotation

- Measures the LOS magnetic field component through rotation of background polarisation
- Requires measures of electron density and path length to recover magnetic field strength
- Not suitable for high-column-density sightlines such as molecular clouds

$$\Delta\psi = \lambda^2 \left(0.812 \int n_e \vec{B} \cdot d\vec{l}\right) = \lambda^2 \mathrm{RM}$$

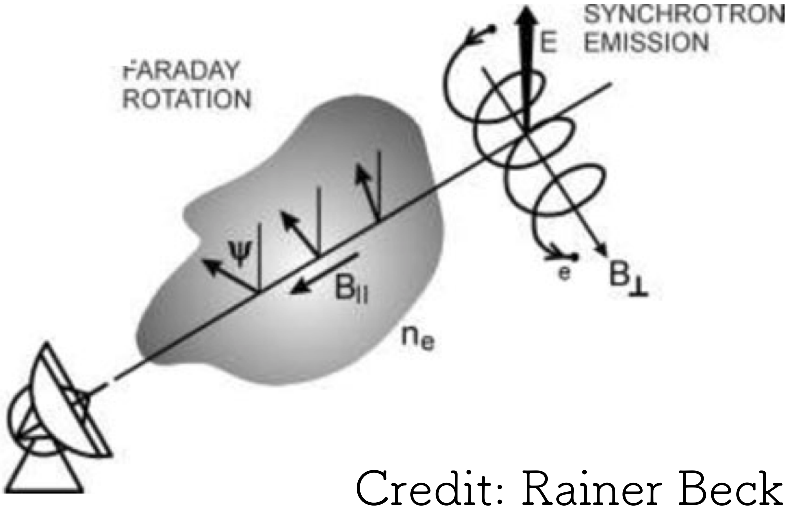

Credit: Rainer Beck

Methods for measuring magnetic fields

Dust emission/extinction polarimetry

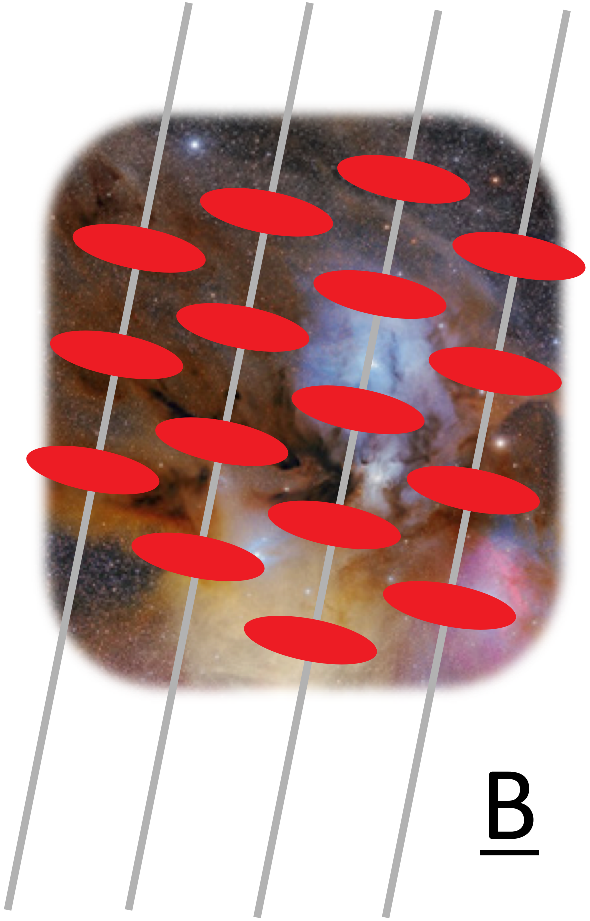

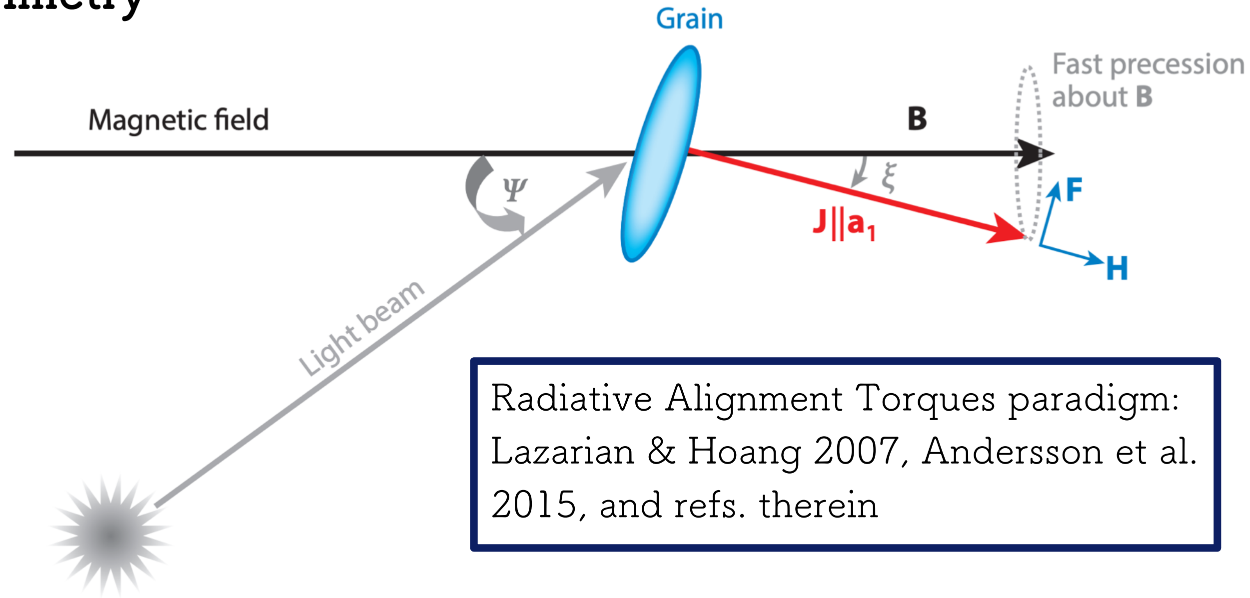

Radiative Alignment Torques paradigm: Lazarian & Hoang 2007, Andersson et al. 2015, and refs. therein

Polarization angle:

$$\theta_p = 0.5 \arctan(U, Q)$$

Polarization fraction:

$$p = \frac{\sqrt{Q^2 + U^2}}{I}$$

Methods for measuring magnetic fields

The Zeeman Effect

- Directly measures the line-of-sight field component
- Requires a paramagnetic species: HI, OH, CN...
- Pencil-beam and very observationally intensive

Faraday rotation

- Measures the line-of-sight magnetic field component
- Requires measures of electron density and path length to recover magnetic field strength
- Not suitable for high-column-density sightlines such as molecular clouds

Dust polarization

- Allows inference of the plane-of-sky magnetic field morphology
- Can be used to map wide areas
- Indirect and subject to LOS and beam integration effects, and to loss of grain alignment

(3) Fields in clouds, filaments & cores

Models of cloud formation

1) Gravitational instability of the Galactic disc
   (Parker instability)
2) Condensations from large-scale turbulence
3) Colliding atomic flows
4) Shell expansions and interactions

Gravitational instability of the Galactic disc

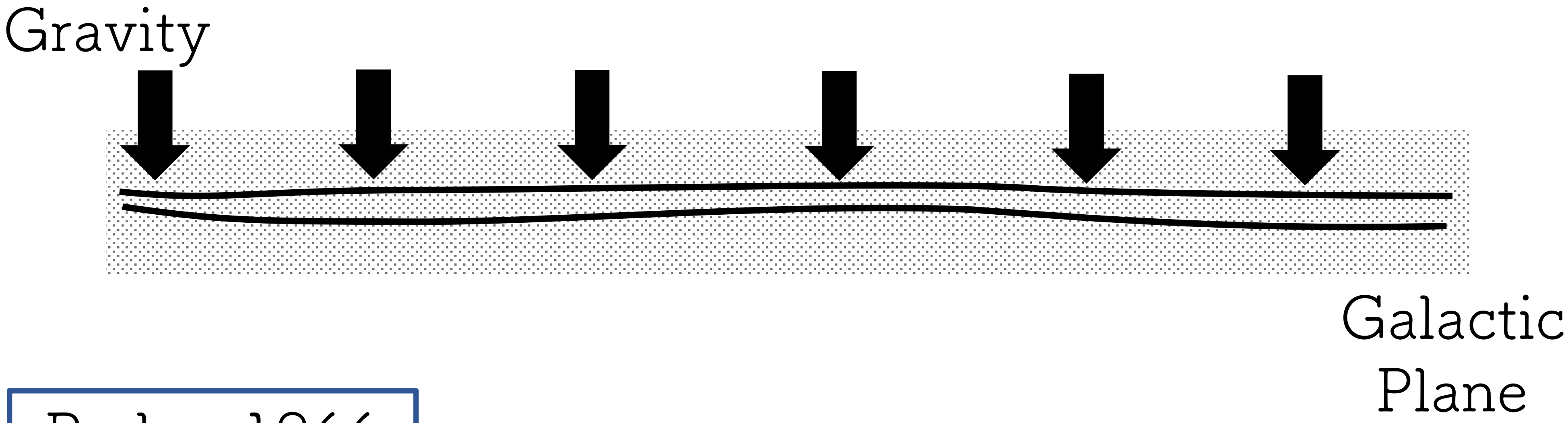

Parker 1966

Gravitational instability of the Galactic disc

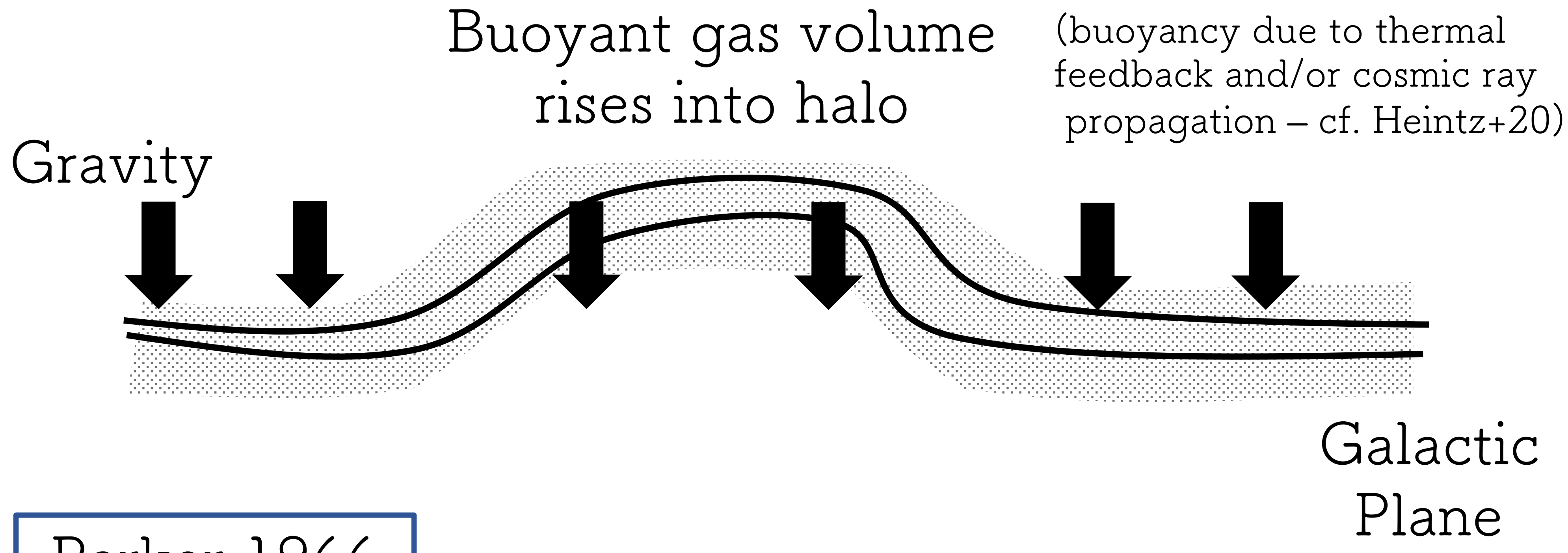

Parker 1966

Gravitational instability of the Galactic disc

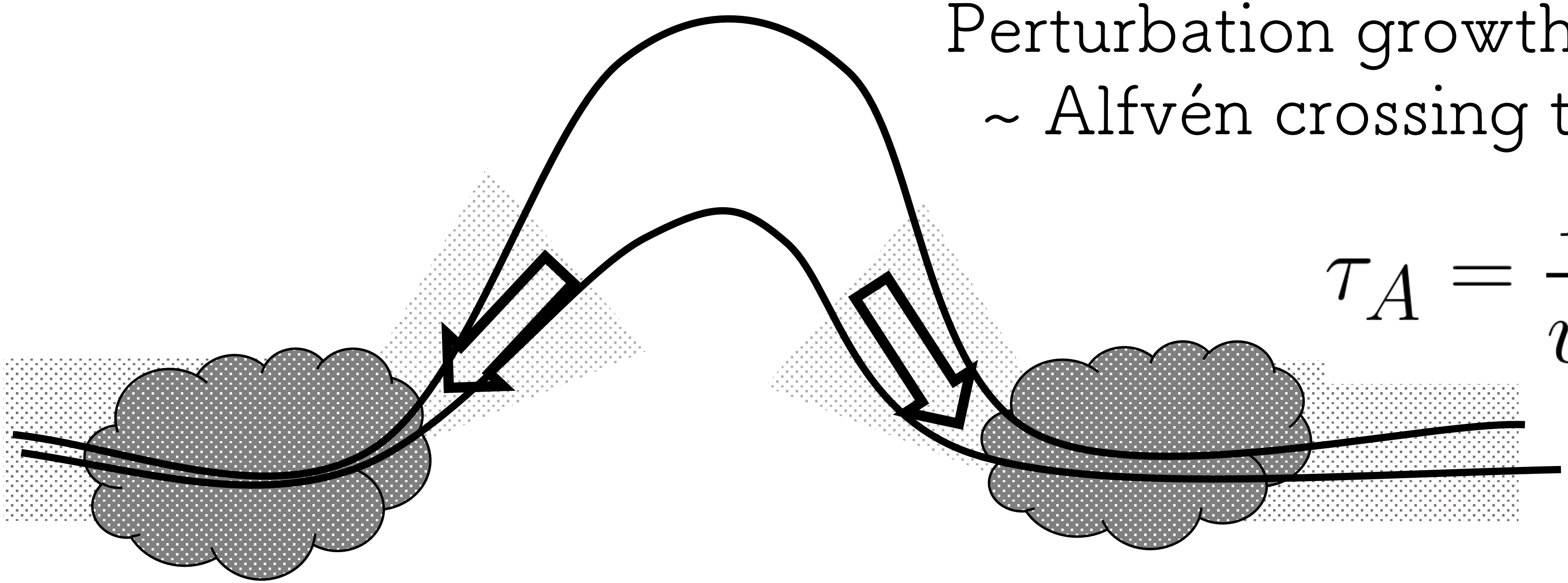

Perturbation growth rate
~ Alfvén crossing time

$$\tau_A = \frac{H}{v_A}$$

Parker 1966

If disc scale height H~100pc and
v_A~10 km/s, **τ_A~10 Myr**

In differentially rotating disks, filamentary clouds form with their major axis perpendicular to the magnetic field

Körtgen et al. 2018

Condensations from large-scale turbulence

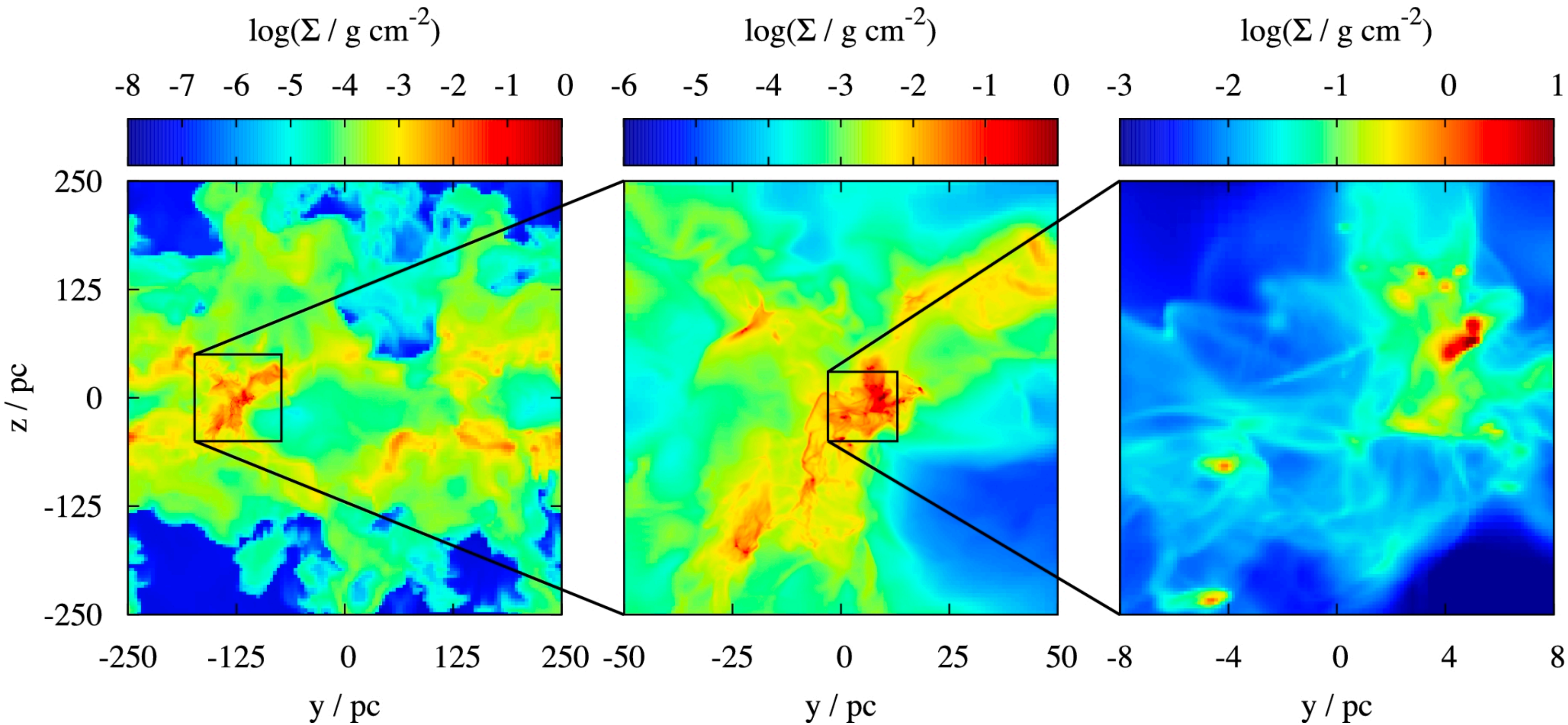

SILCC-Zoom simulation – Seifried et al. 2017

Turbulence driven by differential Galactic rotation and clustered stellar feedback creates shocks, triggering thermal instability and local collapse.

This process occurs over many orders of magnitude in size scale: zooming into clouds from a kpc-scaled box allows high-resolution studies of molecular clouds while preserving the large-scale dynamics of turbulence and magnetic fields.

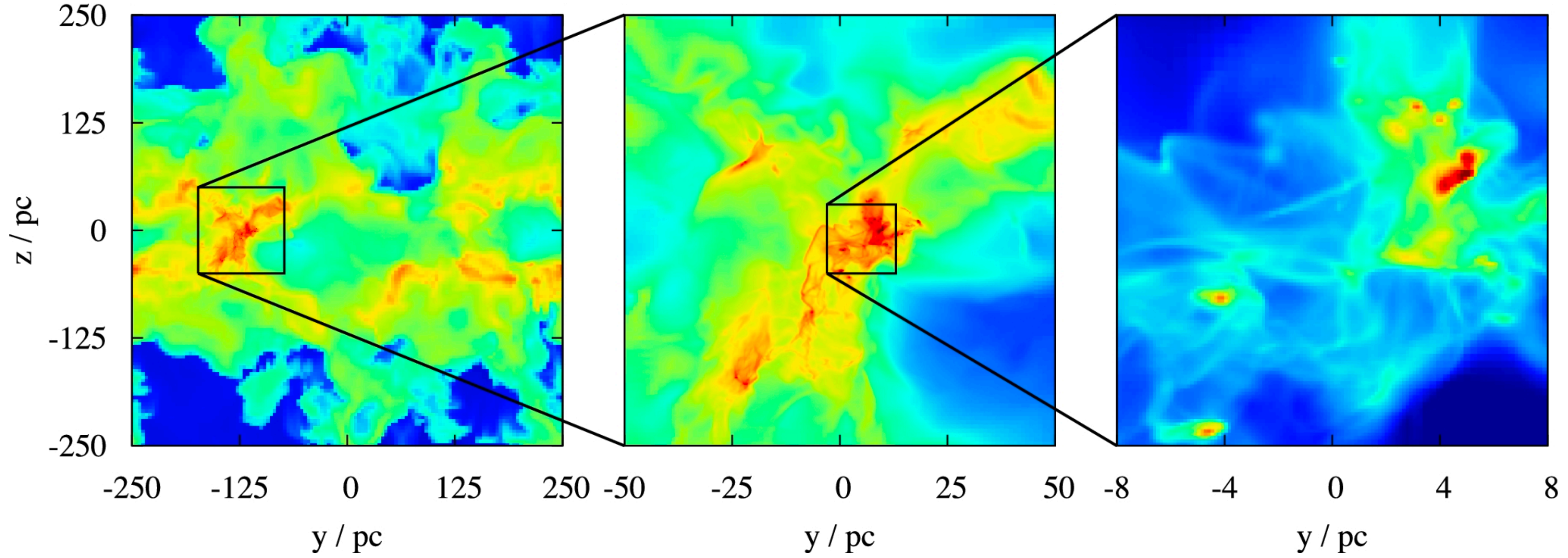

SILCC-Zoom simulation – Seifried et al. 2017

Colliding atomic flows

Hennebelle et al. 2008

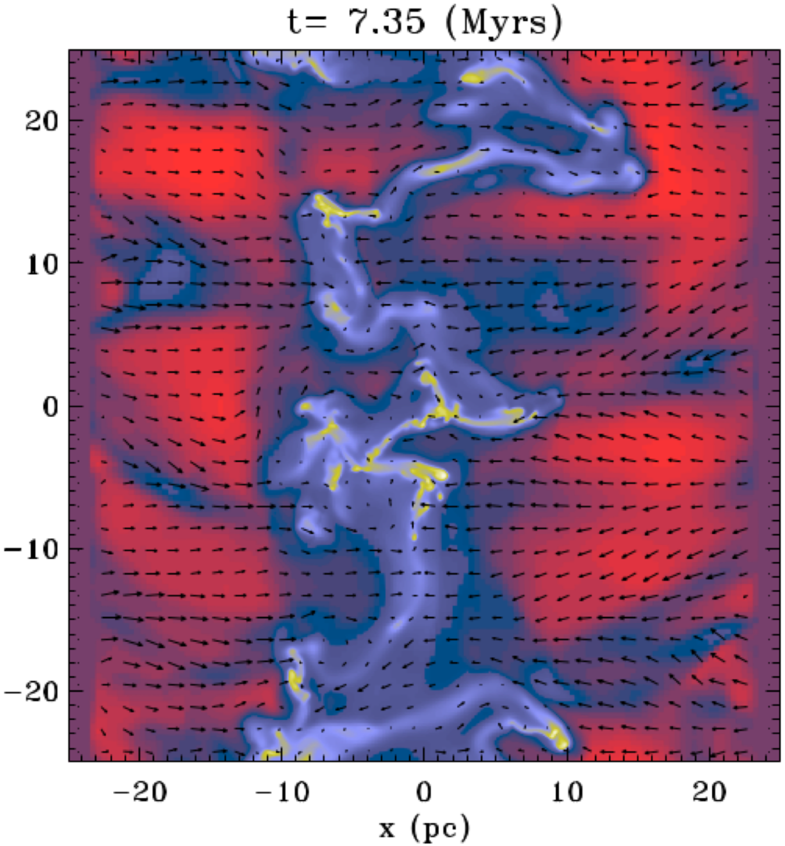

When warm atomic gas flows converge to a shock, a series of fluid instabilities can condense the atomic gas into molecular clouds:

1) Non-linear thin shell instability induces shear
2) Shear transitions to turbulence via Kelvin-Helmholtz instability
3) Condensations within shock become thermally unstable, forming clumps of dense gas

In general, if the magnetic field is misaligned with respect to the gas flow, dense gas formation will be suppressed

⇒ Perpendicular magnetic fields are required for star formation

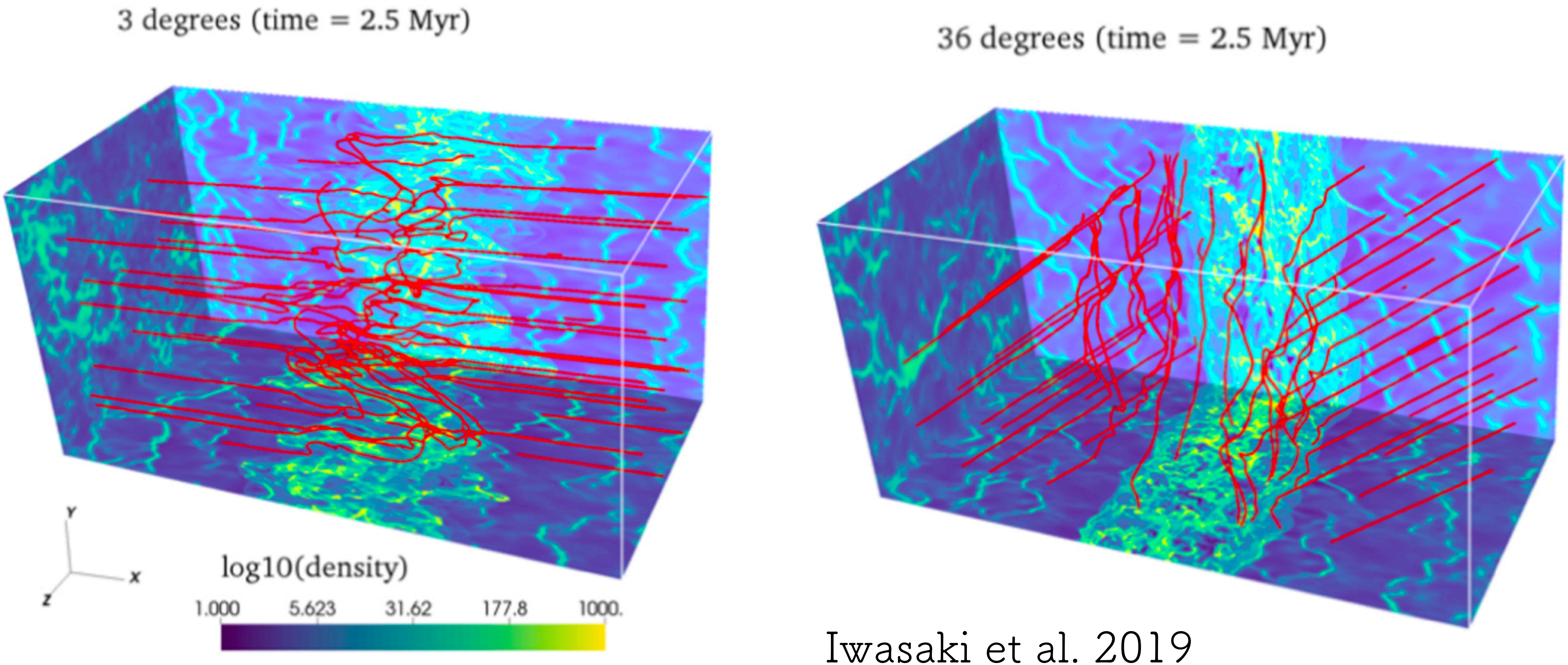

Iwasaki et al. 2019

Shell expansion and interactions

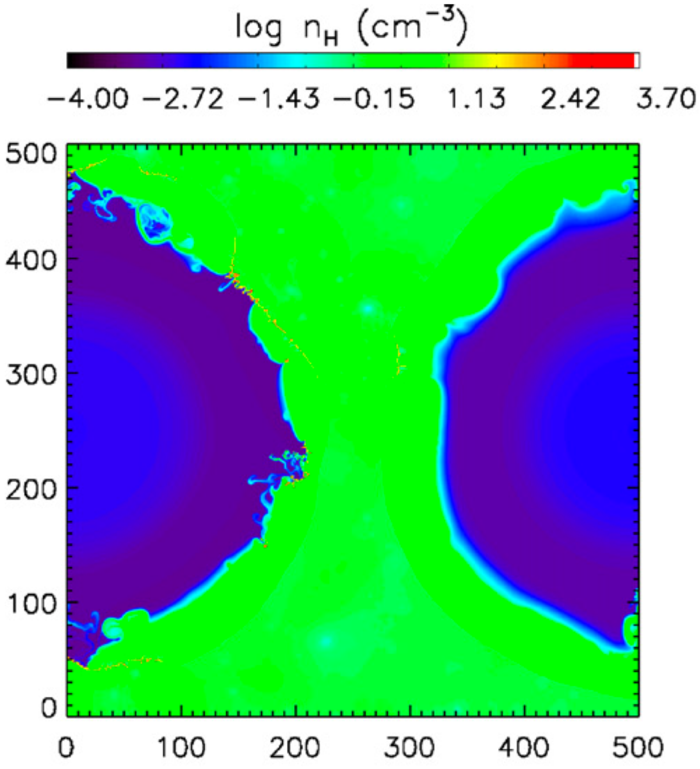

t = 3 Myr

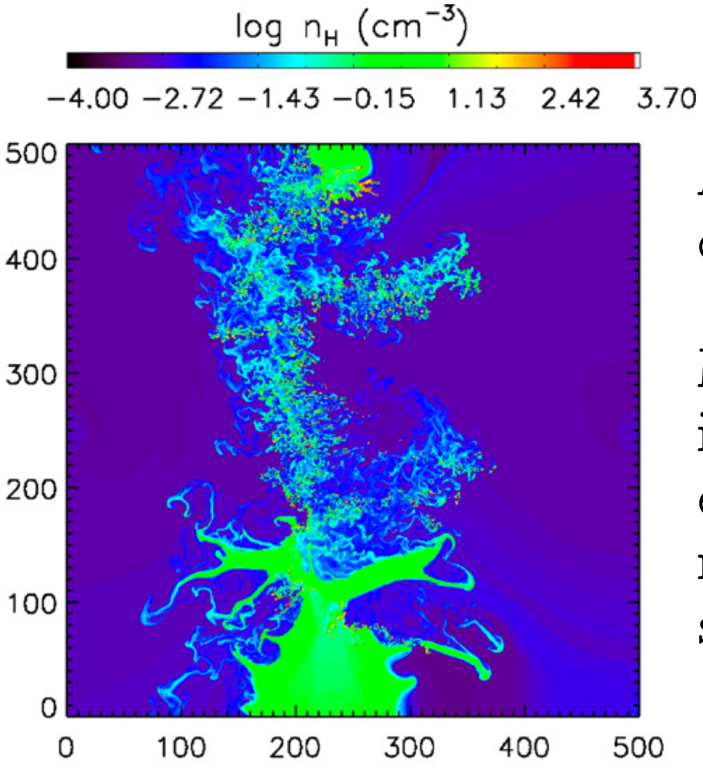

t = 7 Myr

A special case of colliding flows:

Molecular gas forms in the interaction of expanding HII regions or superbubbles

Ntormousi et al. 2011

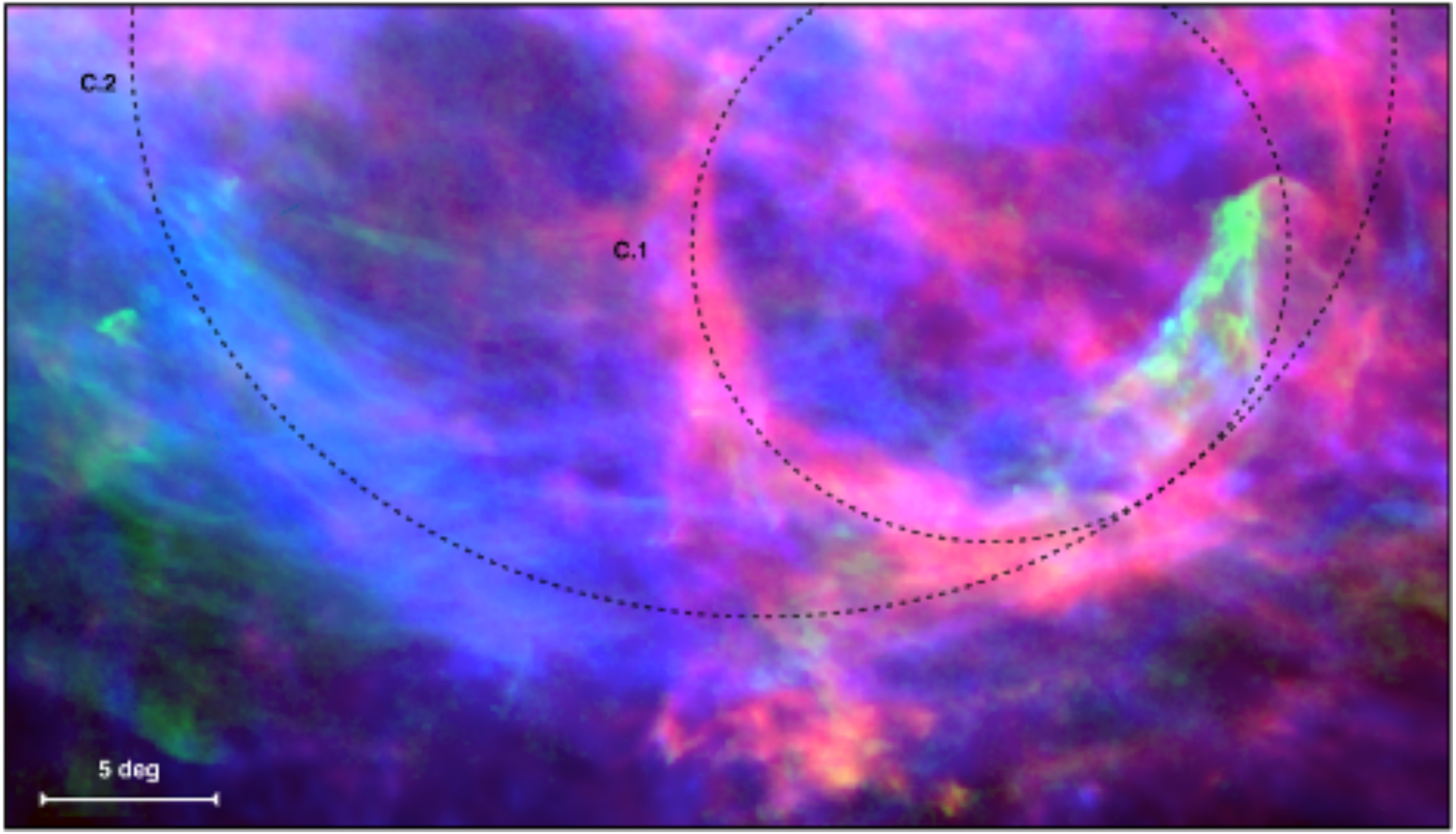

Bracco et al. 2020

However, single-shell interaction is difficult because…

a) Timescales for cloud formation from diffuse atomic medium >> evolution time of shell

b) Magnetic fields may suppress instabilities, and so dense gas formation

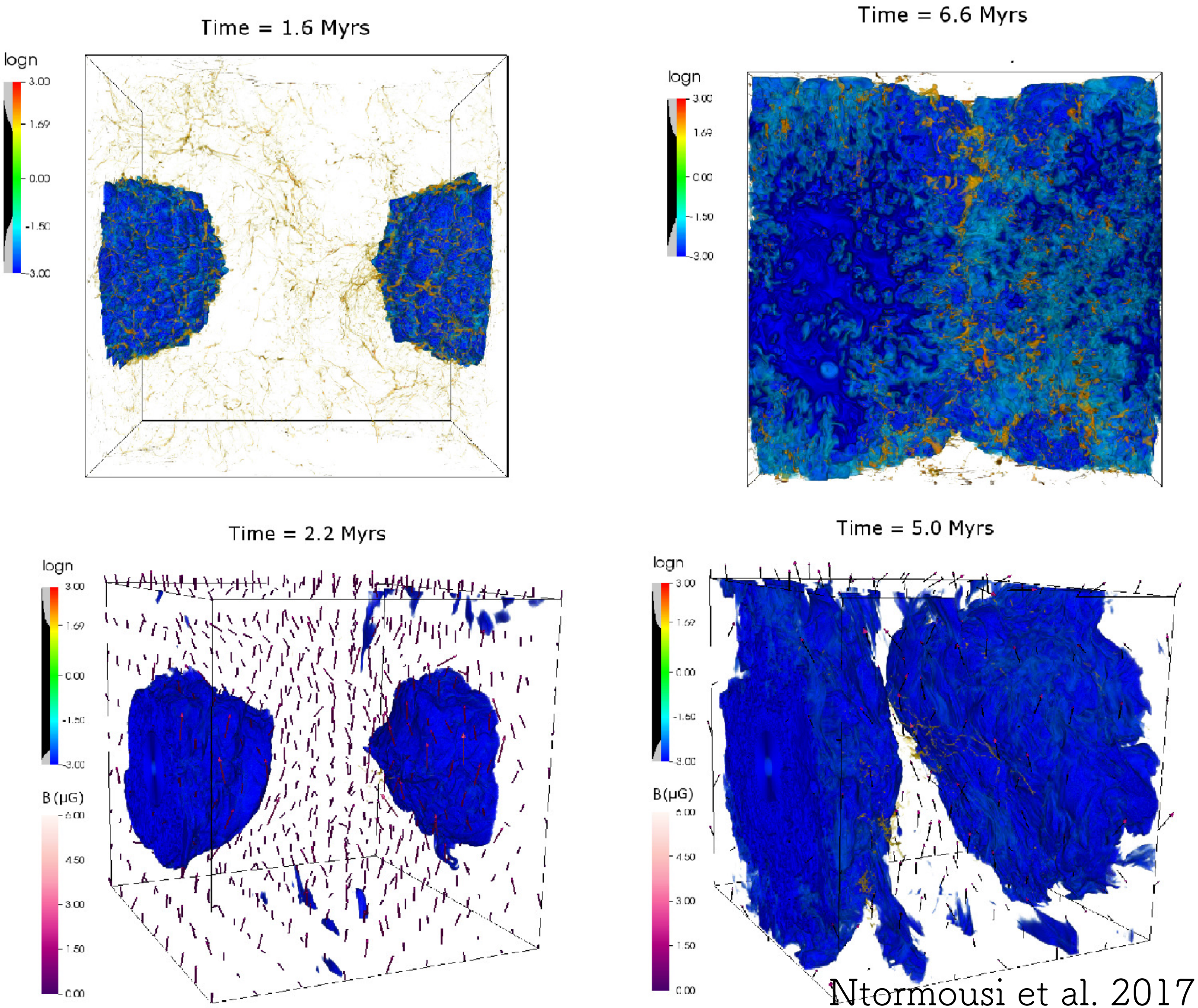

Ntormousi et al. 2017

Multiple-collision models

Network of Expanding Shells

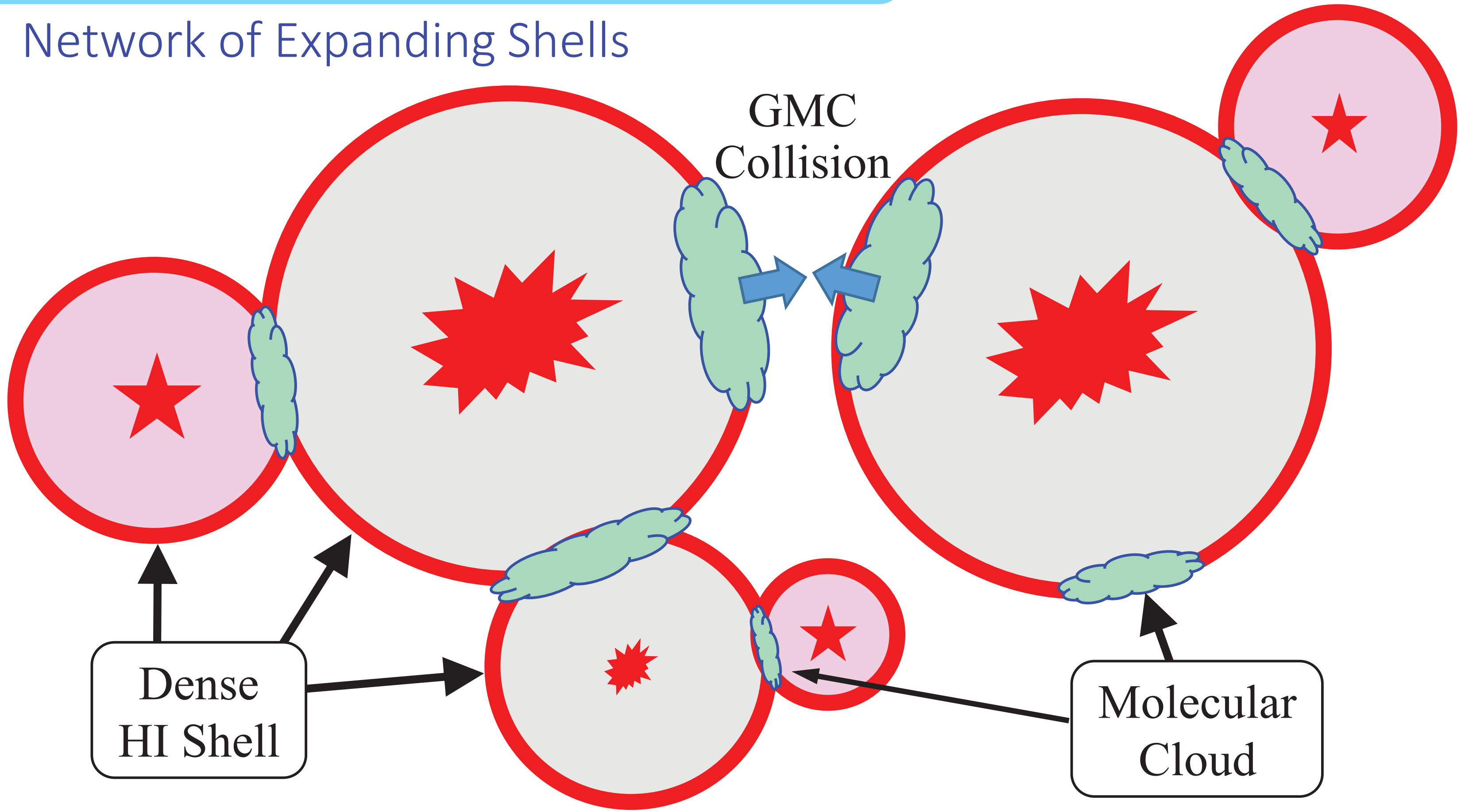

Inutsuka et al. 2015

Multiple-collision models

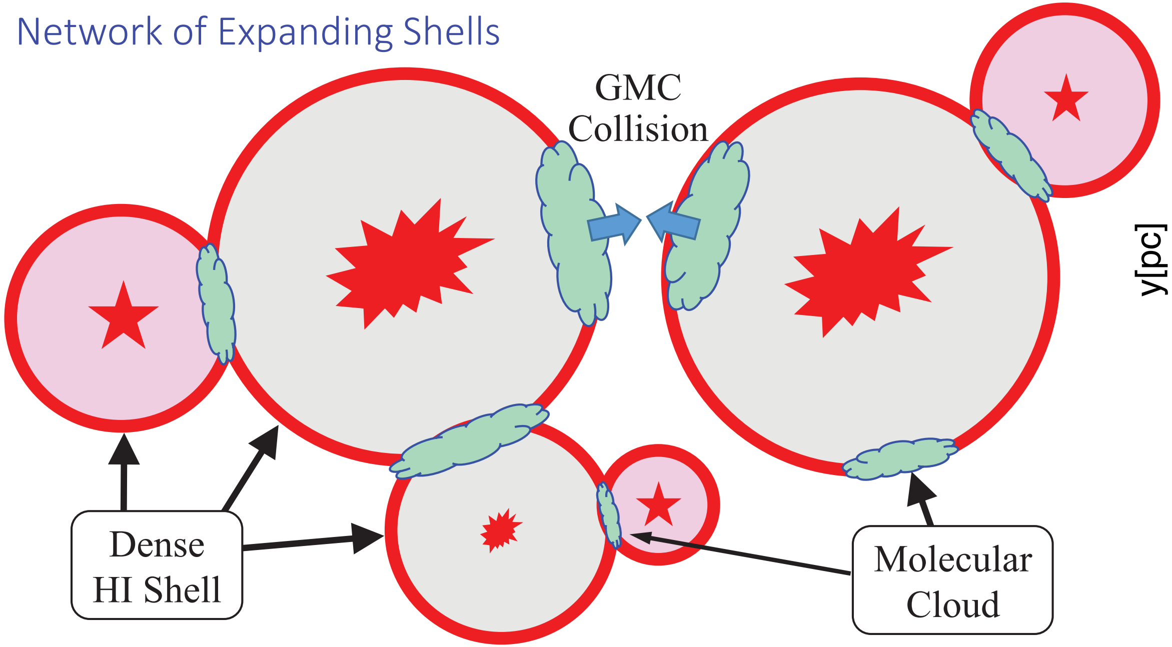

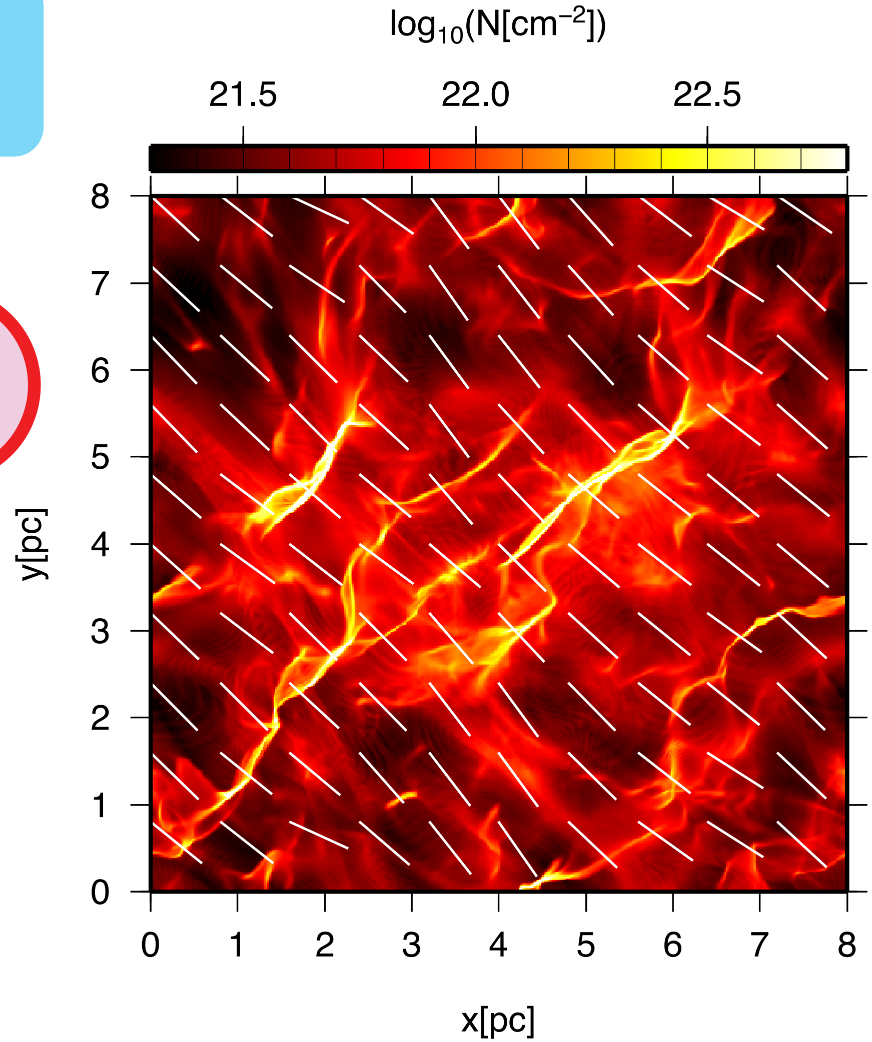

Inutsuka et al. 2015

Observational tests

We need better predictions from models: most predict similar magnetic field geometries, if they make predictions at all

We also need more Zeeman and Faraday rotation measurements of the CNM

The multiple-collision model broadly matches many of the observations, but that doesn't preclude the others doing the same

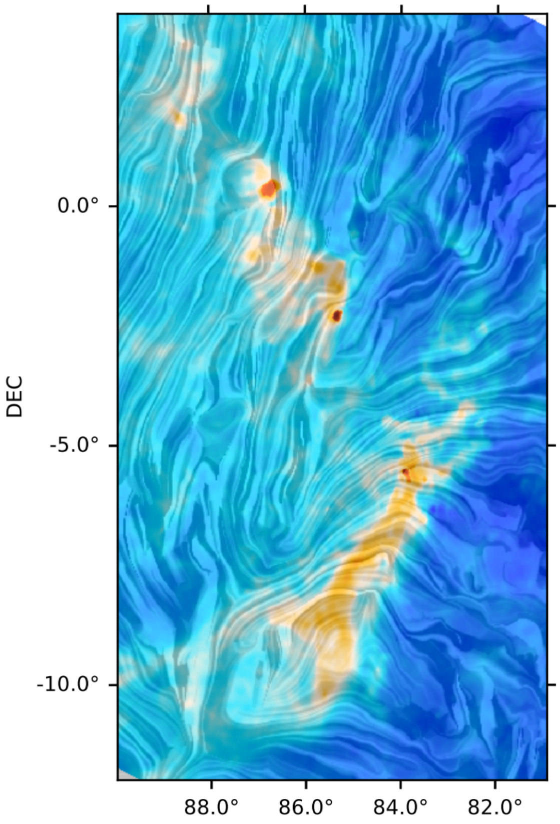

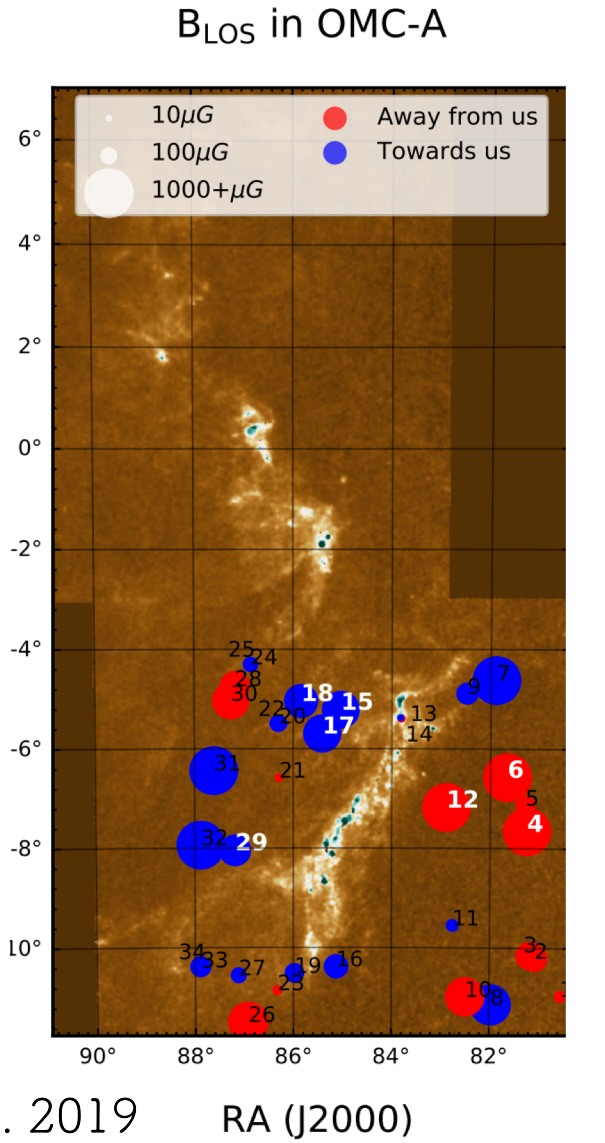

Tahani et al. 2019

Collapsing molecular clouds

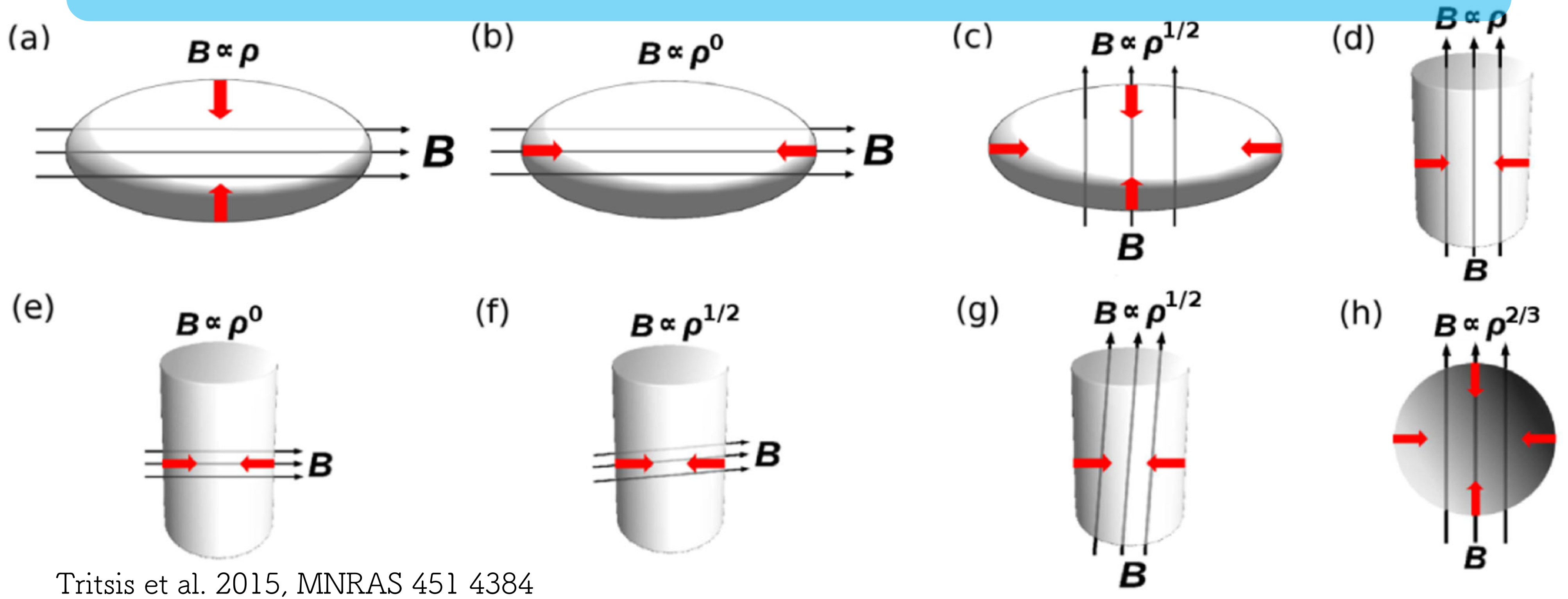

Tritsis et al. 2015, MNRAS 451 4384

Does magnetic field strength increase with gas density?

(I.e.: is the field being compressed by gravitational collapse?)

Strong-field case (e.g. Mouschovias & Ciolek 1999)

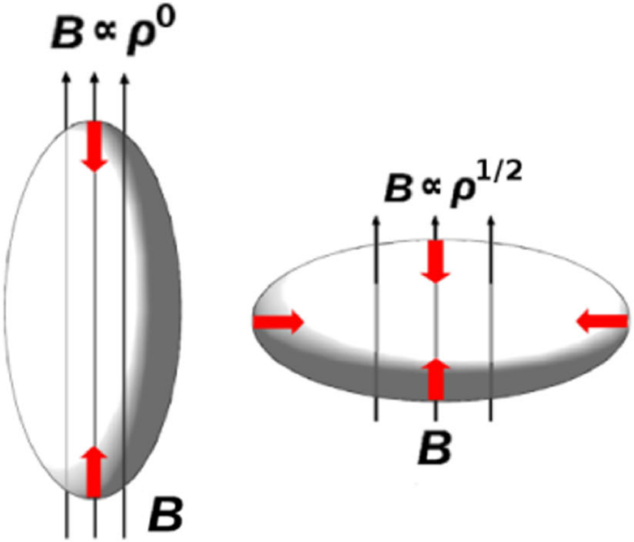

1) Cloud collapses freely along field lines (B constant)
2) Cloud collapses across field lines ($B \sim \rho^{1/2}$)

Weak-field case (Mestel 1966):

Homologous cloud collapse: $B \sim \rho^{2/3}$

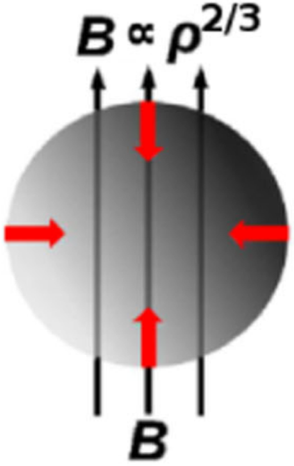

$B \sim \rho^{2/3}$ is unique to spherically-symmetric collapse

Crutcher relation

$$B = \begin{cases} B_0 & (n < n_0) \\ B_0 \left(\frac{n}{n_0}\right)^{\kappa} & (n > n_0) \end{cases}$$

Crutcher et al. 2010:

B constant below 300 cm^{-3}

B ~ $\rho^{0.65}$ above 300 cm^{-3}

Problem solved? Not really:

a) Reanalyses have found indices in the range 0.5-0.72 (Tritsis et al. 2015; Jiang et al. 2020), with the transition density not well-constrained.

b) Clouds aren't collapsing homologously on these scales.

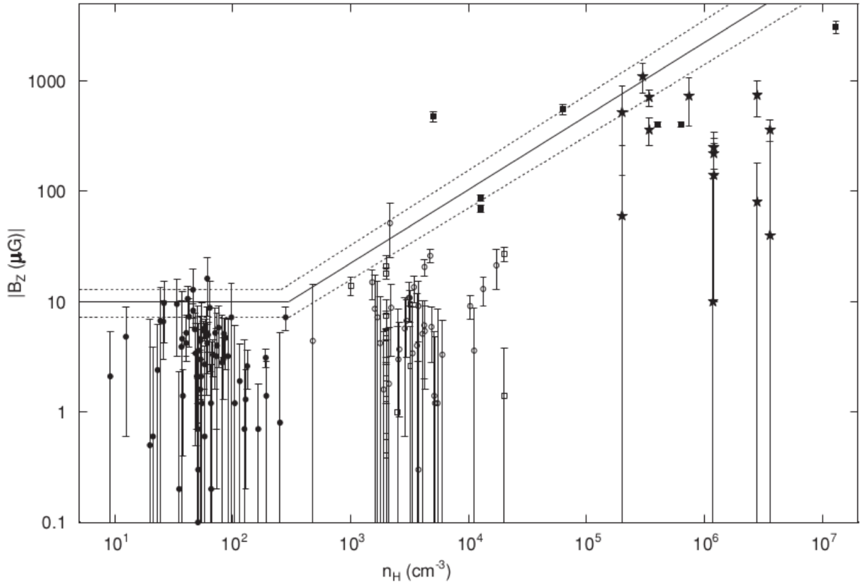

Crutcher et al. 2010, ApJ 725 466

Magnetic fields and cloud structure formation

- In the weak-field (initially supercritical) case, magnetic fields follow gas density structures
- In the strong-field (initially subcritical) case, gas density structures run parallel to the field at low column density, and perpendicular at high column density.
- The transition is <u>somehow</u> related to the transition to gravitational instability

Weak initial field

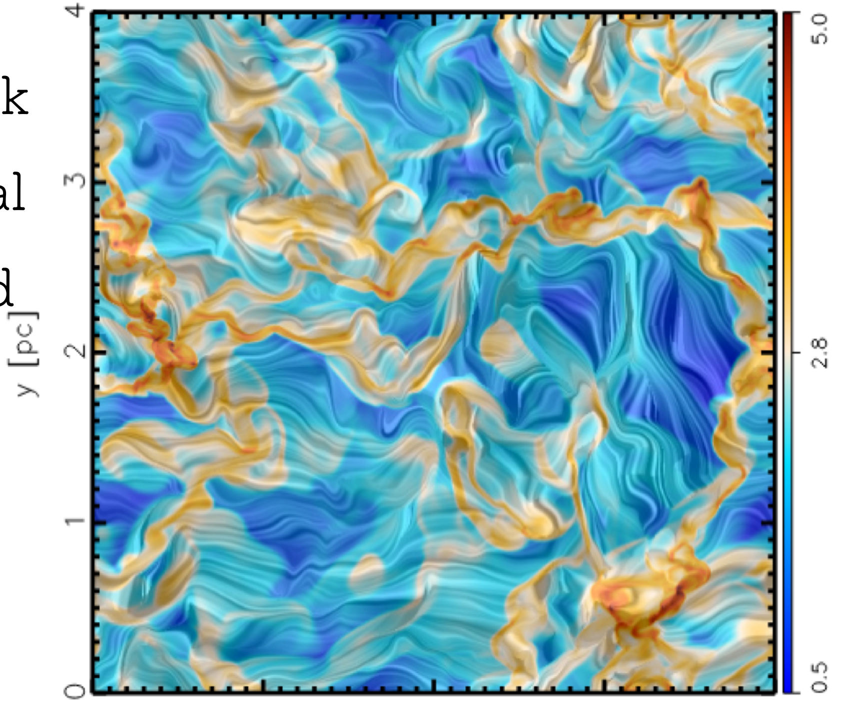

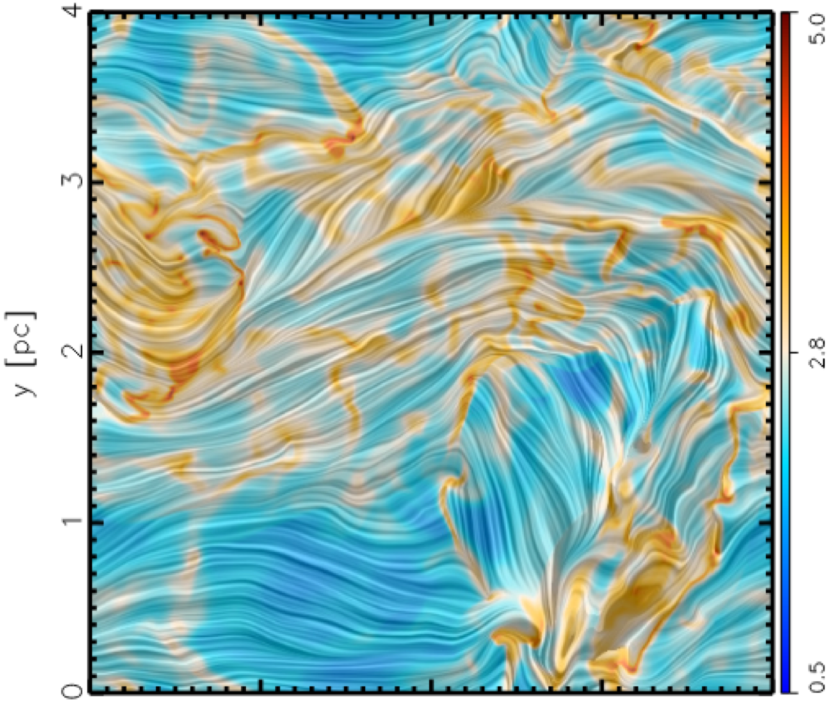

Strong initial field

Soler et al. 2013, Soler & Hennebelle 2017

Magnetic fields and cloud structure formation

- In the weak-field (initially supercritical) case, magnetic fields follow gas density structures
- In the strong-field (initially subcritical) case, gas density structures run parallel to the field at low column density, and perpendicular at high column density.
- The transition is <u>somehow</u> related to the transition to gravitational instability

Taurus Molecular Cloud

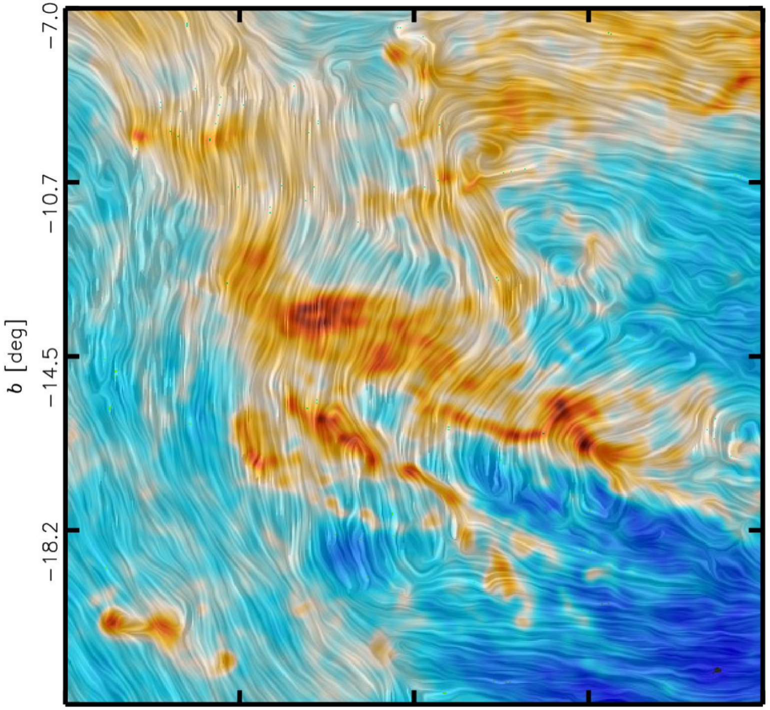

Planck Int. XXV 2016, A&A 586 A138

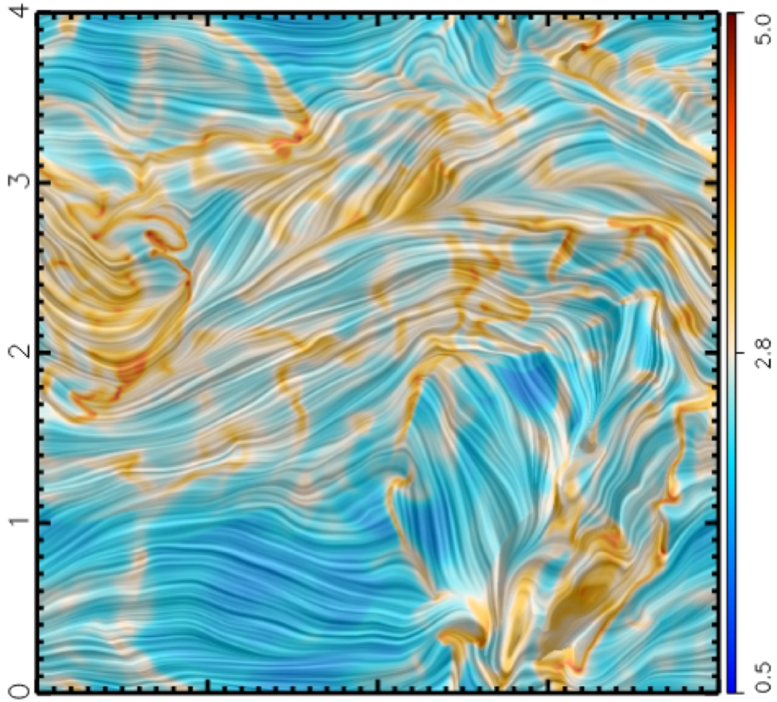

Strong initial field

Soler et al. 2013, Soler & Hennebelle 2017

The Histogram of Relative Orientations

A quantitative measure of how the angle between magnetic field and density structure changes as a function of (column) density (Soler et al. 2013)

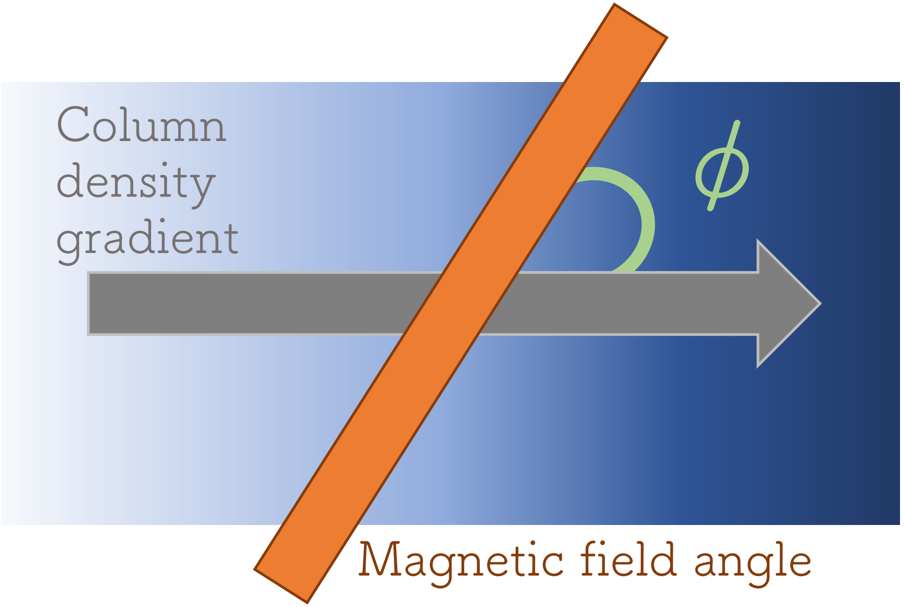

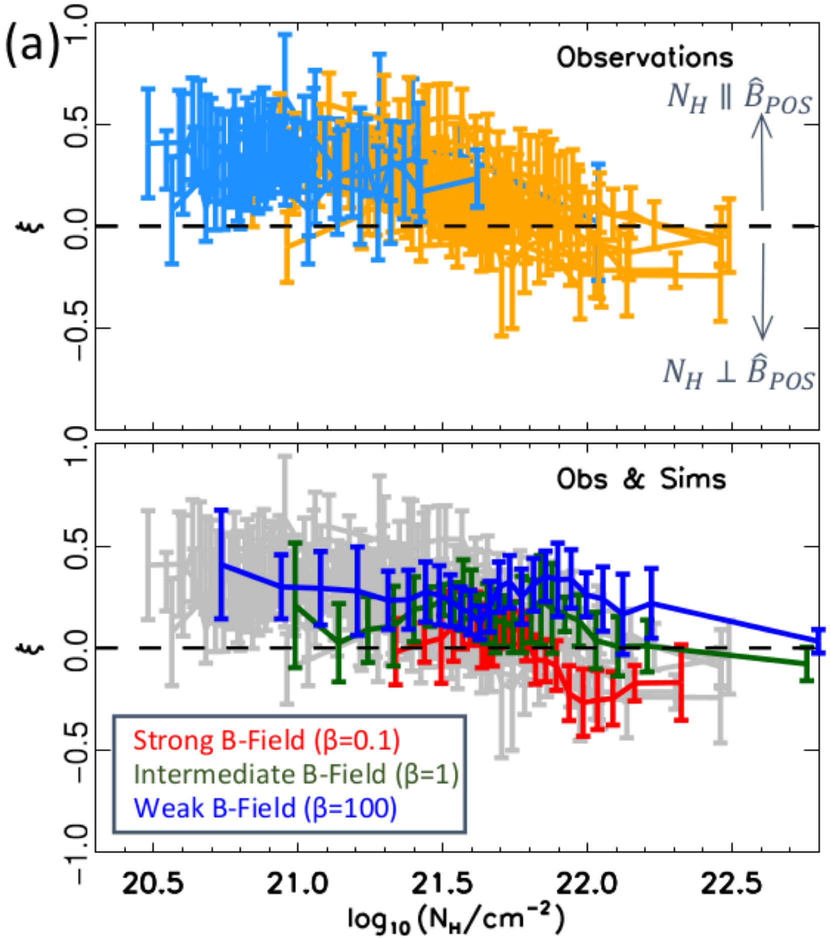

Planck Collaboration 2016 A&A 586 A138

The Histogram of Relative Orientations

Shape factor:

$$\xi = \frac{A_c - A_e}{A_c + A_e}$$

A_c = number of measurements where $|\phi| \leq 22.5^\circ$

A_e = number of measurements where $|\phi| \geq 67.5^\circ$

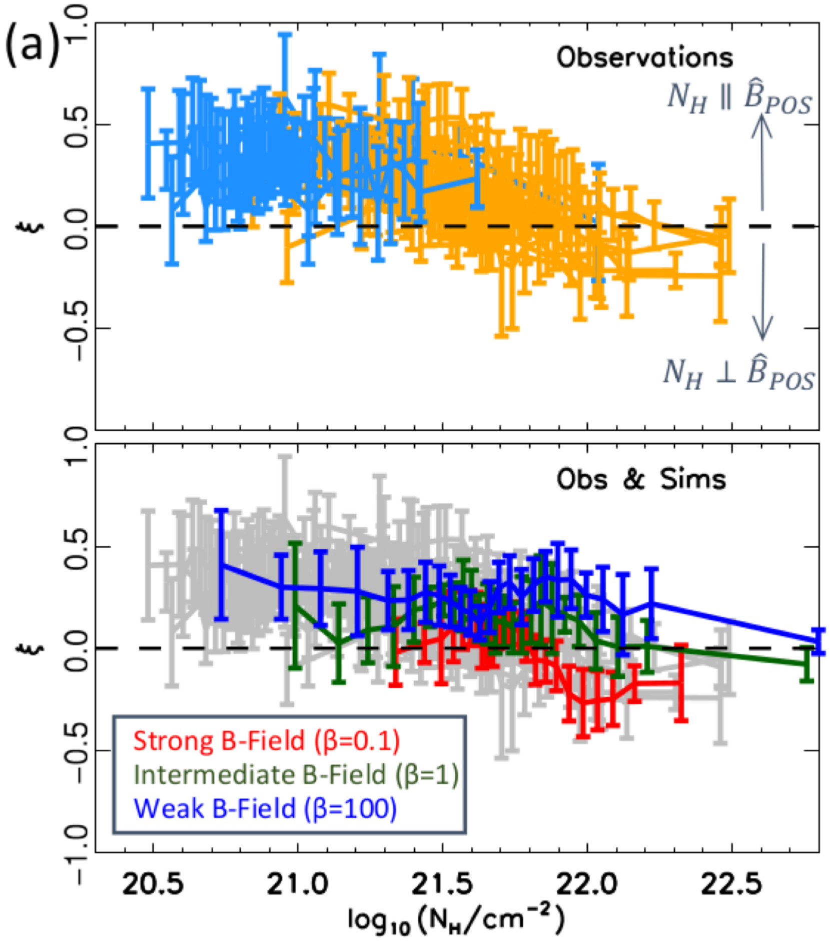

Planck Collaboration 2016 A&A 586 A138

The Histogram of Relative Orientations

A quantitative measure of how the angle between magnetic field and density structure changes as a function of (column) density (Soler et al. 2013)

However: different simulations produce radically different transition densities, and transitions can be created even in simulations without self-gravity (e.g. Barreto-Mota et al. 2021)

We need better observational constraints!

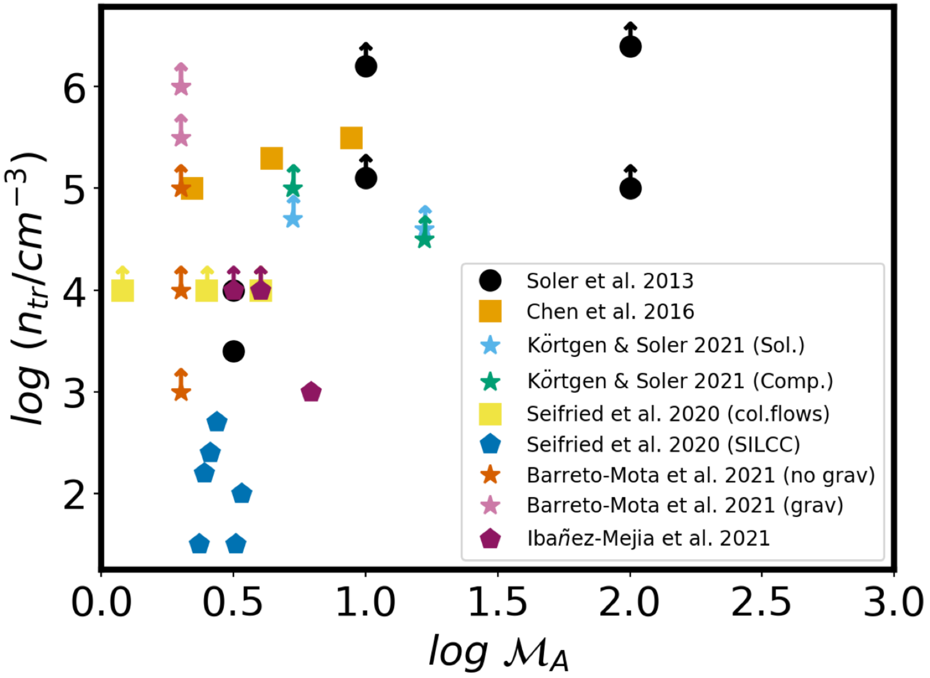

Pattle, Fissel, Tahani, Liu & Ntormousi
PP7 Proceedings, arXiv:2203.11179

The Davis-Chandrasekhar-Fermi Method

Deviation in angle from the mean field direction is taken to be the result of distortion of the field by small-scale non-thermal motions and so to scale with the Alfvén Mach Number (Chandrasekhar & Fermi 1953, Davis 1951).

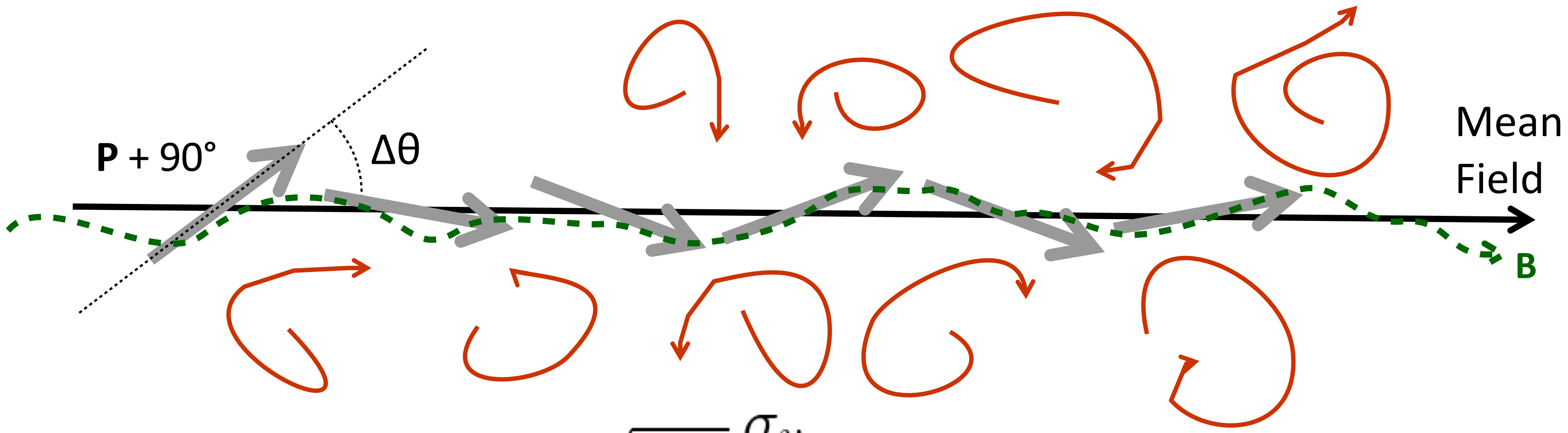

$$B_{\rm pos} = Q\sqrt{4\pi\rho}\,\frac{\sigma_v}{\sigma_\theta}$$

(cf. Crutcher et al. 2004)

Mass-to-flux ratio: $\lambda = 7.6\times10^{21}\frac{N(\mathrm{H_2})\,(\mathrm{cm^{-2}})}{B_{pos}\,(\mu\mathrm{G})}$ Alfvén velocity: $\vec{v}_A = \frac{\vec{B}_0}{\sqrt{4\pi\rho_0}}$ Alfvén Mach N°: $\mathcal{M}_A \sim \frac{\sigma_{\rm NT}}{v_A}$

The Davis-Chandrasekhar-Fermi Method

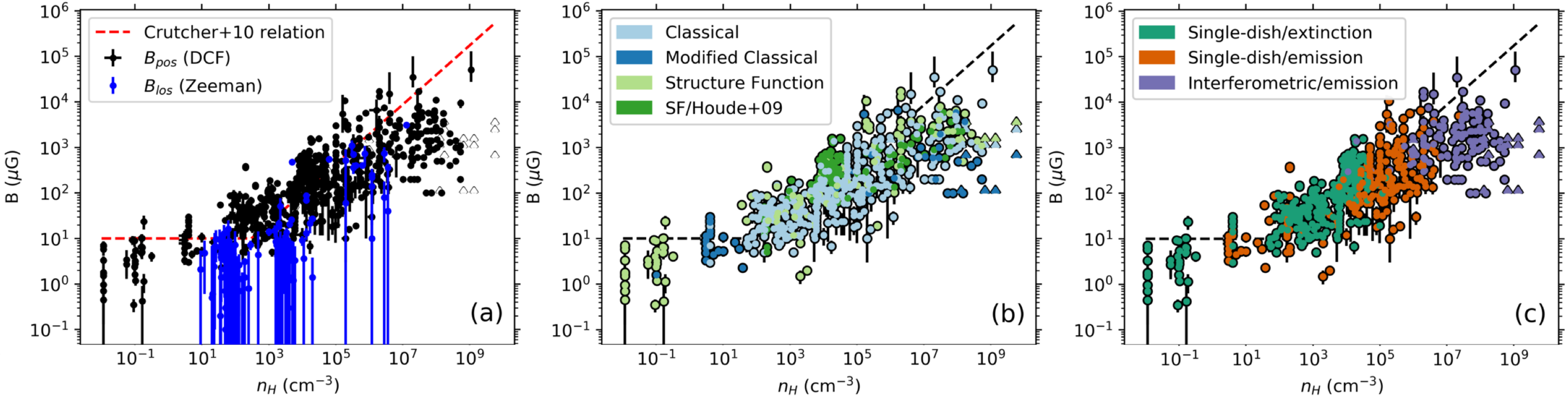

Structure-Function modifications:

- Falceta-Goncalves+08
- Hildebrand+09
- Houde+09
- Lazarian+20

Recent reanalyses:

- Junhao Liu+21a,b,22
- C.-Y. Chen+22
- Pattle+22

More radical reformulations:

- Skalidis & Tassis 21
- P.S. Li+21

At 2001-2021 level of calibration: DCF scales well with Zeeman, but appears to on average overestimate field strength by a factor ~ 3 – 5

Pattle, Fissel, Tahani, Liu & Ntormousi
PP7 Proceedings, arXiv:2203.11179

Both HROs and DCF suggest that molecular clouds are subcritical on large scales

Region	$\lambda_{\rm obs}^{\rm DCF}$	$\lambda_{\rm obs}^{\rm DCF+SF}$
Taurus	0.4 ± 0.4	0.2 ± 0.1
Ophiuchus	0.4 ± 0.4	0.2 ± 0.2
Lupus	0.3 ± 0.2	0.2 ± 0.1
Chamaeleon-Musca .	0.4 ± 0.3	0.2 ± 0.2
Corona Australis (CrA)	0.9 ± 0.9	0.3 ± 0.3
Aquila Rift	0.3 ± 0.2	0.1 ± 0.1
Perseus	0.3 ± 0.3	0.2 ± 0.2
IC 5146	0.5 ± 0.3	0.3 ± 0.2
Cepheus	0.3 ± 0.1	0.1 ± 0.0
Orion	0.3 ± 0.3	0.2 ± 0.2

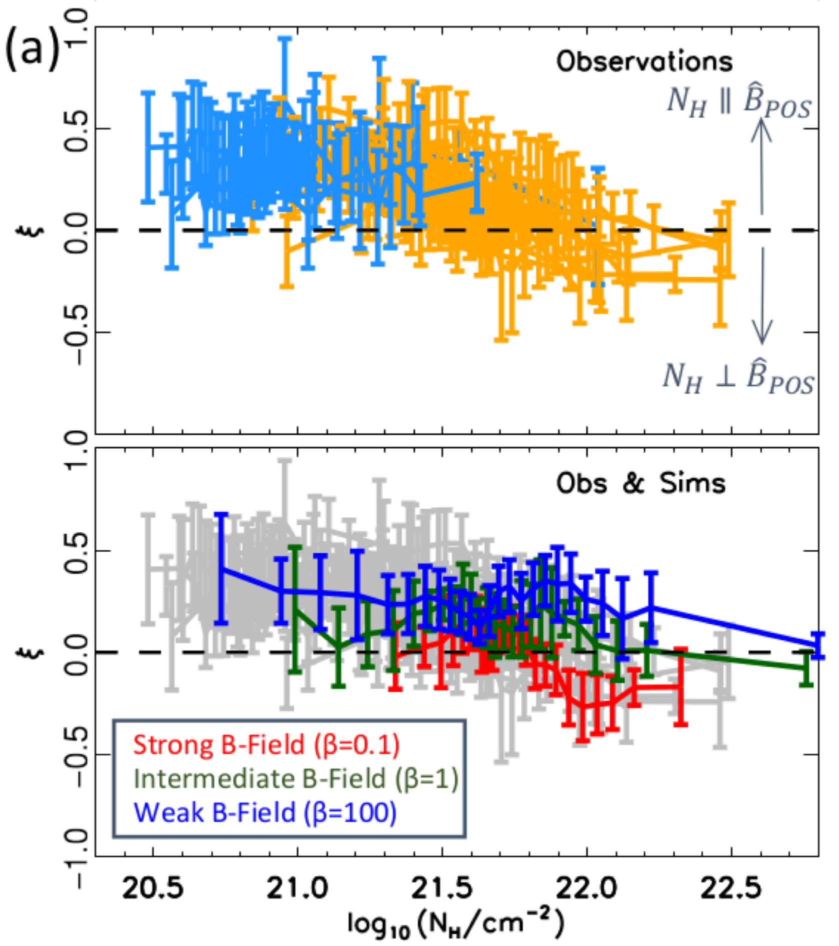

Planck Collaboration 2016 A&A 586 A138

Magnetic fields in low-mass filaments

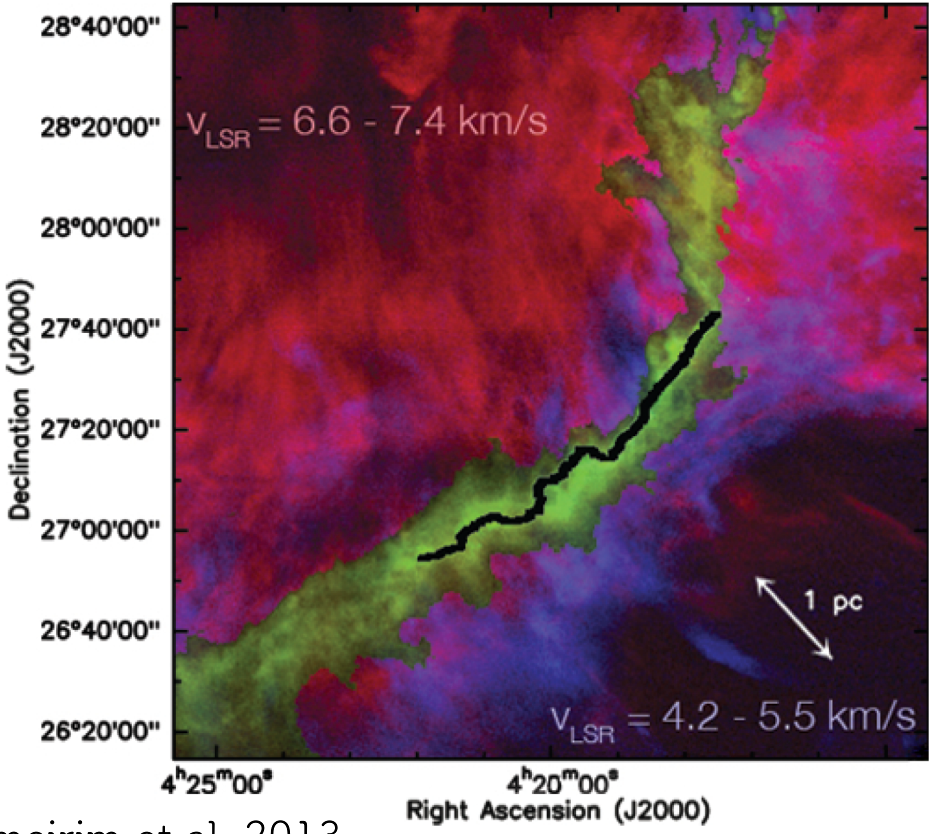

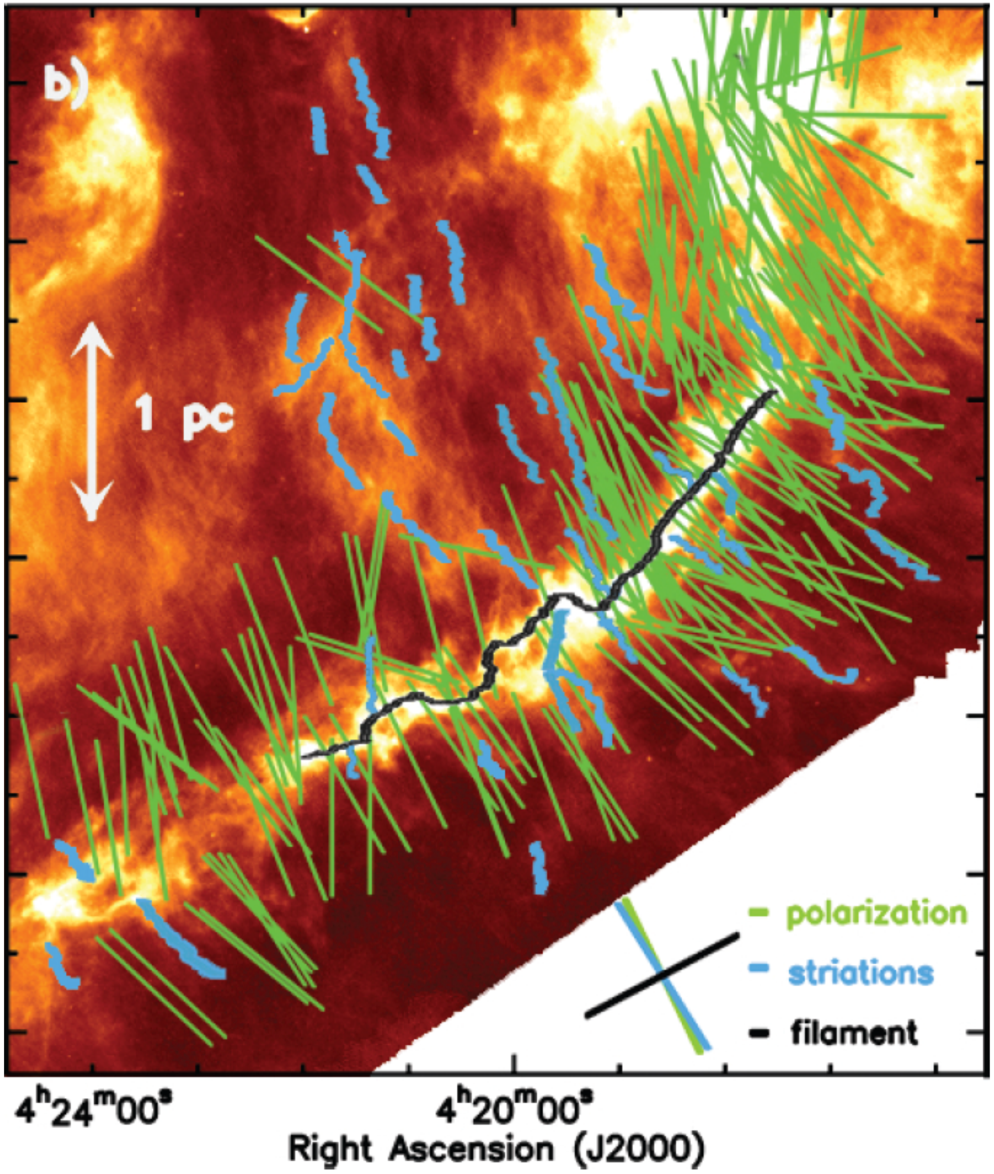

Palmeirim et al. 2013

Perseus NGC 1333

Doi et al. 2020

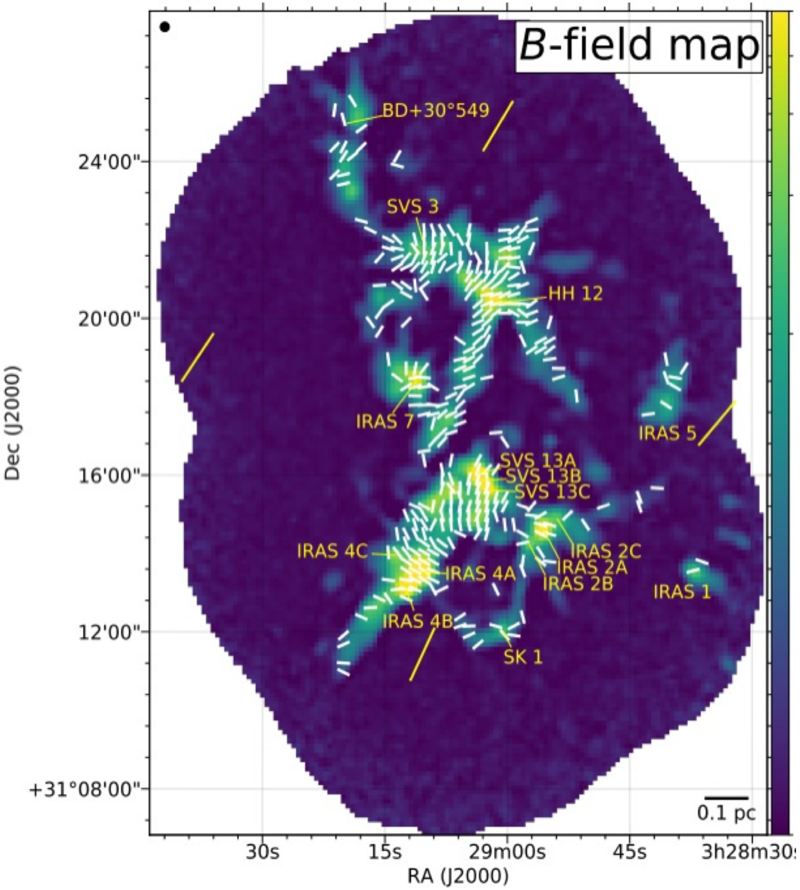

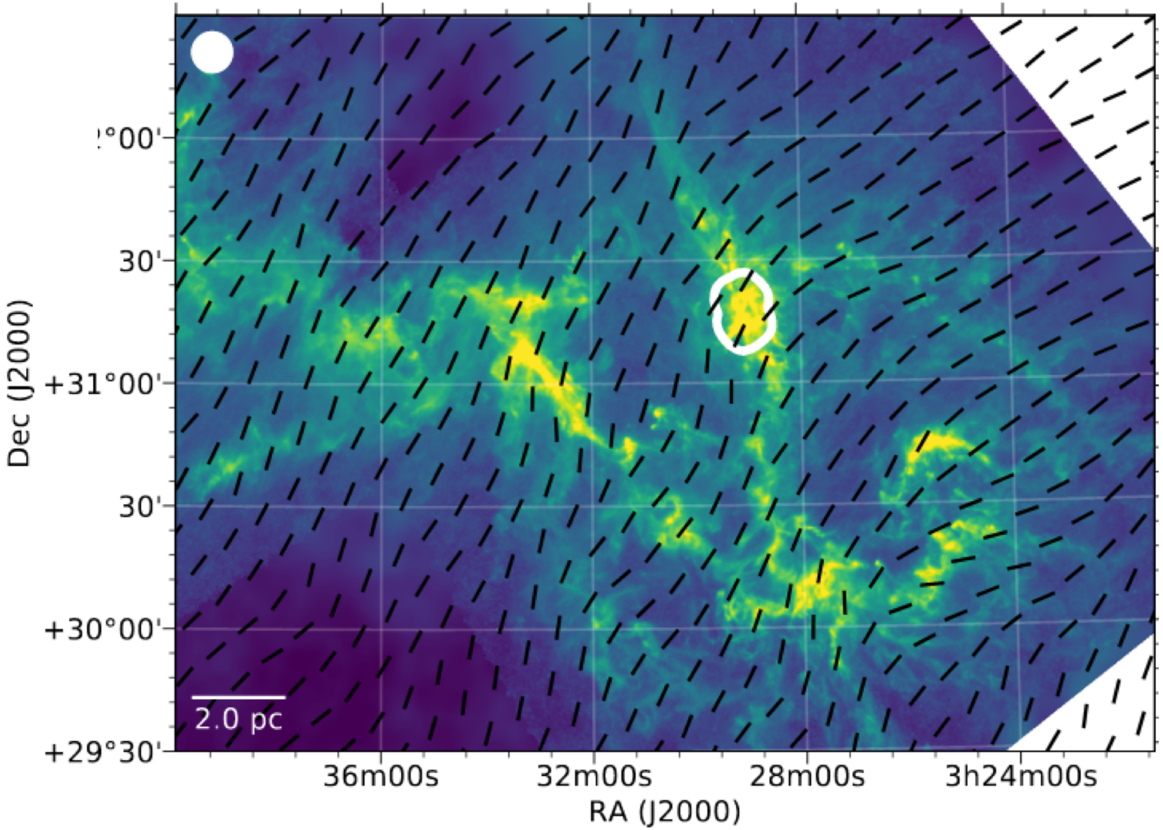

Low-mass filamentary star formation at a distance ~ 300 pc. Observations show reasonable agreement between filamentary and large-scale magnetic field directions in north of region; significant discrepancies exist in the south.

Perseus NGC 1333

A range of field/filament orientations in projection: statistically consistent with the magnetic field being perpendicular to the density structures in 3D.

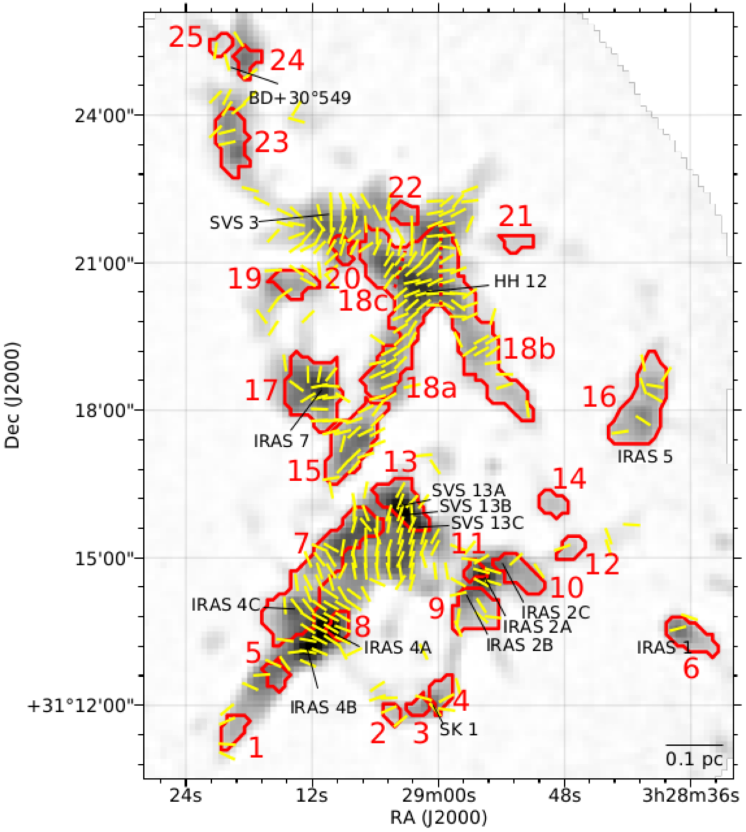

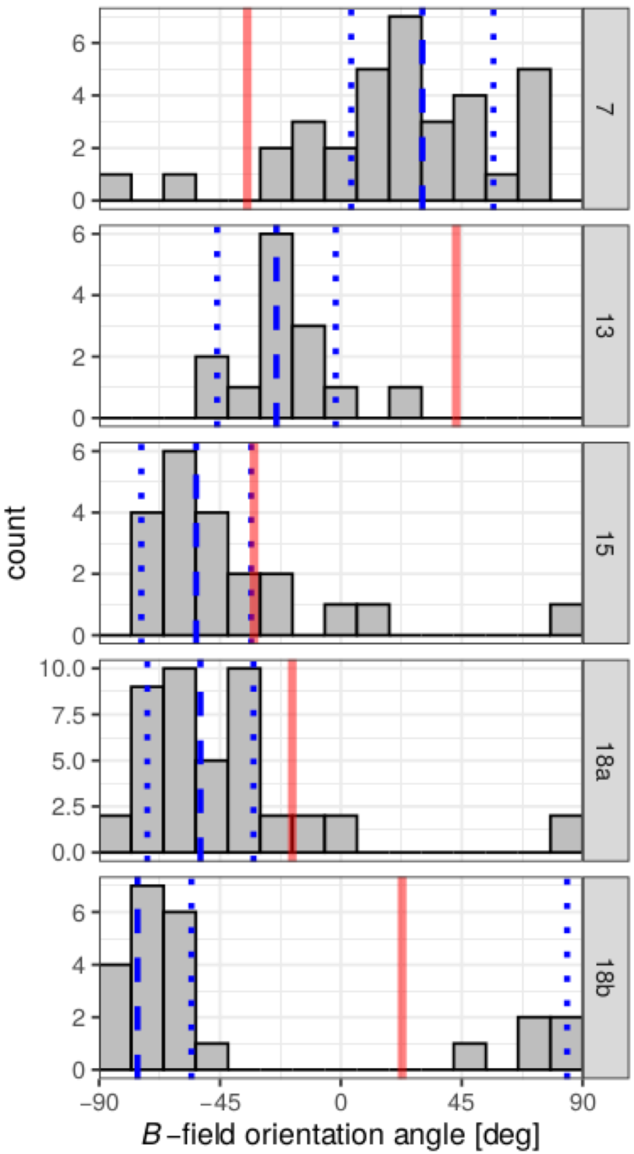

Doi et al. 2020

Magnetic fields in hub-filament systems

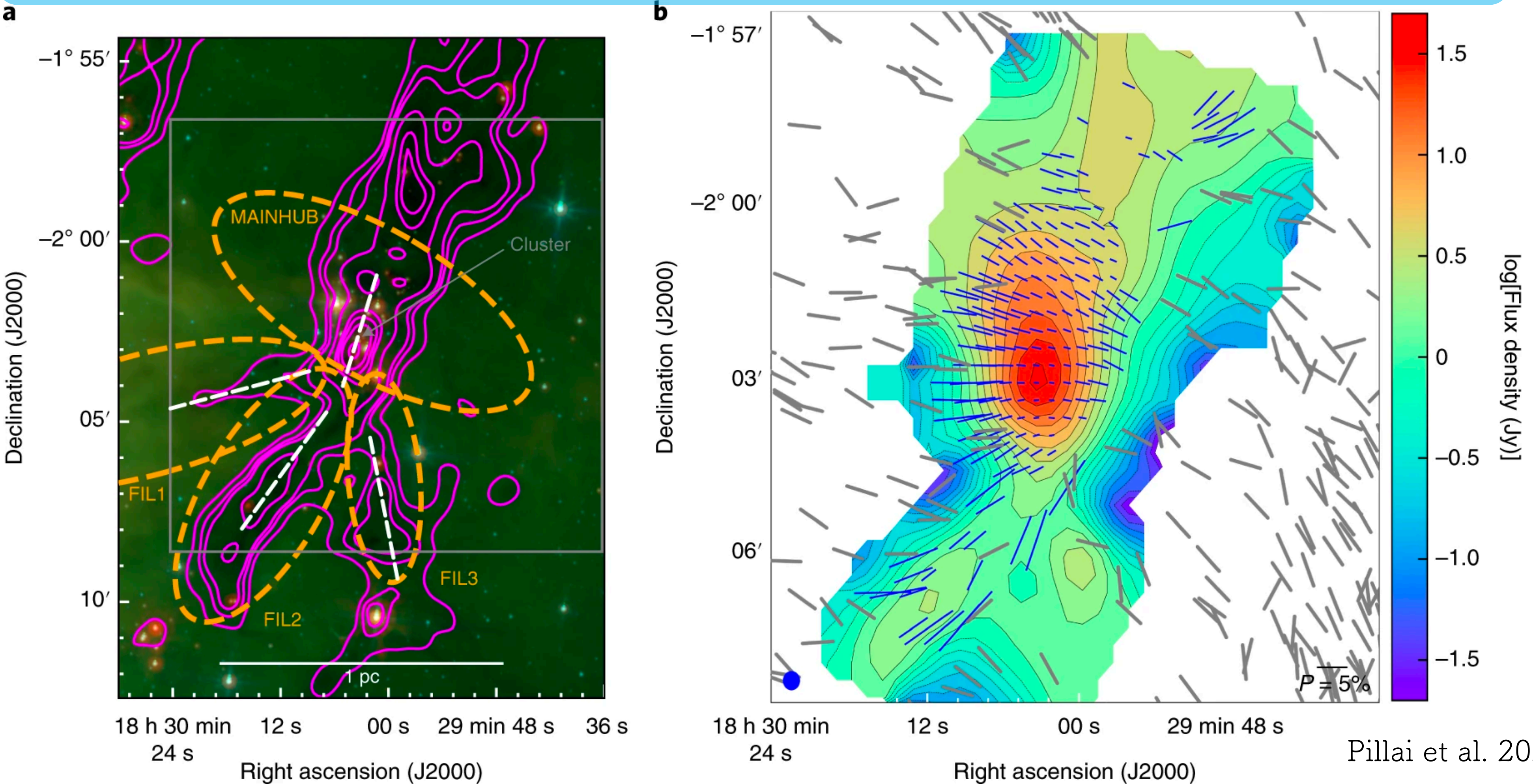

Pillai et al. 2020

NGC 6334: Subfilaments

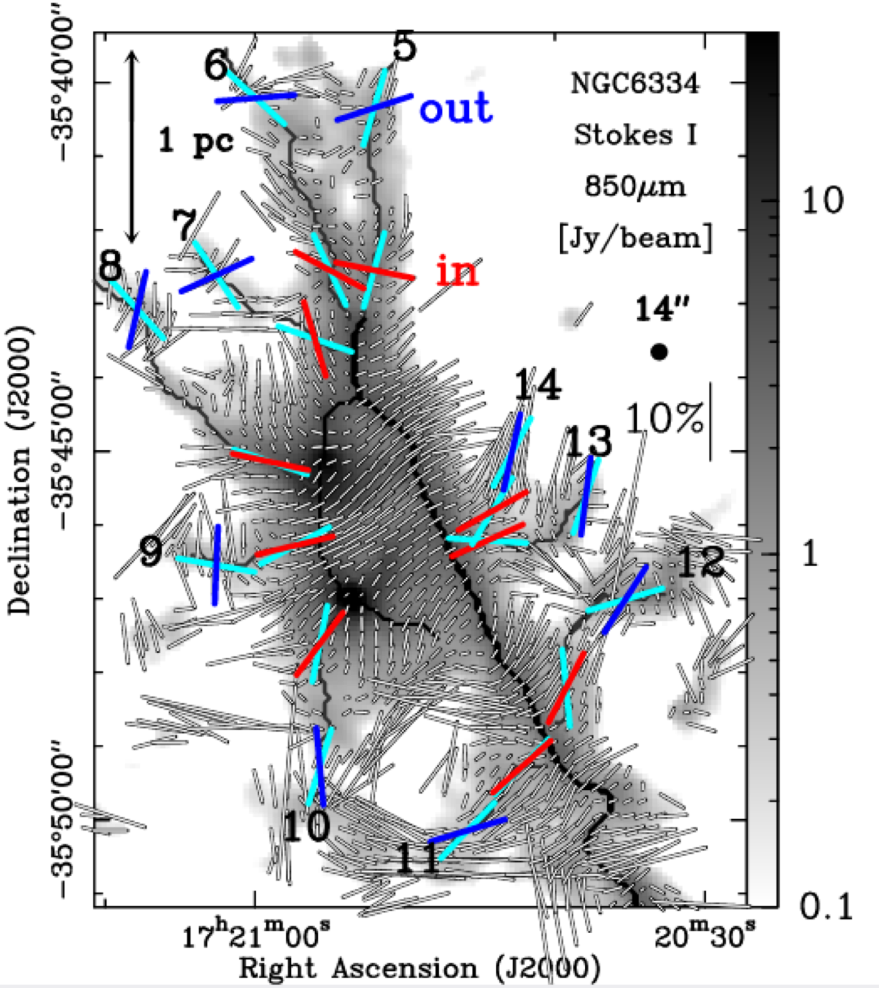

Field rotates from being mostly perpendicular to mostly parallel as the sub-filaments merge with the ridge and hubs.

The sub-filaments are magnetically supercritical at their far ends, becoming magnetically subcritical near the ridge and hubs: **low- and high-mass star formation modes in the same cloud?**

Arzoumanian et al. 2021

Prestellar Cores

A gravitationally bound over-density which will go on to form a single star or stellar system

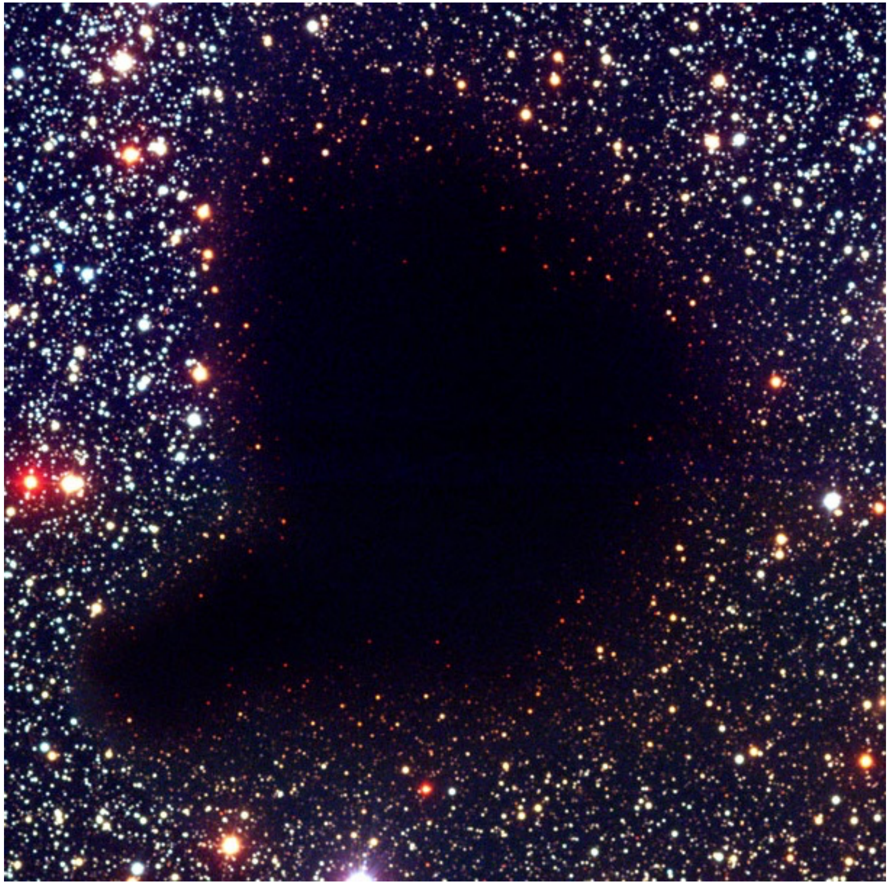

Alves et al. 2001

Jeans Mass

$$M_{\rm J} = \frac{4\pi}{3}\frac{c_{\rm S}^3}{G^{3/2}\rho^{1/2}}$$

An object with $M >> M_J$ is a strong candidate for magnetic support

If non-thermal motions can be taken to represent a hydrostatic pressure (the microturbulent assumption; Chandrasekhar 1951), then $c_s \rightarrow (c_{\rm S}^2 + \sigma_{v,\rm NT}^2)^{0.5}$

Ambipolar diffusion

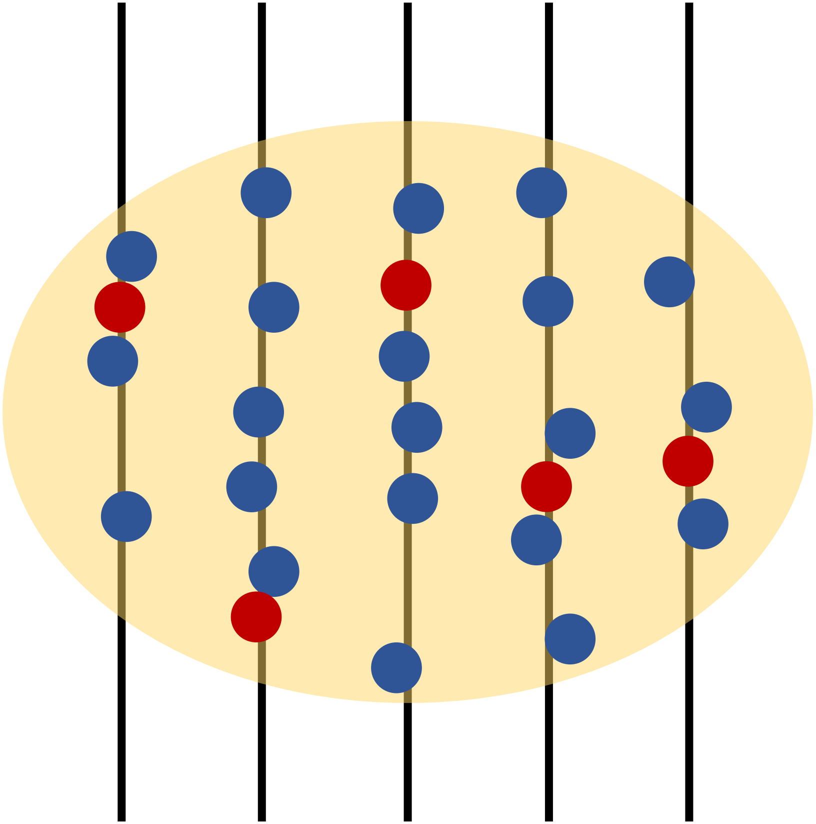

An initially magnetically subcritical, flux-frozen starless core

Ambipolar diffusion

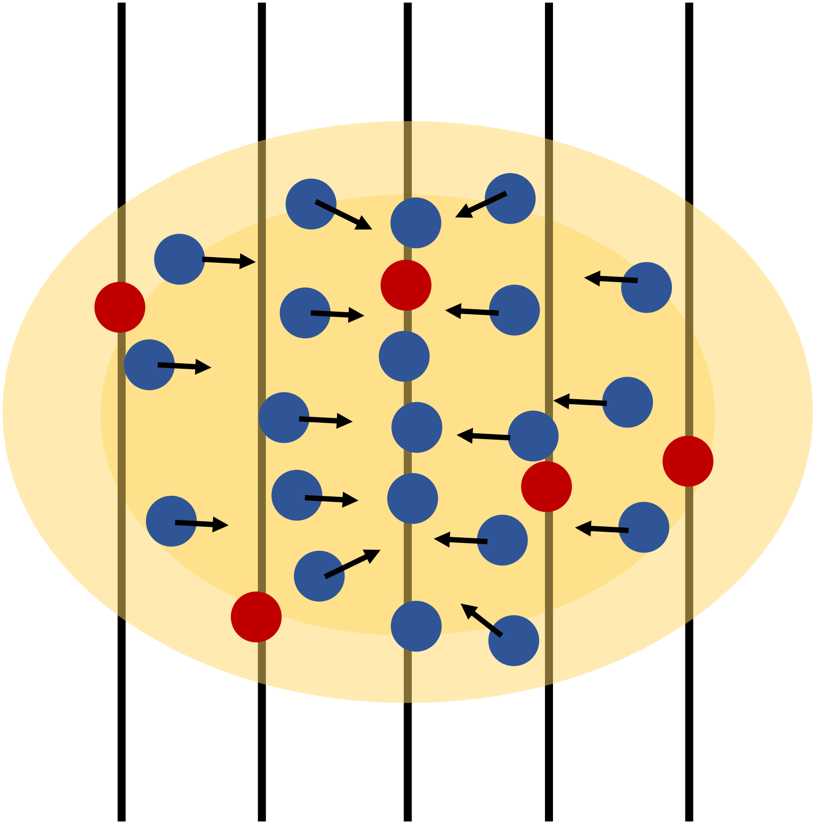

The ionization fraction drops, so the ion-neutral collision rate reduces

Neutrals start to drift inwards under gravity. Ions stay frozen to the magnetic field

Ambipolar diffusion

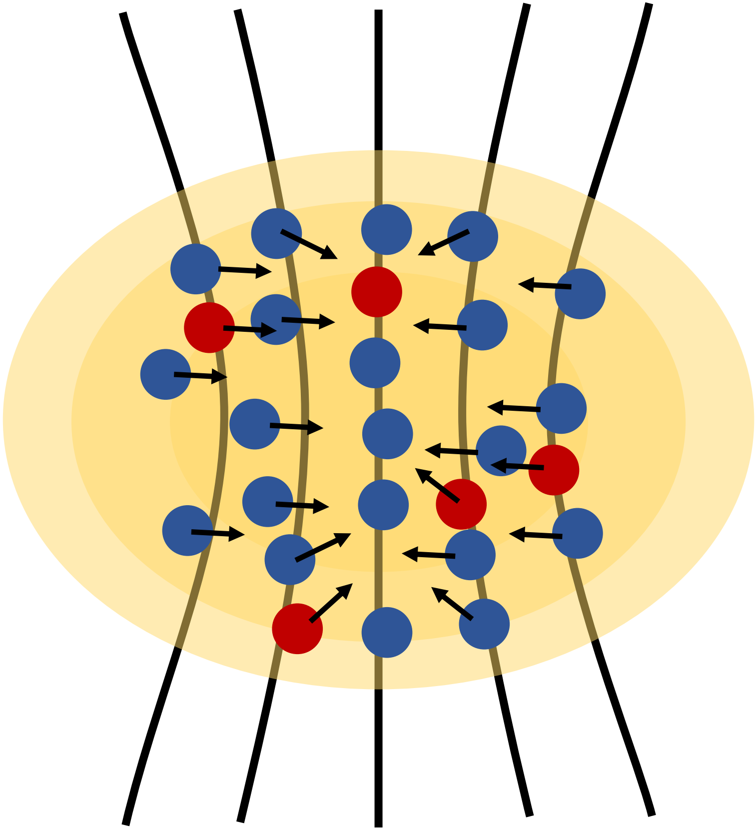

Once the core becomes magnetically supercritical, the ions fall inward too, dragging the field with them

This creates a characteristic **hourglass morphology**

This indicates a magnetic field that used to be dynamically important

Ambipolar diffusion timescale

Ion-neutral coupling holds while $t_{AD} > t_{ff}$

Freefall time: $$t_{ff} = \left(\frac{3\pi}{32G\rho}\right)^{0.5}$$

Ambipolar diffusion (ion-neutral drift) timescale:

$$t_{AD} = \frac{L^2}{\lambda_{AD}} \qquad \lambda_{AD} \propto \frac{B^2}{x_i n_n^2} \qquad x_i \propto \sqrt{\frac{\zeta}{n_n}}$$

Observed magnetic fields in prestellar cores

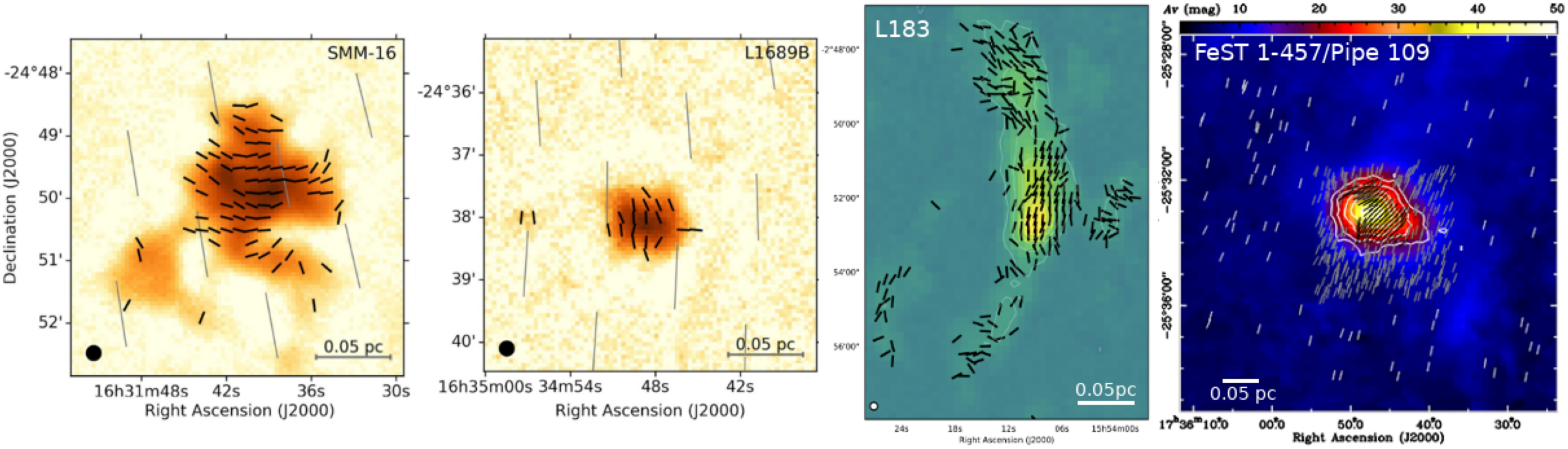

Magnetic fields are typically consistent with being parallel to the core minor axis in 3D, suggesting that cores preferentially collapse along the magnetic field direction (cf. Basu 2000). However, they generally do not show clear hourglasses

L-R: Pattle et al. 2021, Karoly et al. 2020, Alves et al. 2014

Hourglass fields in protostellar cores

Low-mass protostellar core:
NGC 1333 IRAS 4A

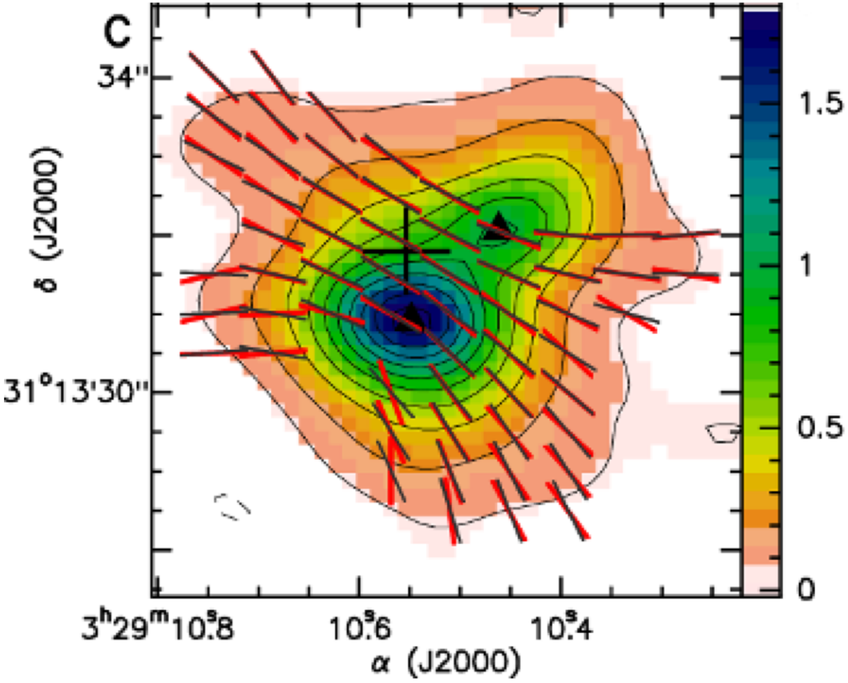

Girart et al. 2006

Massive cluster-forming core:
G240.31+0.07

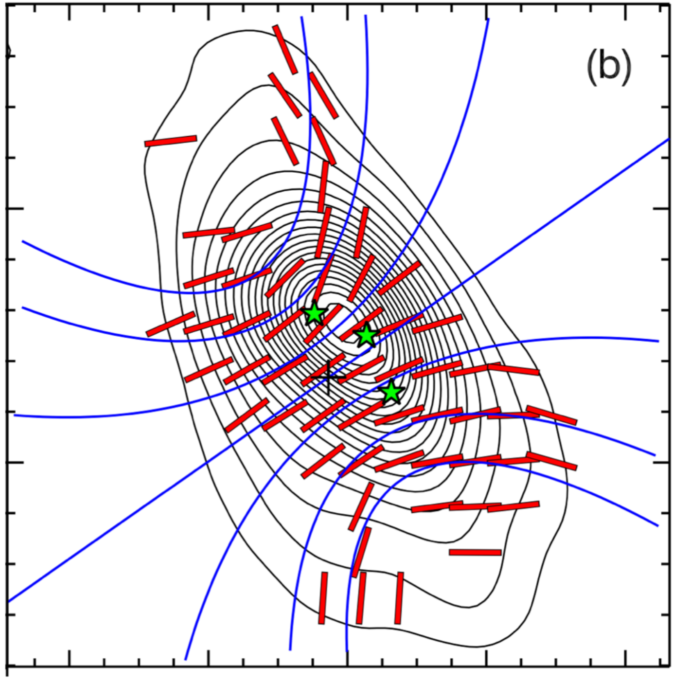

Qiu et al. 2014

Measuring μ_Φ in core envelopes with HINSA

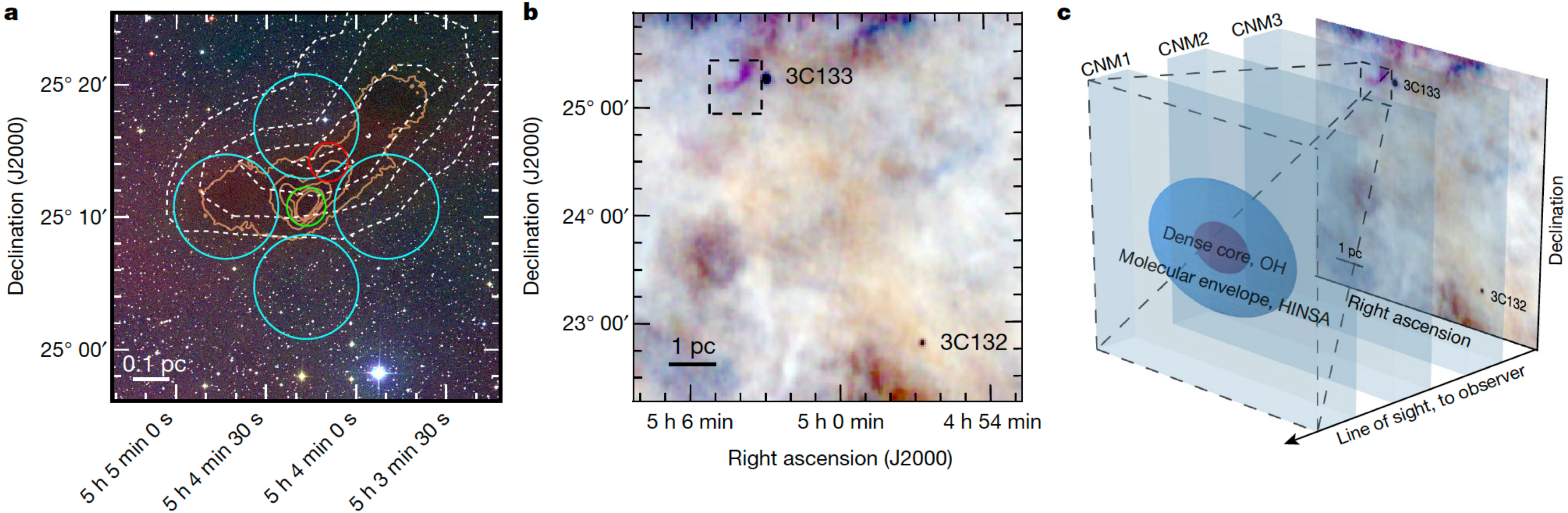

HINSA: HI In Self-Absorption

Can measure the Zeeman effect in density regimes not accessible in emission

Ching et al. 2022

Measuring μ_Φ in core envelopes with HINSA

Tracer/cloud	λ^c
H I_{3C132}/CNM1	0.18 ± 0.07
H I_{3C133}/CNM1	0.10 ± 0.04
HINSA/envelope	3.5 ± 0.3
OH/core	2.5 ± 0.4

Suggests that L1544 formed from gas that was already supercritical

Ching et al. 2022

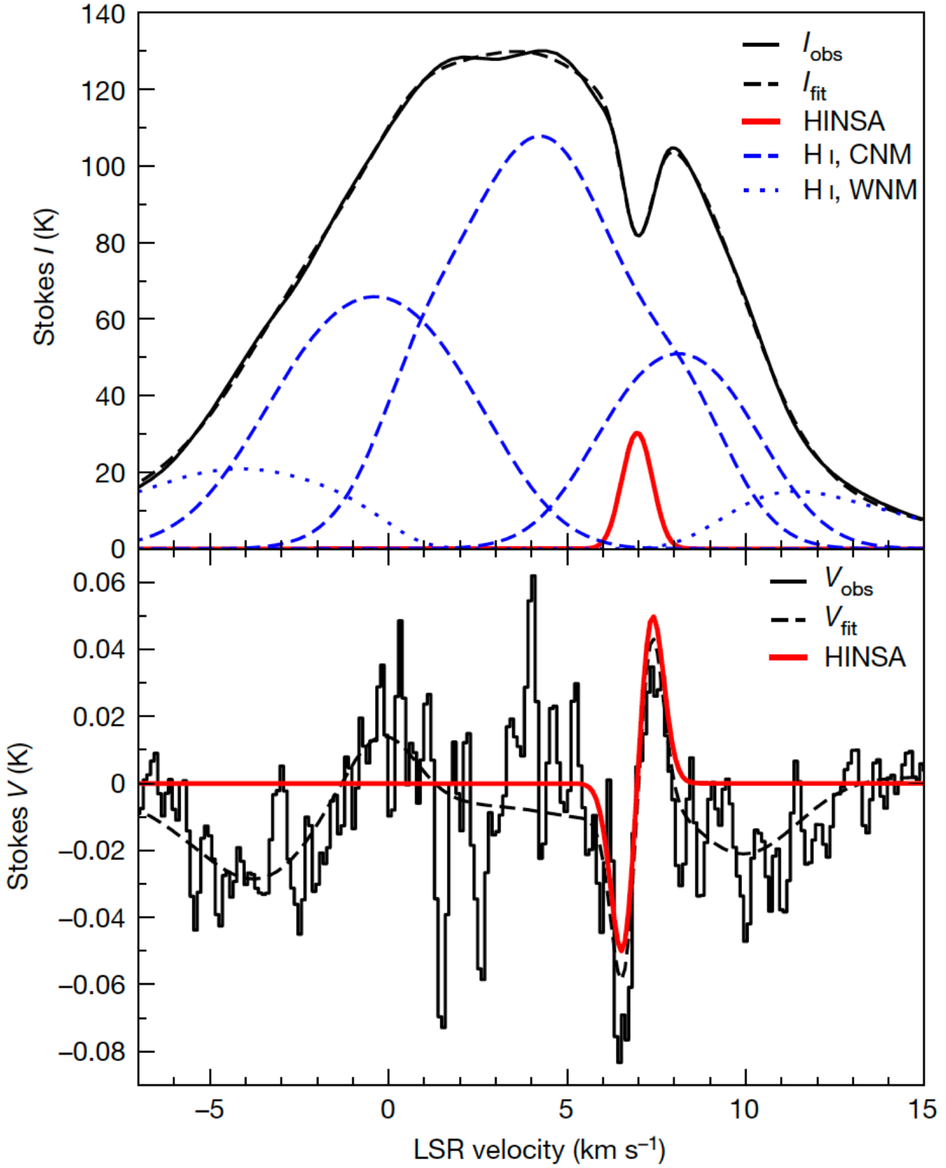

High-mass prestellar cores?

Candidates typically identified through Jeans Mass arguments: large magnetic fields implicitly required for support

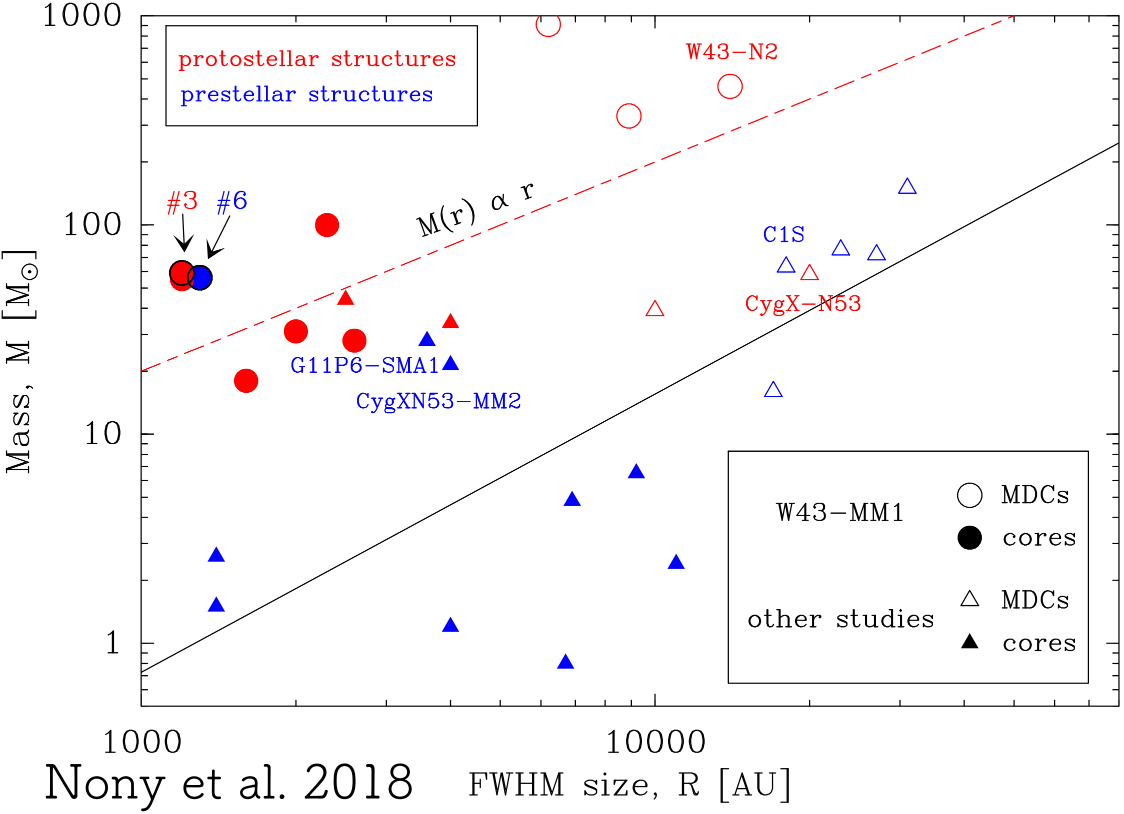

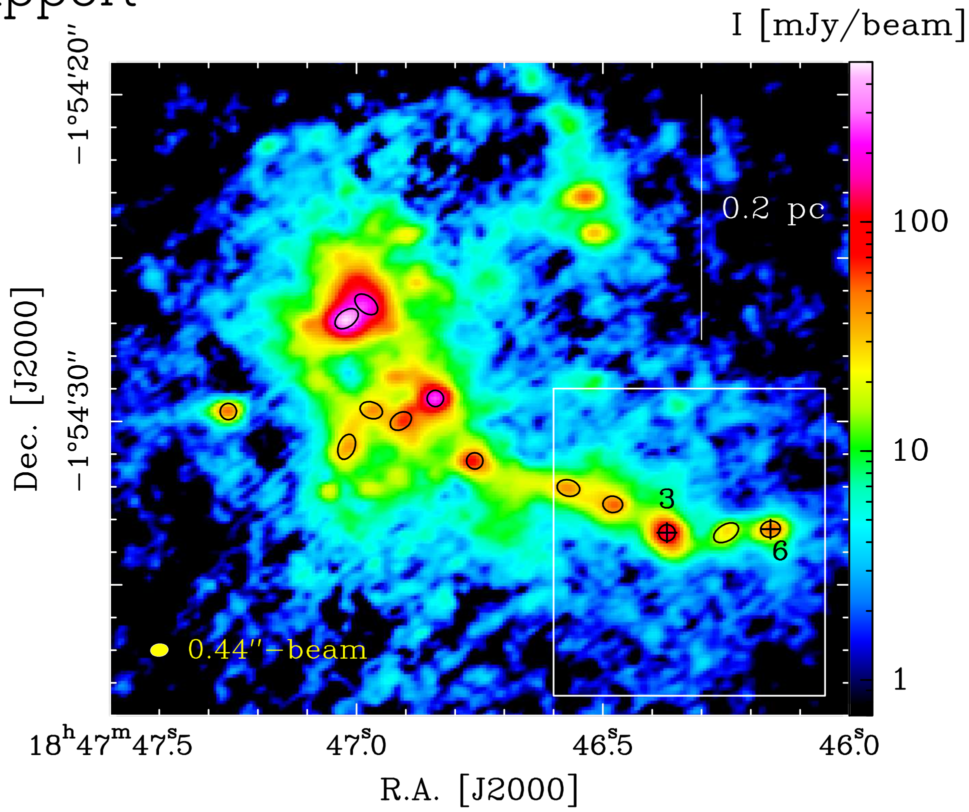

Nony et al. 2018

(4) Fields and feedback

Magnetic fields and outflow feedback

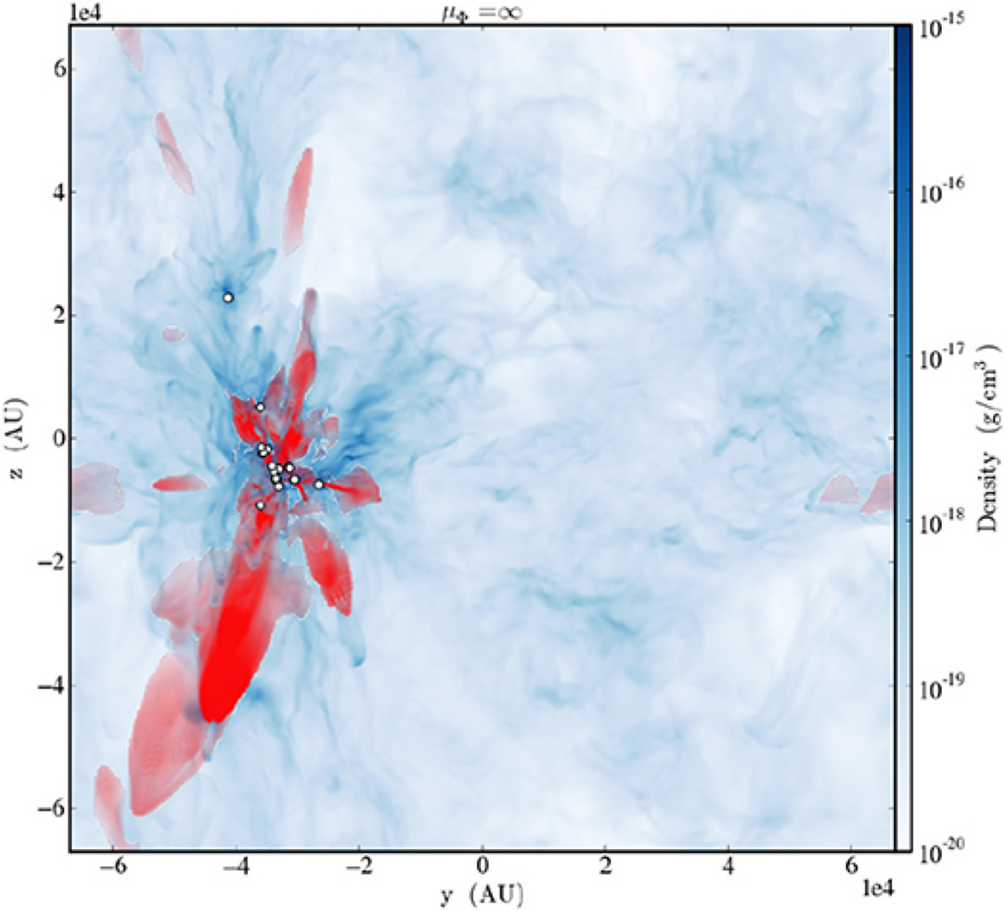

Without a magnetic field

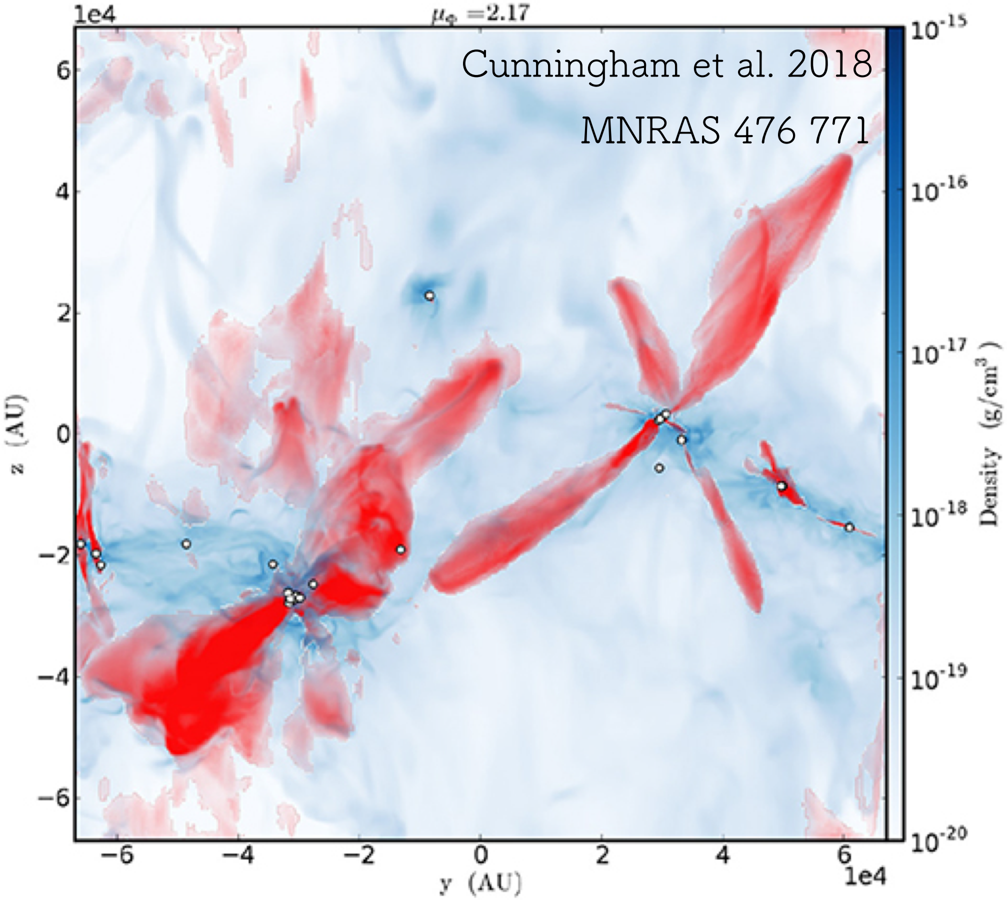

With a magnetic field

Magnetic fields may play a crucial role in setting star formation efficiency:

a) **Within a star-forming core**, by removing mass and angular momentum, and preventing further accretion

b) **Over molecular clouds**, by propagating outflow feedback, and so inducing turbulent motions, over large volumes

cf. Krumholz & Federrath 2019

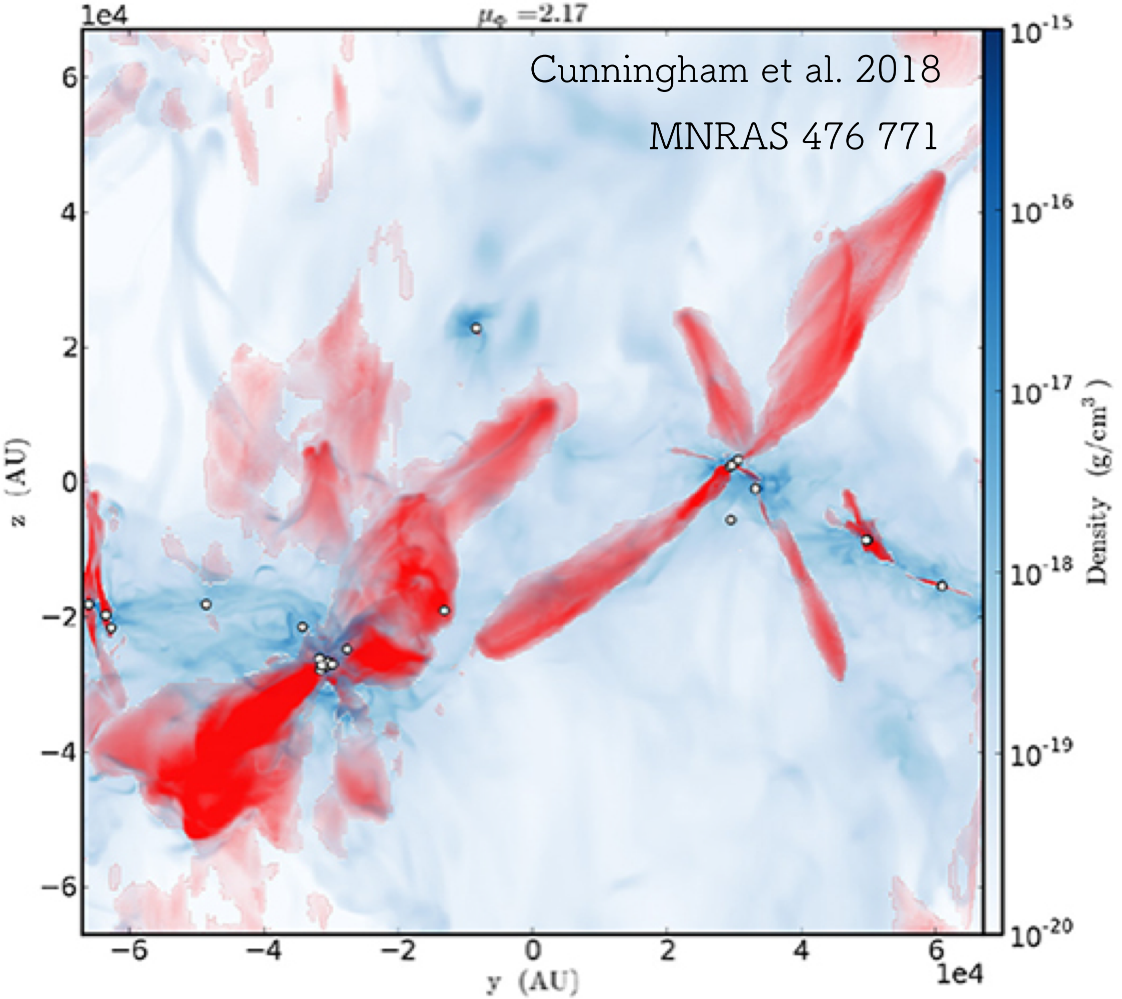

Magnetic fields and stellar feedback

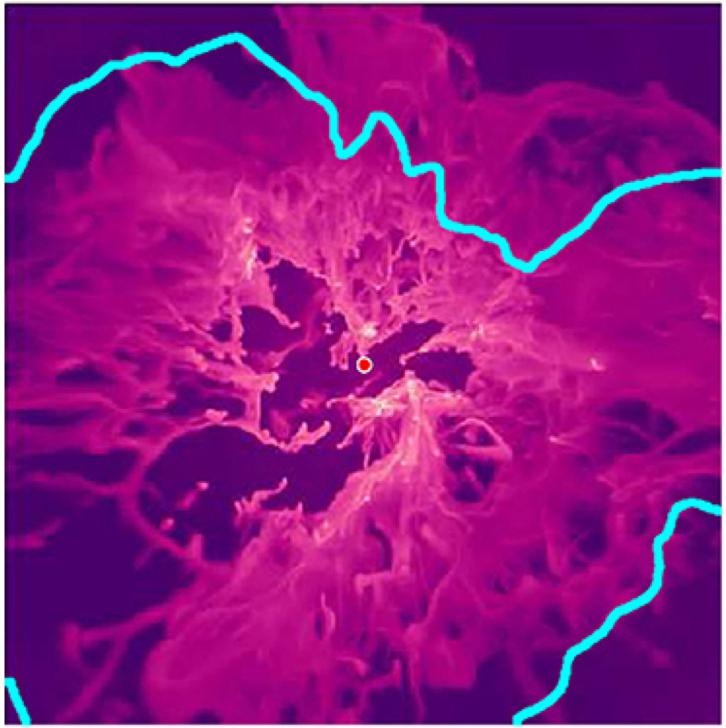

Without a magnetic field

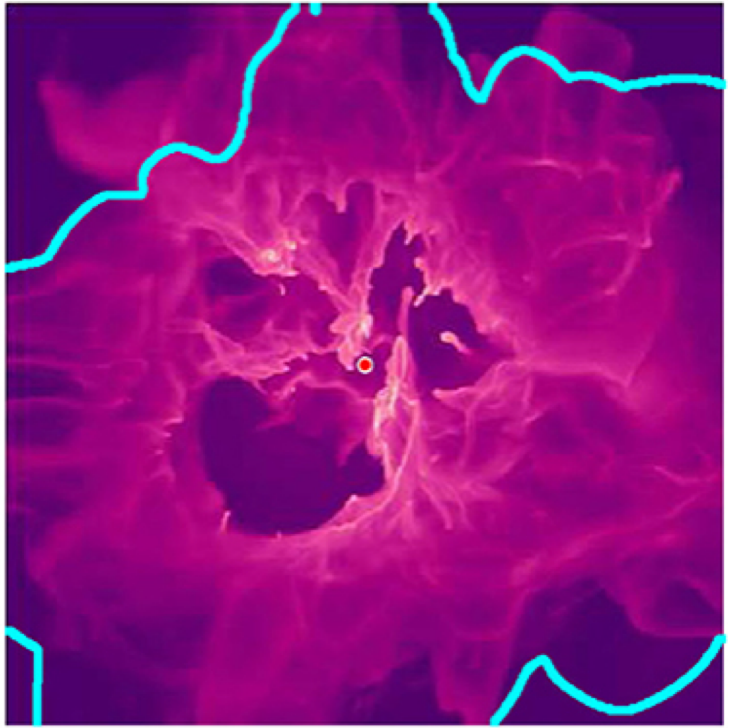

With a magnetic field

Magnetic fields may play a role in HII region confinement?

Geen et al. 2015

Magnetic fields under feedback

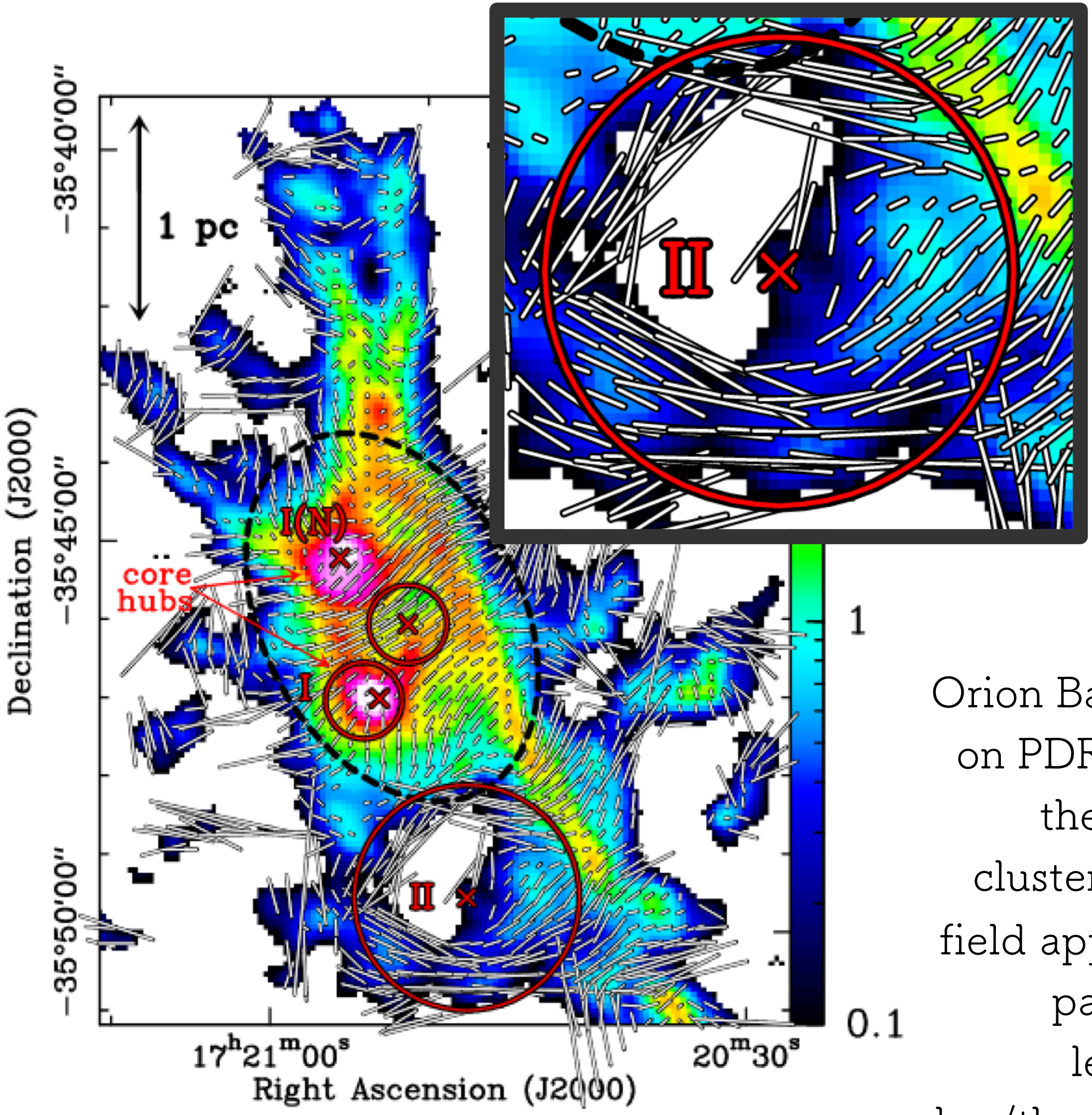

Arzoumanian et al. 2021

NGC 6334: Approximately concentric B-field patterns ("shell-like structures") around HII regions – perhaps indicating magnetic field compression? (Tahani et al., ApJ in press)

Orion Bar: an edge-on PDR, bordering the Trapezium cluster. Magnetic field appears to run parallel to the length of the bar/the shock front.

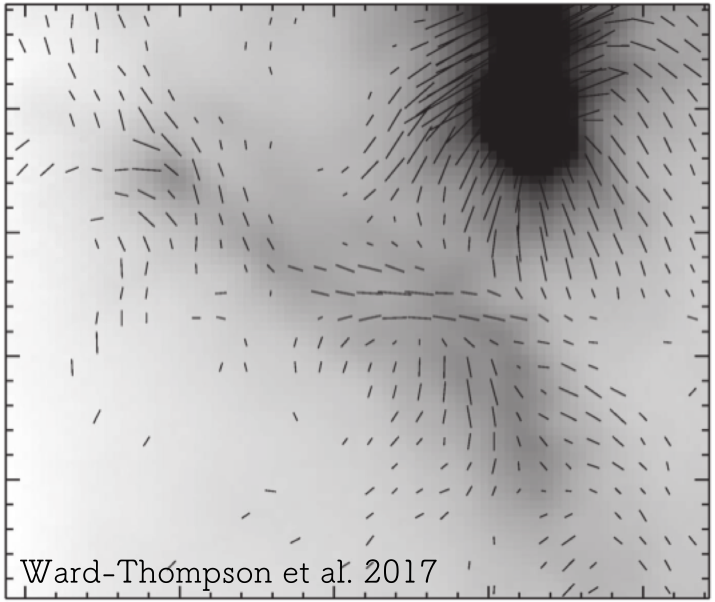

Ward-Thompson et al. 2017

(5) Galactic magnetic fields

Galactic magnetic fields

Magnetic fields are initially generated by small-scale supernova-driven turbulent dynamos

The turbulent seed fields are then amplified and maintained by a galactic dynamo

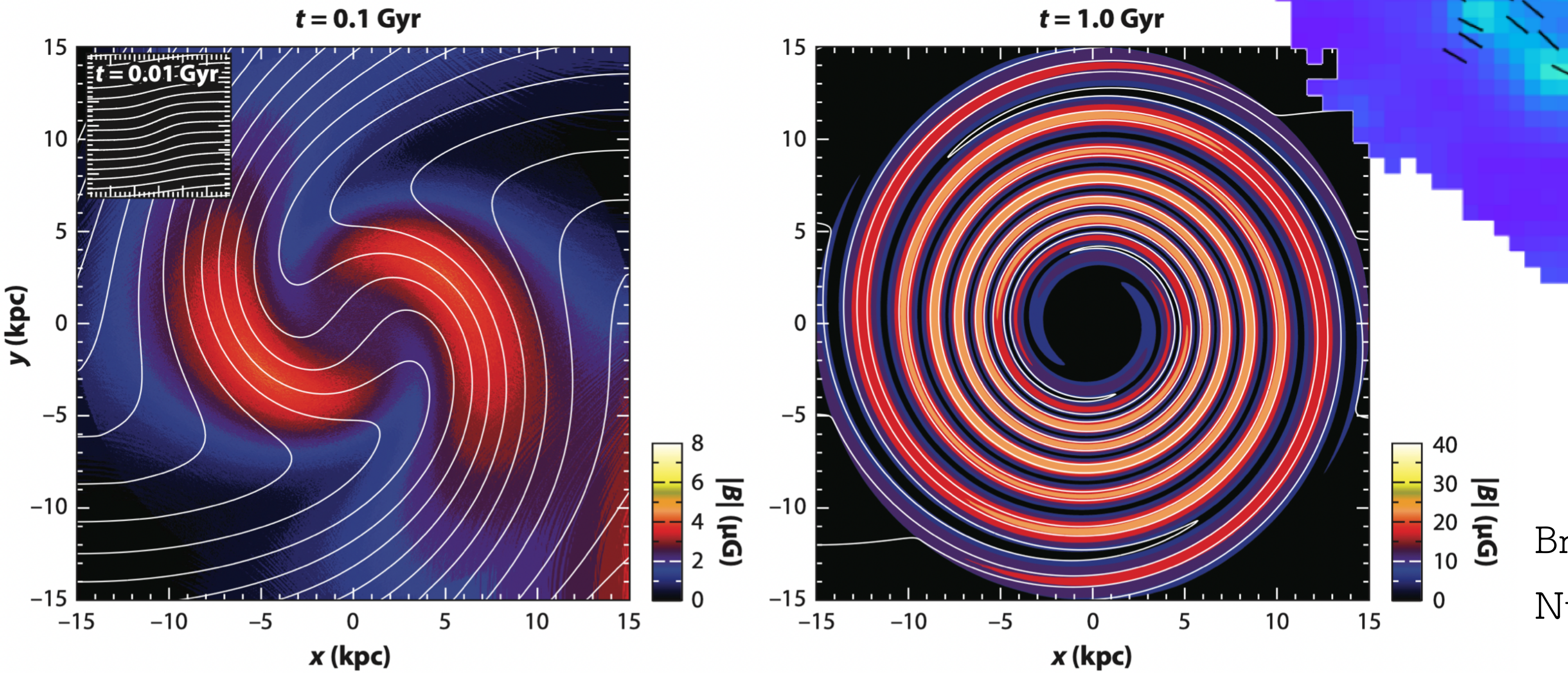

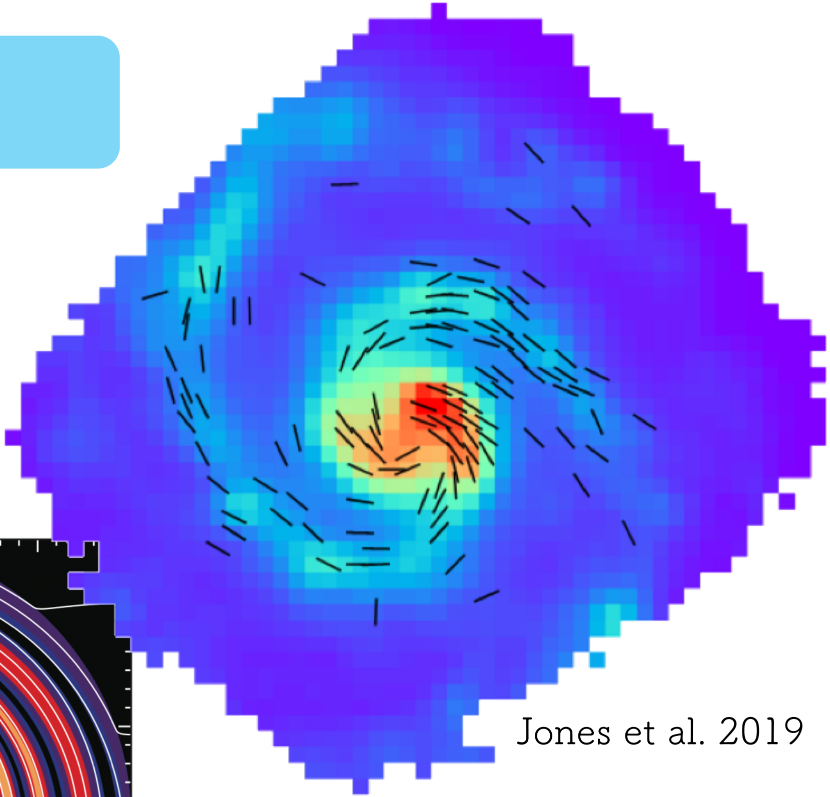

Jones et al. 2019

Brandenburg & Ntormousi 2023

The SOFIA SALSA Survey

Lopez-Rodriguez et al. 2022

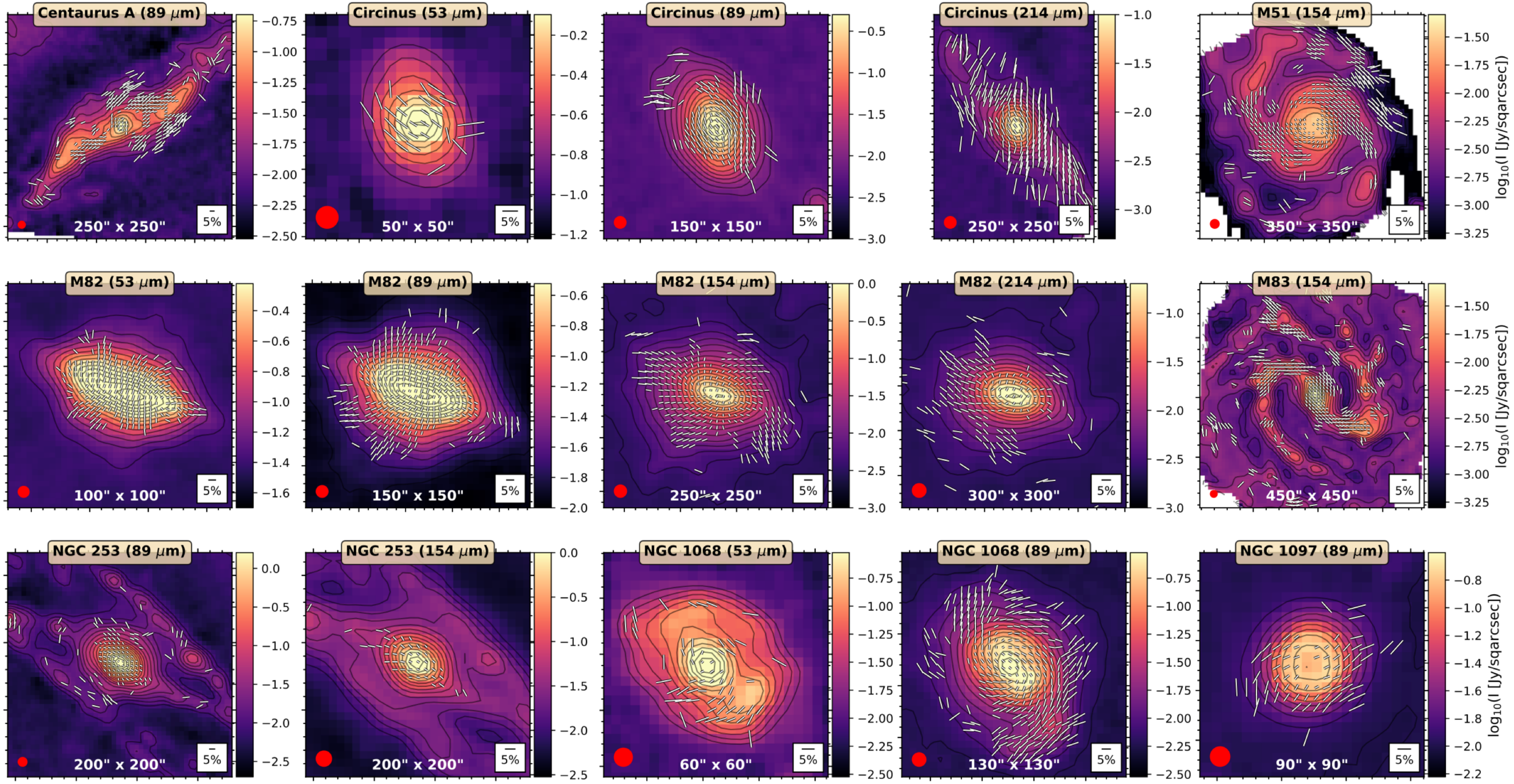

Star formation feedback can disrupt dynamo fields

NASA, ESA, Hubble Heritage Team (STScI/AURA)

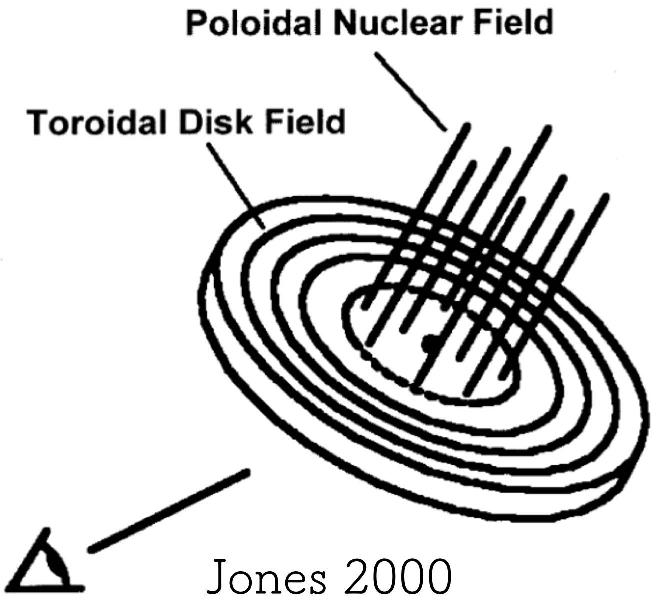

Jones 2000

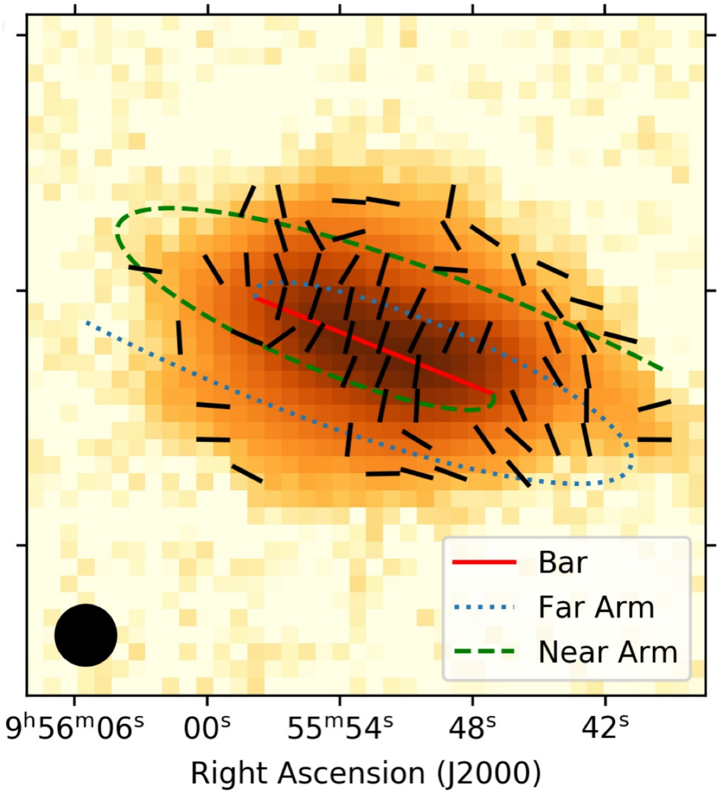

Pattle et al. 2021, MNRAS 505 684

Mismatched spiral arms vs. magnetic arms

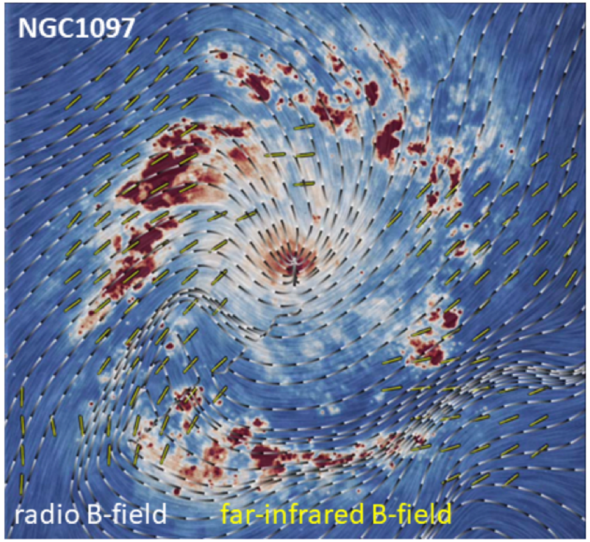

Magnetic fields aligning with warped disk

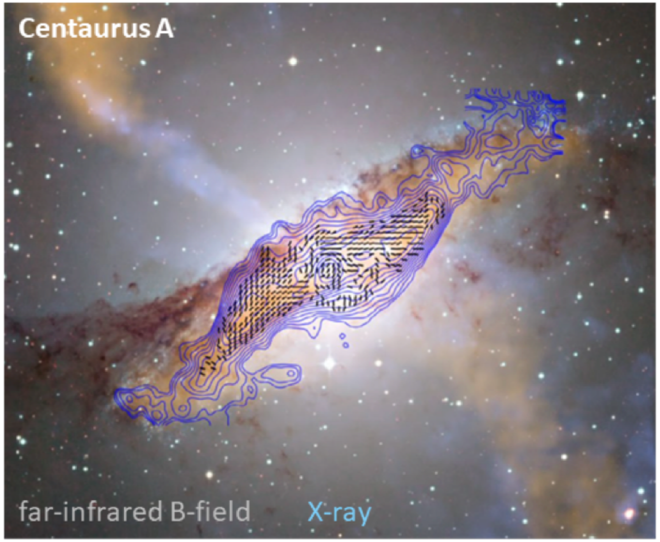

Magnetic fields in starburst-driven outflows

Misaligned spiral arms vs. magnetic arms

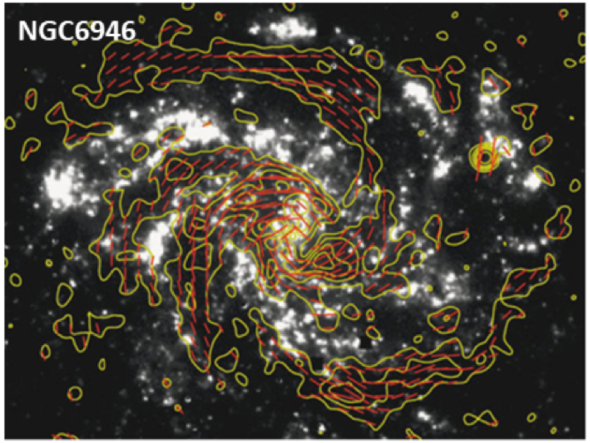

Misaligned radio and far-infrared B-field

Magnetic fields and structure and star formation

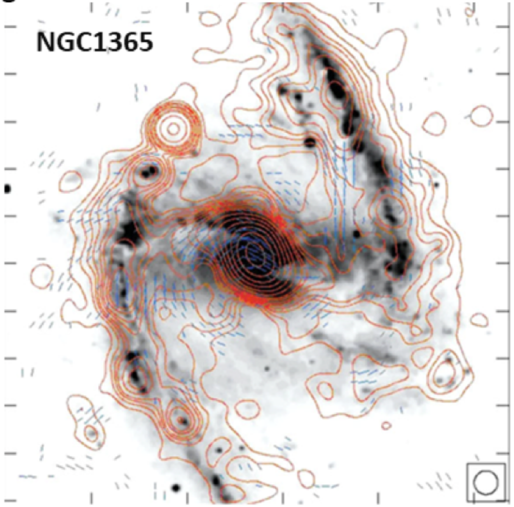

Liu et al. 2024, arXiv:2403.01202

(6) Future facilities

Current facilities

Dust emission

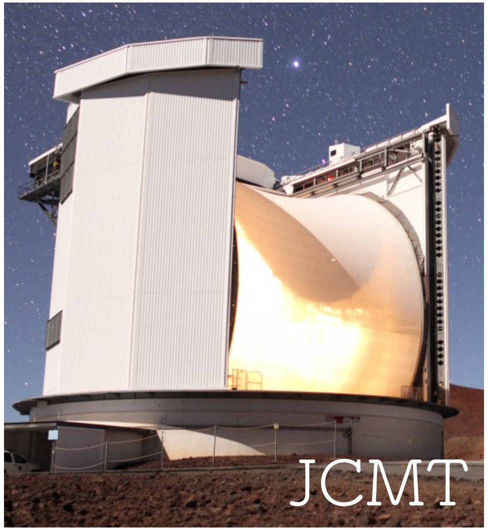

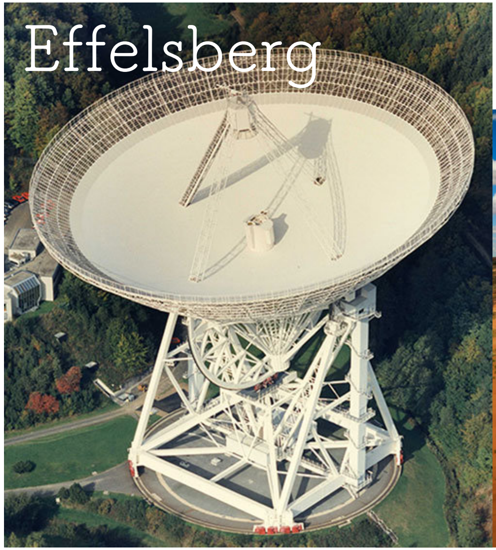

Faraday rotation

Zeeman splitting

Current facilities

Dust emission

Faraday rotation

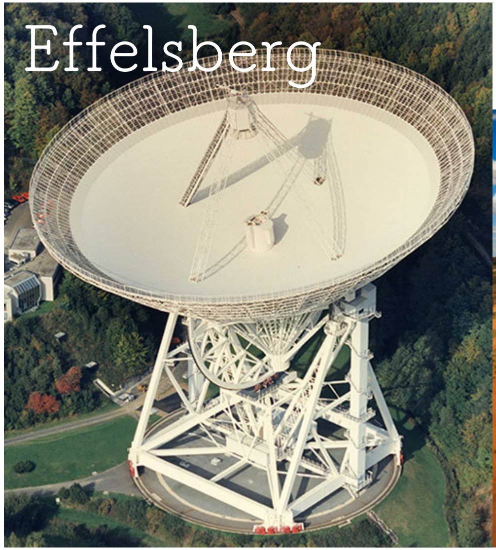

Zeeman splitting

PRIMA

PRobe far-Infrared Mission for Astrophysics

Selected for Phase A study!

12-month mission concept study underway

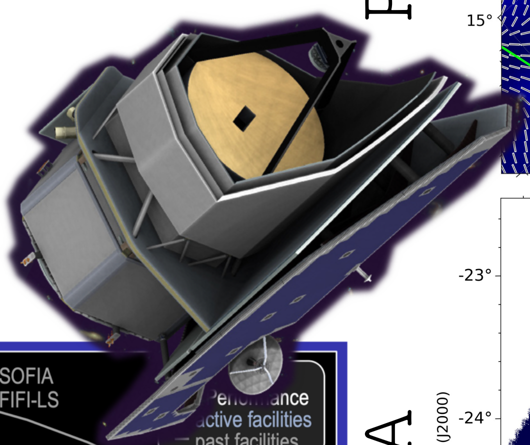

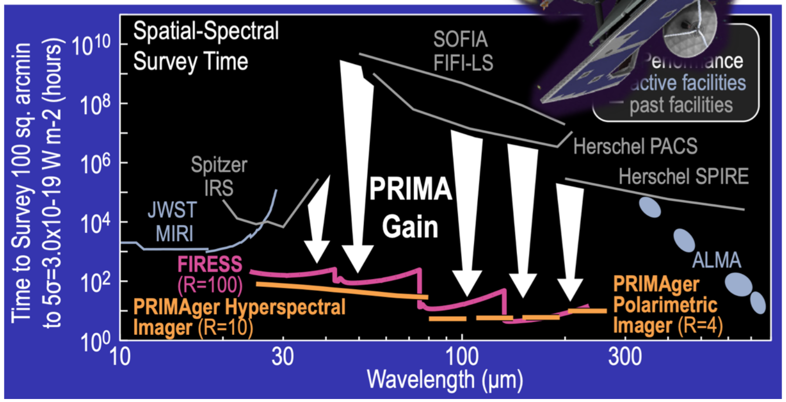

https://prima.ipac.caltech.edu/

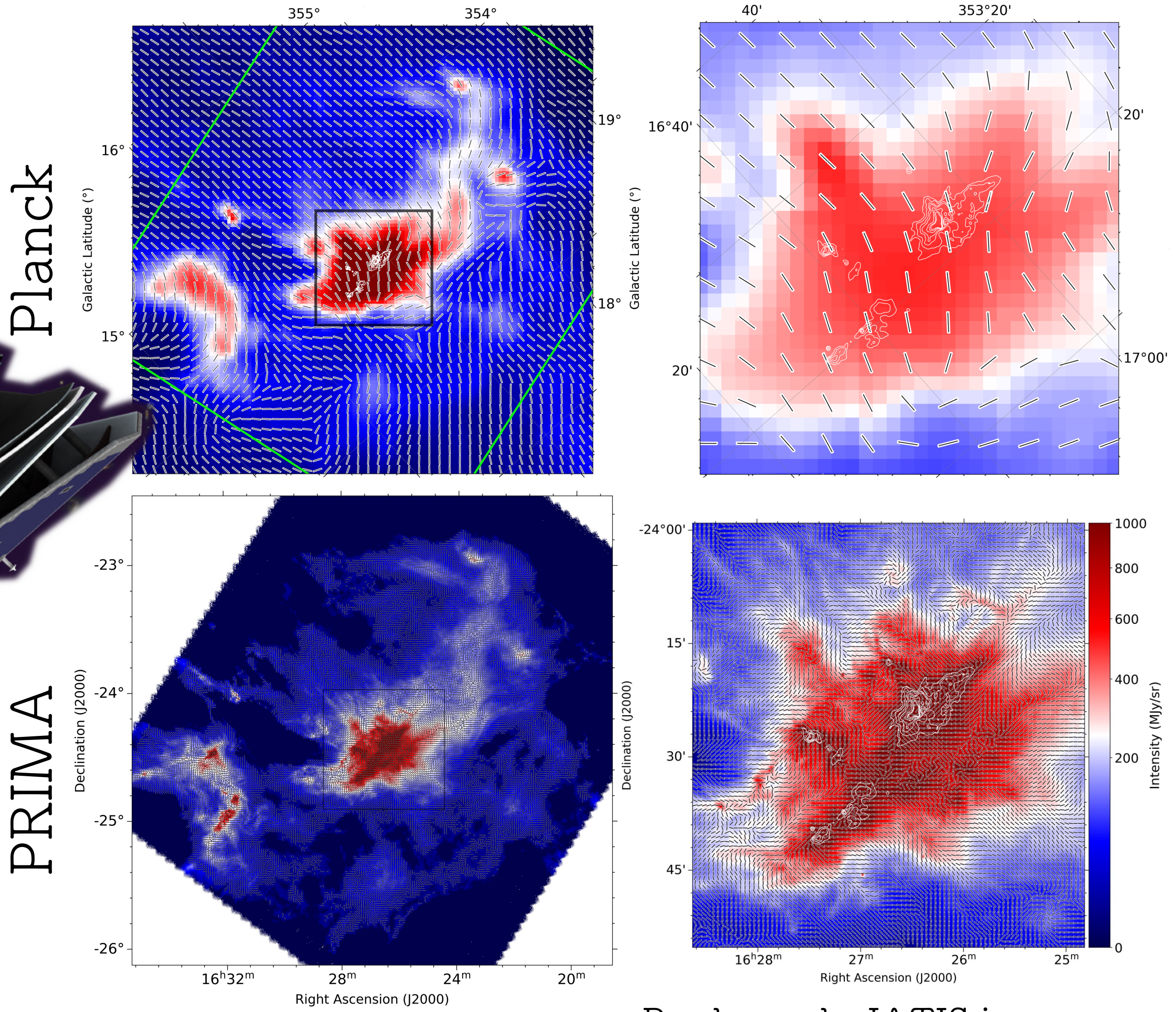

Pattle et al., JATIS in press

AtLAST
The Atacama Large Aperture Submillimetre Telescope

- A 50m-diameter single-dish submillimetre telescope with a 1 square degree field of view, located on the Atacama Plateau
- Aiming to be the first fully sustainable telescope
- Horizon Europe-funded design consolidation study began this year
- Aiming for first light in mid 2030s

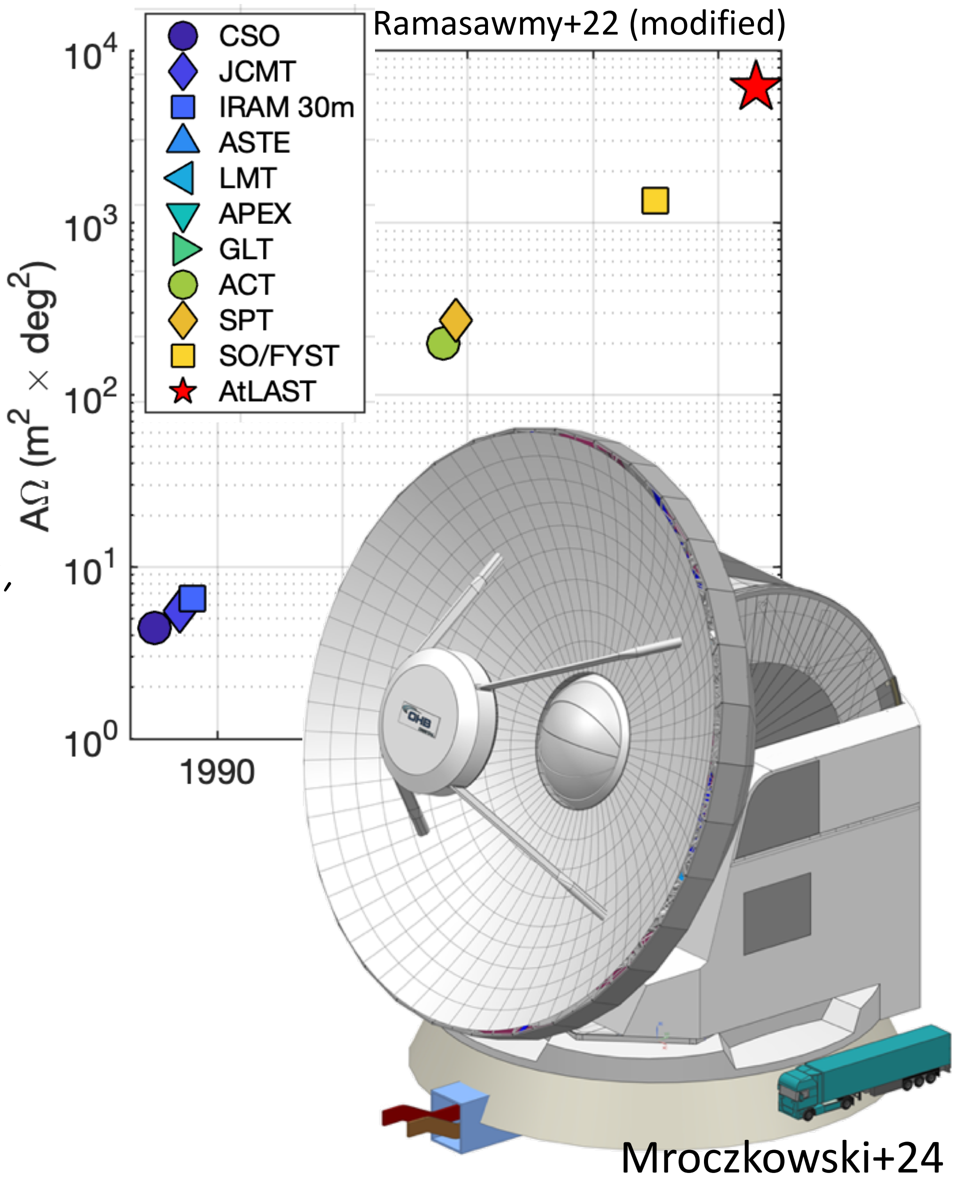

The Square Kilometre Array (SKA)

- Under construction in Australia (SKA-Low) and South Africa (SKA-Mid)
- Will be suitable for Zeeman HI, OH and HINSA, and Faraday rotation
- **First science data expected in 2027!**

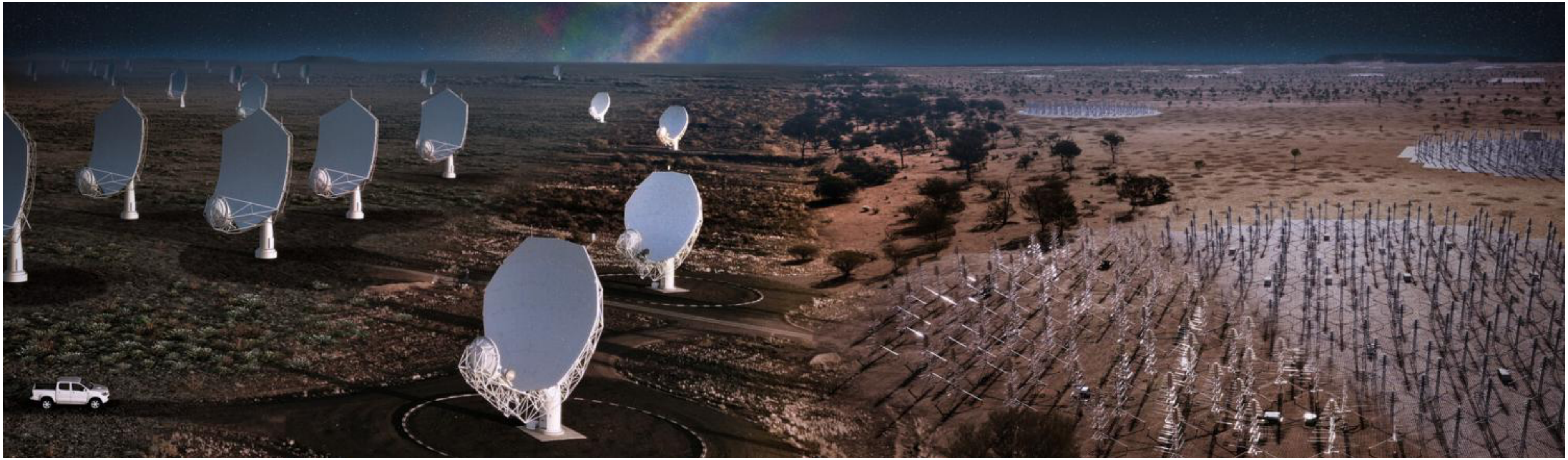

Magnetic fields thread the ISM on all size scales: what dynamical role do they play?

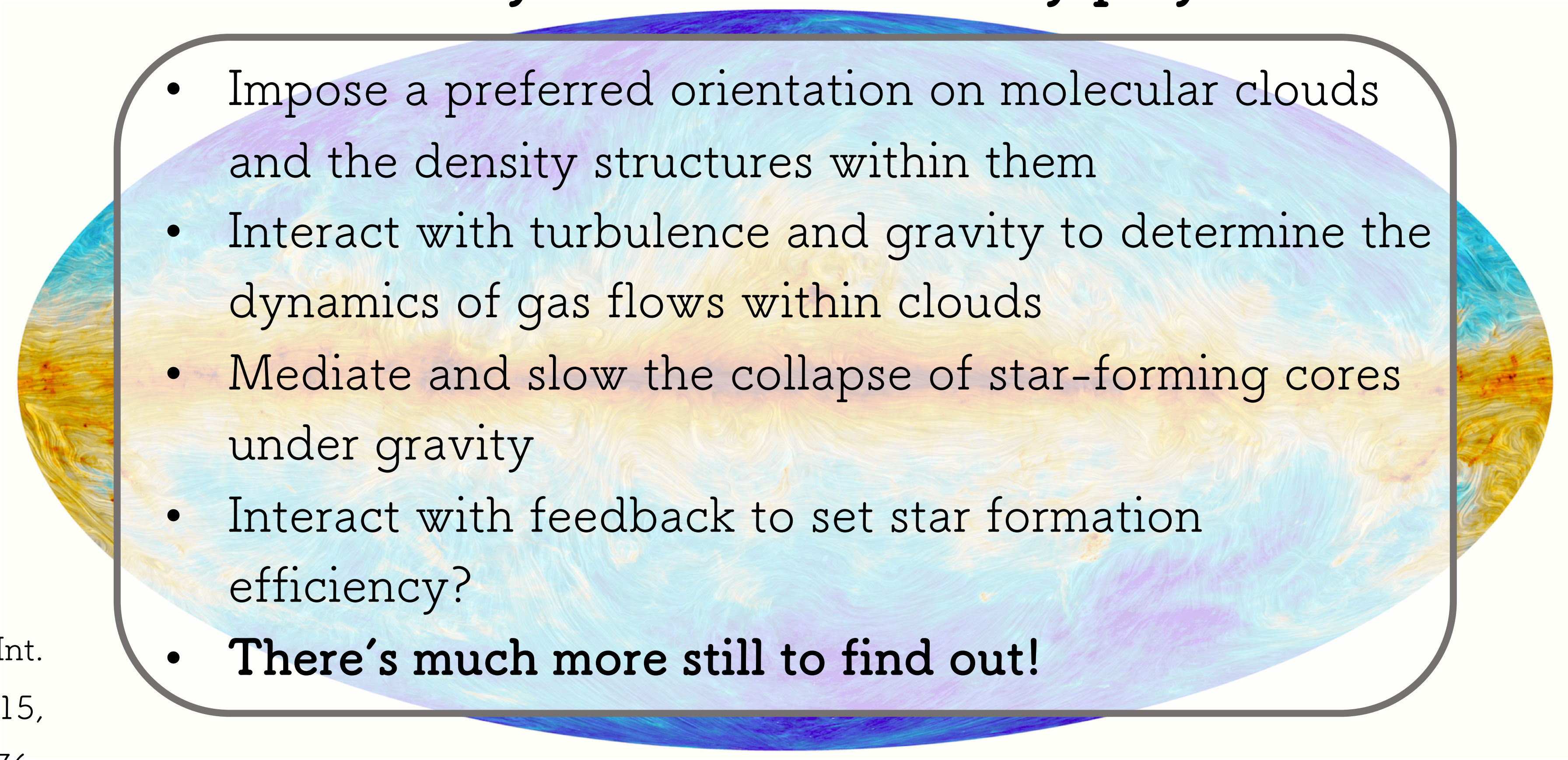

- Impose a preferred orientation on molecular clouds and the density structures within them
- Interact with turbulence and gravity to determine the dynamics of gas flows within clouds
- Mediate and slow the collapse of star-forming cores under gravity
- Interact with feedback to set star formation efficiency?
- **There's much more still to find out!**

Planck Int. XIX 2015, A&A 576 A104

Thank you!